Stratigraphic correlation and depositional setting of the Early Weichselian (MIS 5d-a) sediments and surrounding Pleistocene and Holocene sediments in the Dutch Offshore, Southern North Sea; A regional perspective from seismic interpretation and sediment core data

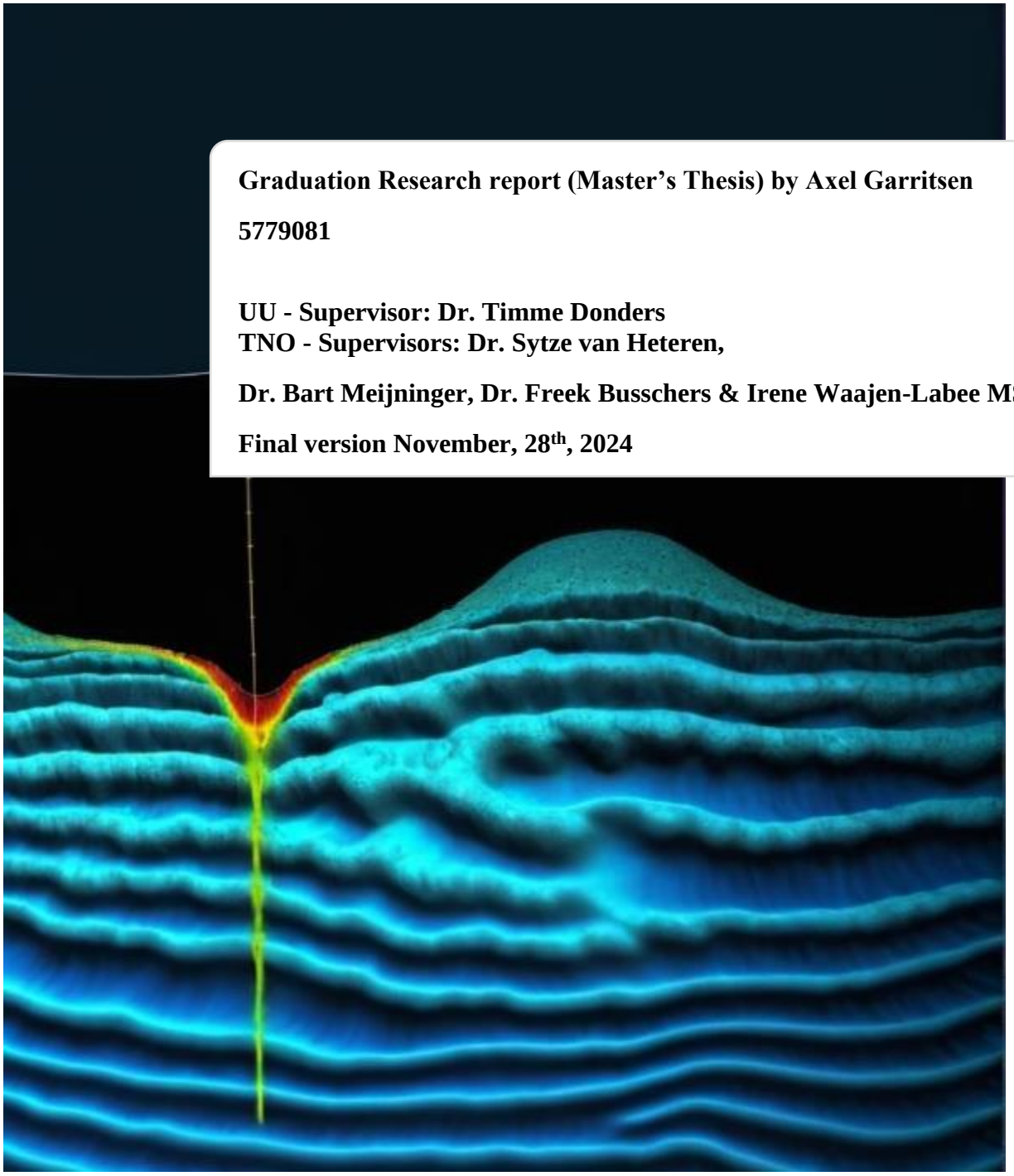

Graduation Research report (Master's Thesis) by Axel Garritsen

5779081

UU - Supervisor: Dr. Timme Donders
TNO - Supervisors: Dr. Sytze van Heteren,

Dr. Bart Meijninger, Dr. Freek Busschers & Irene Waajen-Labee MSc.

Final version November, 28th, 2024

TNO Geological Survey of the Netherlands Part of TNO

Universiteit Utrecht Faculty of Geosciences

Table of contents

Front cover: Art Impression using artificial intelligence and the terms “seismic data” and “seafloor” among others, made by author at openart.ai.

Abstract

Coastal nearby deposits from the Eemian (MIS 5e) and the Early Weichselian (MIS 5d-a) can provide relevant context about past climate and sea level fluctuations. From this perspective, the Brown Bank Formation is also interesting. The Brown Bank Formation is largely consisting of clay-rich laminated deposits in the southern North Sea area, that are mainly deposited in regressive lagoonal or submerged deltaic settings during the Odderade interstadial (MIS 5a) of the Early Weichselian and the transition to the Early Pleniglacial (MIS 4). Given, there is still significant uncertainty about the depositional environment in which the Brown Bank Formation formed and its spatiotemporal variability and the transition into the lateral contemporary facies. More research into the Brown Bank Formation is welcome. In addition, better understanding of this can lead to new insights into sea level fluctuations and climate change in the Weichselian and also for the current Holocene/Anthropocene.

Therefore, this study provides a seismostratigraphic interpretation of 2D high resolution seismic survey data (100 km of PES and sparker data in the Dutch part of the southern North Sea, acquired by the Flanders Marine Institute). In which, several seismic facies units have been distinguished (Unit A-G) based on reflection configurations. The stratigraphic interpretation was acquired using comparison with local described sediment cores and a neighboring seismic survey line of the Hollandse Kust West Windfarm project, that was interpreted in this study as well. Ultimately the stratigraphic interpretation consists of the following lithostratigraphic units: the Southern Bight Formation, the Naaldwijk Formation, the Boxtel Formation, the Kreftenheye Formation, the Brown Bank Formation, the Eem Formation, the Egmond Ground Formation and the Yarmouth Roads Formation, from top to bottom.

The discovery of the absence of a lateral transition of the characteristic Brown Bank facies with the fluvial domain, within the length of the seismic survey line, can be seen as the most important insight gained. In addition, the fact that the Brown Bank Formation contains an erosive vertical transition with the Kreftenheye and Boxtel Formations everywhere. Furthermore, this study has provided insights about the depositional environment of the Brown Bank Formation based on the facial character and geomorphology in the seismic data.

1. Introduction

The idea that there have been one or more ice ages and that multiple changes have taken place in the landscape, nature and climate has become increasingly popular since the beginning of the 19th century, thanks to scientists such as Louis Agassiz (1807-1873) (Fagan, 2009). Over the course of the 20th century, this idea became also accepted by the general public. The ice-pushed ridges (or glacio-tectonic structures), moraines and erratic boulders serve as proof of this in the Dutch landscape. The same holds for the many finds from the Southern North Sea area of megafaunal remains of extinct animals such as *Megaloceras giganteus* (giant deer) and *Mammuthus primigenius* (the woolly mammoth) or animals that were only known from faraway places with a colder or deviating climate such as *Rangifer tarandus* (reindeer), *Ovibos mooschatus* (muskox), *Delphinapterus leucas* (beluga) and *Odobenus rosmarus* (walrus) (Mol & Bakker, 2022; Post, 2022). Besides, there are palynological records in which one or more cold-climatic episode(s) are identified on the basis of the occurrence of pollen assemblages of cold-bearing vegetation, such as from sediments of the Drenthe lake; Mekelermeer (Bohncke & Wijmstra, 1988).

Previously, climatic changes and their accompanying environmental and biodiversity changes were mainly the subject of curiosity. However, in the second half of the 20th century, these have become part of fundamental research to understand and anticipate on, the climatic effects in the future. An example of such an effect is sea-level rise. In the current relatively warm interglacial (the Holocene (MIS 1; Marine Isotope Stages are alternating cool and warm intervals which are deduced from stable oxygen isotope data from deep sea sediment core samples; Cai et al., 2010)) global sea-level has risen since the glaciers retreat at the end of the last glacial (the Weichselian, MIS 5d-2) and is still rising today (with 2.9 mm per year in the Netherlands; Taal, Deltares, 2023).

Given the low elevation compared to sea-level in the Netherlands, sea-level rise due to climate change is a major problem for the Netherlands. Therefore, historical sea-level fluctuations are studied to gain understanding about which conditions existed during sea-level rises and what factors are driving sea-level rises and are decisive for the present and future sea-level. Therefore, the Eemian (MIS 5e), an earlier interglacial and climate analogue to the Holocene, with similar sea-level behavior and the Weischselian Early Glacial (MIS 5d-a), a general cooler period than today, in which climatic colder stadials and warmer interstadials and associated sea level fluctuations alternated, are studied as well. Sea-level was also rising relatively rapidly during the Eemian and reached a higher level (about 6-9 meters higher than today; Zagwijn, 1983) than the current sea-level, which is the highest level since the start of the Holocene (Mathys, 2010).

Certain deposits from the Eemian and from the transition times to the cooler Early Glacial (Early Weichselian, MIS 5d-a) and Early Pleniglacial (MIS 4) are being studied from the interest in, among other things, historical climate and sea-level fluctuations, in particular the Brown Bank Formation (previously named: Brown Bank Member; Cameron et al., 1989; Waajen et al., 2024). In addition, these deposits are interesting for landscape development studies. Because these deposits provide an archive of relatively nearshore depositional environments and their relatively detailed changes from a period when few onshore deposits have been preserved. Besides, there is practical curiosity for these deposits due to the infrastructure of the North Sea, including the construction of wind farms (Eaton et al., 2020;

Cartelle et al., 2021). The study of deposits from this transition during MIS 5 is being carried out within the North Sea Research Project of the Dutch Geological Survey of TNO. That research project aims to better map the geology of the North Sea and to correlate this offshore geology with the better studied onshore geology of the Netherlands. This research project was an important driver for this study.

However, for a research project named VER-SKAN, on connecting the key areas in the Quaternary geology and archaeology of the Dutch North Sea (which was subsidized by the Cultural Heritage Agency of the Netherlands), a 2D high resolution seismic survey line was acquired by the Flanders Marine Institute (VLIZ). With a length of 100 km, from the offshore sand extraction pit near the Maasvlakte (The Maasvlakte is a man-made harbor peninsula, part of the Port of Rotterdam and built up from offshore sands) in the Southeast to the Brown Bank (a submarine ridge on the Dutch side of the North Sea border with the United Kingdom) in the Northwest along several cored locations (view Fig. 9) This seismic survey line connects two distinct and relatively well-studied areas in the North Sea, the coastal Maasvlakte and Eurogeul areas as well as the Brown Bank area further offshore, and is a potential tool for their correlation. Therefore, the interpretation of this seismic line ('the VLIZ Line') contributes to their correlation.

Because the Maasvlakte was constructed by dredged sands which proved rich in Pleistocene fossils and artefacts, it has an extensive history of paleontological and archaeological finds and is one of the richest sites in the North Sea area. The history of the Maasvlakte has been explained by Van Ginkel et al. (2014). Recent outlines of the Quaternary palaeontological sites of the North Sea and the found land mammal fauna and the archaeologic finds (prehistoric human tools) of the North Sea area are provided by Mol & Bakker (2022) and Amkreutz (2022) respectively. Hijma et al. (2012) provided a stratigraphic context for the archaeological and palaeontological finds through a detailed geological reconstruction of the southern Dutch coast and offshore area. Decades of geological and occasional archaeological and paleontological research on the Maasvlakte and Eurogeul areas, including the sand nourishment finds, has led to many hypotheses about the subsurface, the geo-archaeological history of these areas and how these past landscapes can be reconstructed.

In addition to the sand nourishment sites, there are also large quantities of Pleistocene mammalian remains and more rarely, however, over the past century, substantial amounts of artifacts retrieved from the North Sea by fishermen with their beam trawlers. It became known that many finds had been made in the area around Brown Bank. This led to an interdisciplinary scientific investigation to discover more about the Mesolithic archaeology of the Brown Bank area (Missiaen et al., 2021).

In recent years, large-scale geological research has been carried out in regions where new wind farms are planned. To assess the conditions of the subsurface for foundations of wind turbines, thorough geophysical surveys and geotechnical and geological site investigations are carried out. In addition, it helps to prevent geo-archaeologically and stratigraphically important areas from being destroyed or becoming inaccessible (Rijksdienst voor Ondernemend Nederland, 2019; Eaton et al., 2020; Cartelle et al., 2021).

Named after the Brown Bank is the Brown Bank Formation (previously known as the Brown Bank Member); clay-rich laminated deposits that are believed to have been deposited during the Early Weichselian (Cameron et al., 1992; Waajen et al., 2024), supposedly in regressive

marine, lagoonal to deltaic settings. The Brown Bank Formation is distributed in the central part of the Southern North Sea (view Fig. 6) and is usually present at about 5 meters below the seabed. Cameron et al. (1992) published the gathered information on the sedimentary facies of the Brown Bank Formation by the British and Dutch Geological Surveys. Since then, the depositional environment of the Brown Bank Formation has been broadly known. However, more clarity about the depositional environment is desirable. Namely, was the environment shallow marine, lagoonal-intertidal, supratidal, lacustrine, or deltaic? In addition, was it a salt brackish or fresh water environment? Cameron et al. (1992) did also publish the current known distribution of the Brown Bank Formation. Since then, more has become known, including discoveries of remnant deposits south of the Eurogeul (Hijma et al., 2012). Nevertheless, it is desirable to obtain more precise understanding of the spatial arrangement of the Brown Bank Formation. In addition, the question arises whether there was spatiotemporal variability in the depositional environment(s) of the Brown Bank Formation? Eaton et al. (2020) do suggest that there is spatial variability because the depositional facies of the Brown Bank Formation units in their offshore East Anglia study area, may differ from those further south. Several authors have also written about temporal variation within the Brown Bank Formation. According to Bicket and Tizzard (2015), there would be a division with a sandier lower unit that was associated with topographic lows and the underlying Eem Formation and an upper unit richer in clay. Eaton et al. (2020) reportedly found only this upper unit in their study area. Furthermore, this upper unit was found to be divided into a more silt-rich unit below a more clay-rich unit (Eaton et al., 2020). Another question that remains is: What is the vertical and lateral transition into the lateral contemporary facies of the Brown Bank Formation? In particular, is the connection between the Brown Bank Formation and the fluviatile domain of the Meuse and Rhine rivers preserved? Furthermore, of the mode, pace and timing of environmental and climatic changes that occurred in the Southern North Sea during the Weichselian is still much unclear. Although the recently published study Waajen et al. (2024) has gathered a large amount of information about this, by combined analysis of 2D acoustic reflection profiles and a geochemical and geochronological analysis of sediment cores. With this, Waajen et al.(2024) provided a new framework for the stratigraphy, the depositional environment and the depositional age of the Brown Bank Formation at its type locality, which is somewhere between 70 to 80 ka, which is around the transition from the Odderade interstadial (MIS5a) into the Early Pleniglacial (MIS4). However, more research is welcome to better understand and resolve questions about the distribution of the Brown Bank Formation and the depositional environment(s) in which it formed and the changes that occurred therein/with it.

To answer these questions and to contribute to the gathering of the necessary insights, the 2D seismic survey data are examined and interpreted in this study. More precisely, units are distinguished in the seismic data based on geometry and seismic facies, including reflection configurations and interpreted in terms of depositional environments and stratigraphically labeled and compared for ground-truthing with sediment cores from close to the VLIZ line. With the aim of improving the understanding of the stratigraphy and depositional environmental changes of the Early Weichselian (MIS 5d-a) succession in particular and the surrounding Middle Pleistocene (MIS 13-6), Eemian (MIS 5e), Middle and Late Weichselian (MIS 4-2) and Holocene (MIS 1) succession in this area as well.

Therefore, this study attempts to answer the following research question: What is the vertical and lateral stratigraphic succession shown on the newly acquired southern North Sea seismic line and how can this be environmentally interpreted? An attempt is made to answer this

question for the Early Weichselian sediments in more detail compared to the surrounding sediments. Sediment core data from the TNO archives that are useful for this research are integrated to make more reliable interpretations. The results of the seismic interpretation of the VLIZ line include a series of screenshots, the clean data, a location map of the data segments, a diagram depicting the different units and their seismic facies, a schematic cross-section of the VLIZ line, and a stratigraphic diagram. Furthermore, new insights gained with this study about the Quaternary stratigraphy of the Dutch North Sea can help in the search for interesting new locations for collecting sediment cores. This study also serves as support for an ongoing PhD-project between Utrecht University and the Dutch Geological Survey of TNO on the subject with the non-binding title: "the Early Weichselian in the southern North Sea".

2. Geologic setting and climatic history of the Southern North Sea area

2.1 Developmental and climatic history

The North Sea Basin originates from Late Jurassic and Early Cretaceous rifting (Eaton et al., 2020; Laban & Van der Meer, 2022), this was not always accompanied by accumulation space creation. For example, during the alpine orogeny, inversion took place in the Dutch subsurface and in the Southern North Sea. From the Mid-Miocene, constant subsidence has taken place in the entire North Sea basin, providing accumulation space for large river systems to prograde to (e.g. Eridanos, Rhine, Meuse, Scheldt, Thames, Humber; Laban & Van der Meer, 2022).

During the Quaternary the North Sea area encountered multiple sea level lowstands during the glacial times that exposed shallow continental shelves and thus turned the North Sea partially to largely into dry land. Glaciers at lands bordering the Northern North Sea grew substantially during the glacial times (Scandinavian and British highlands) and ultimately reached the Southern North Sea, leaving ice-pushed sediment ridges, valleys and glacial till behind in this area. The sea level lowstands alternated with highstands during the interglacials, in which temperate marine conditions prevailed in the area (Busschers, 2007; Hijma et al., 2012; Eaton et al., 2020; Cartelle et al., 2021; Laban & Van der Meer, 2022). The multiple marine-terrestrial-marine transitions and associated depositional and erosional processes, have led to a relatively complex stratigraphic record in the Southern North Sea (Mellett et al., 2013; Eaton et al., 2020; Eaton et al., 2020; Laban & Van der Meer, 2022). The diverse climatic and developmental history of the Southern North Sea is outlined below. Furthermore, a geologic timetable and other relevant information about the geologic history of the Southern North Sea study area is summarized in Figure 1.

Elsterian/ Anglian glaciation (MIS 12)

Estimated age: ~478 - ~424 ka

During the culmination of this glacial time did glaciers extend to the Northern part of the Netherlands, while ice sheets reached its southernmost extent of the entire Quaternary period, covering a large part of East Anglia (Eaton et al., 2020; Laban & Van der Meer, 2022). During the previous sea level high stands was Great Brittain still an peninsula that was connected through the Weald-Artois Anticline with the Central European mainland (Laban & Van der Meer, 2022). During the Elsterian a melt-water lake formed South of the glaciers that at some point drained through the Weald-Artois Anticline, which resulted in the development of the Strait of Dover. Scouring marks in the English Channel serve as evidence for the formation of a waterfall through which the meltwater lake drained (Mellet et al., 2011; Laban & Van der Meer, 2022). However, Mellet et al. (2011) reported that no constructional or sedimentological evidence of a possible catastrophic flood was found in the English channel. Furthermore, subglacial-formed paleovalleys filled with glaciolacustriene sediments from the Elsterian Glaciation, that are part of the Peelo formation, are present in the Northern Netherlands and parts of the North Sea. However, these sediments and valley systems are almost absent beneath 53° latitude and close to the VLIZ line (Cameron et al., 1989; Eaton et al., 2020; Laban & Van der Meer, 2022).

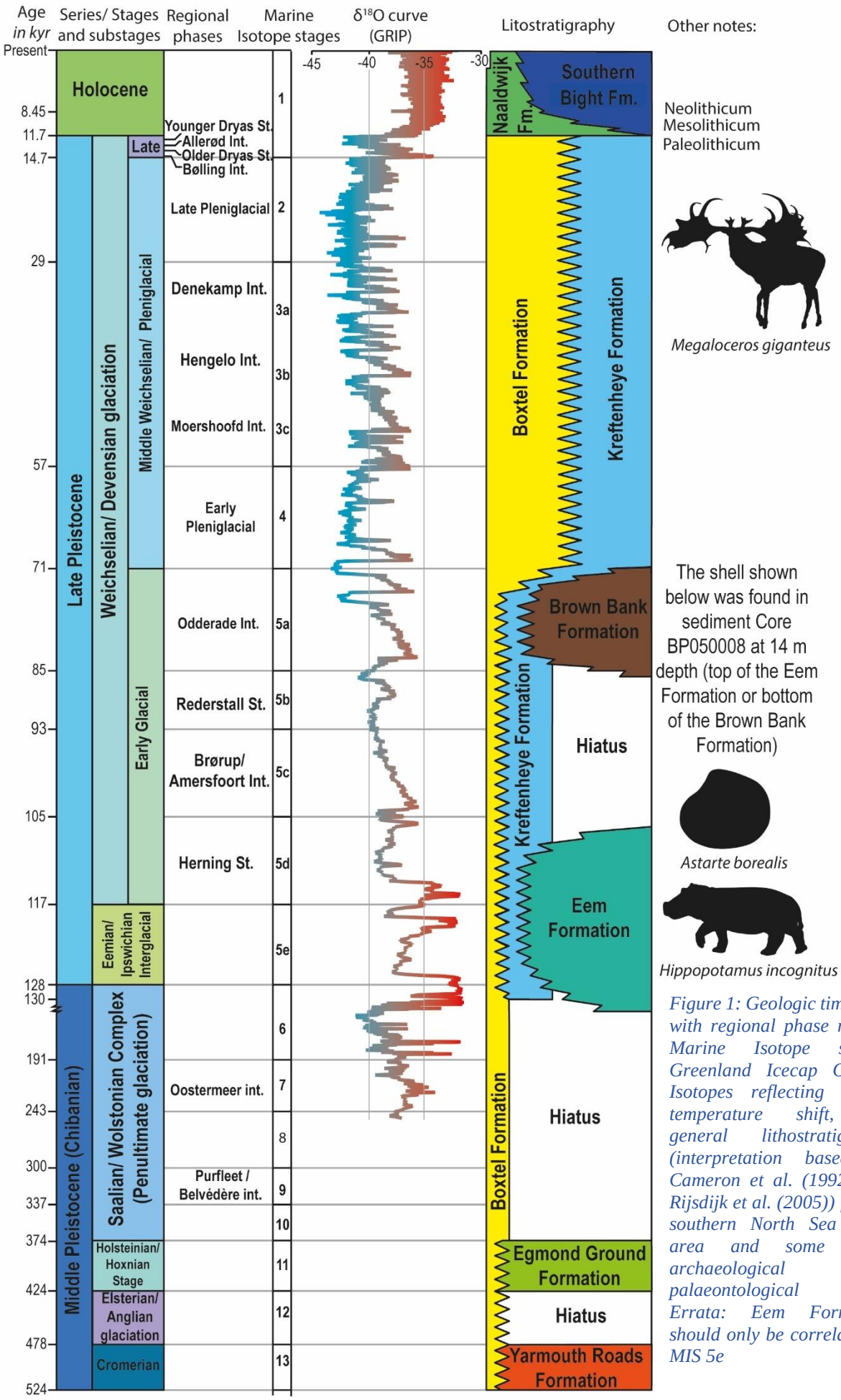

Figure 1: Geologic timetable with regional phase names, Marine Isotope stages, Greenland Icecap Oxygen Isotopes reflecting global temperature shift, the general lithostratigraphy (interpretation based on Cameron et al. (1992) and Rijsdijk et al. (2005)) for the southern North Sea study area and some other archaeological and palaeontological notes. Errata: Eem Formation should only be correlated to MIS 5e

Holsteinian/ Hoxnian interglacial (MIS 11)

Estimated age: ~424 - ~374 ka

Sea level high stands up to 13 or 20 meters above present level, occurred during this interglacial while depositing the marine sediments of the Egmond Ground Formation in the Southern North Sea, which is locally present around the VLIZ seismic line. (Cameron et al., 1989; Laban & Van der Meer, 2022 & references therein). Climatic conditions of the Holsteinian Southern North Sea area were similar to, or little warmer than, the Holocene's temperate conditions. However, the connection between the North Sea and the English channel was closed again as a result of which the warm gulf stream waters were only able to reach the North Sea from the North. (Laban & Van der Meer, 2022).

The Saalian Complex, the penultimate glaciation (MIS 10-6)

Estimated age: ~374 - ~130 ka

The Saalian Complex covers a period where very cold, glacial conditions and relatively temperate intervals prevailed in the Southern North Sea. Base level dropped up to 120 meters (Mellet et al., 2011). Especially the End-Saalian (MIS 6) has shaped the Dutch topography as a result of the glaciers, part of the Scandinavian ice sheet, that reached the central Netherlands, leaving behind several glacigenic landforms (Cartelle et al., 2021; Laban & Van der Meer, 2022). Some of these are recognized today as hills and ridges of tens of meters in height. The Veluwe, the highest push-moraine in the Netherlands, peaks at 109.9 m above sea level. On the Texel-Gaasterland-line are overridden ice-pushed structures found that are formed in an earlier icesheet advance, whereafter the icesheet progressed more South (Peeters et al., 2015). Around 160 ka, glaciotectonic deformation reached a zone fifty kilometers west of today's Haarlem coast (Cartelle et al., 2021). These deposits are grouped in the Drente Formation. The VLIZ line is probably not intersecting the Drente Formation distribution. There was no connection between the Scandinavian ice sheet and the British ice sheet in the central or southern North Sea (Laban & Van der Meer, 2022). Furthermore, a proglacial lake formed during the late Saalian ice sheet expansion that might have flooded large parts of the North Sea and formed a waterfall off the ridge at the Strait of Dover. However, similar to the Elsterian southern North Sea lake, despite some indications, undisputable evidence for both the lake and the waterfall is lacking (Busschers et al., 2008; Mellet et al., 2011; Peeters et al., 2015; Laban & Van der Meer, 2022). Nevertheless, lake systems arose in the deeply scoured subglacial basins when the Saalian ice sheet collapsed (Busschers et al., 2008; Peeters et al., 2016). Furthermore, wind-blown sands of the Boxtel Formation, deposited during the Saalian-complex, are sparsely preserved and often incised by rivers. Furthermore, locally in the Southern North Sea are the wind-blown sands of the Tea Kettle Hole Formation and the proglacial silty clays and fluvioglacial outwash sands and silts of the Cleaver Bank Formation present, which are deposited during the Saalian Complex as well (Cameron et al., 1989; BGS, 2024a; BGS, 2024b).

Eemian/ Ipswichian or penultimate interglacial (MIS 5e)

Estimated age: ~130 - ~115 ka

The cold climatic periglacial conditions that existed in the Netherlands during the Saalian gave way to a temperate climate during the Eemian interglacial (MIS 5d-5e), which was comparable

to warmer than today (Laban & Van der Meer, 2022). This warming was accompanied by a transgression that flooded the entire North Sea area and formed a sea basin that extended into the mouths of the Rhine and Meuse as well as into a valley, that had formed north of the ice-driven ridges in the central Netherlands, which turned this valley into a lagoon and estuary (Busschers et al., 2007; Peeters et al., 2015; Peeters et al., 2016). This transgression left behind the Eem Formation, also along the VLIZ line (Cameron et al., 1992; TNO-GDN, 2022f). During the Eemian the Rhine ran through the IJssel valley and drained into the estuary between Urk and Gaasterland. The Maas largely followed its current route, however, flowed slightly more to the North, along the southern tip of the Utrechtse Heuvelrug. The Meuse flowed into an estuary near present-day Zoetermeer. (Busschers et al., 2007; Peeters et al., 2015; Peeters et al., 2016). During the Eemian, the global sea level reached six meters above the present (Zagwijn, 1983; Peeters et al., 2015; Cohen et al., 2022). The warm Gulf Stream was able to reach the Southern North Sea via the strait of Dover resulting in the migration of mollusk species from the South (Van der Valk, 2022).

Weichselian Early Glacial (MIS 5d-5a)

Estimated age: ~115 - ~71 ka

The Weichselian Early Glacial (MIS 5a-5d) was a climatically varying period with cool stadials (e.g. Herning (MIS 5d) and Rederstall (MIS 5b)) with limited tree growth and more temperate interstadials (e.g. Amersfoort (MIS 5c), Brørup (MIS 5c) and Odderade (MIS 5a) (These ages are correlated with some uncertainty to the Marine Isotope Stages. The same holds for the aforementioned stadials) with coniferous boreal forest and accompanying sealevel fluctuation between approximately -15 and -50 m compared to current sea level (Zagwijn, 1992; Mellet et al., 2011; Waajen et al., 2024). After the Eemian, the climate cooled down and a regression took place, resulting in a sea level drop of about 40 meters, relative to the Eemian high stand. As a result of which the Rhine and Meuse deltas prograded into the Southern North Sea while incision took place upstream (Busschers et al., 2007; Peeters et al., 2016; Waajen et al., 2024). The Brown Bank Formation reflects the Early Glacial in the Southern North Sea Area and along the VLIZ line. To the Brown Bank Formation pertain the (at least partially brackish) lagoonal or (mainly freshwater) deltaic deposits that were formed at or near the river mouth of the prograding Rhine and Meuse rivers in large parts of the southern North Sea (view figure 2). (Cameron et al., 1989; Laban, 1995; Hijma et al., 2012; Eaton et al., 2020; Laban & Van der Meer, 2022; Waajen et al., 2024). However, there is still much uncertainty about the generally low-energy depositional environment and uncertainty about the age of the Brown Bank Formation. Nevertheless, the recent publication of Waajen et al. (2024) concluded that these deposits have most likely been formed during the Odderade (MIS 5a) interstadial. Eaton et al. (2020) mention that certain sedimentary changes and dune-scale bedforms in the Brown Bank Formation in the British sector are providing evidence for episodic (relative) sea level changes within the Early Glacial. Furthermore, Hijma et al. (2012) mention that the swampy Brown Bank delta plain could have been an ideal lowland habitat for (Neanderthal) hunter-gatherers.

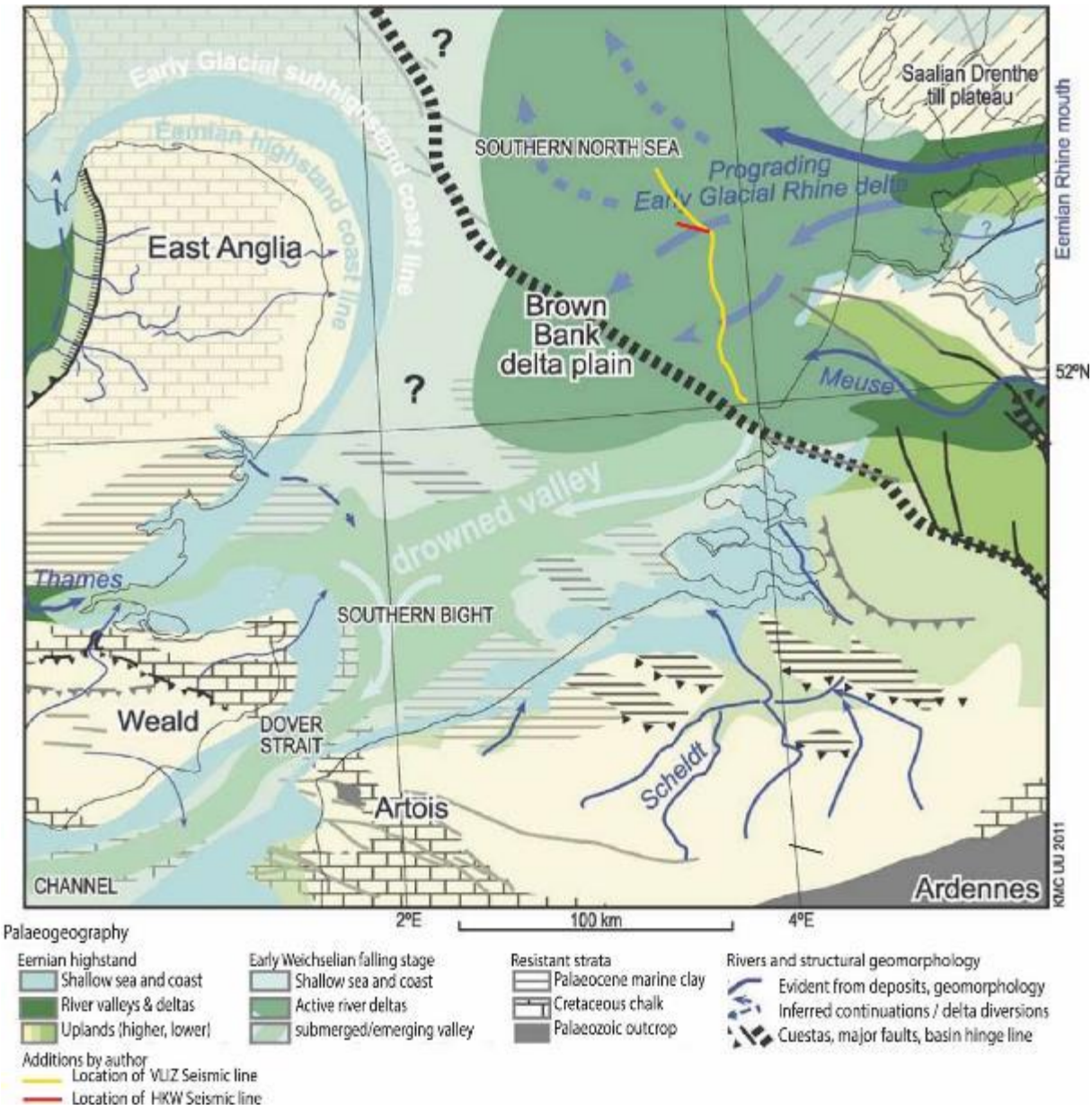

Figure 2: Paleogeographic reconstruction of Southern North Sea area during the Weichselian Early Glacial (MIS 5d-a), with addition of the locations of the seismic lines used in this study. Ref: Hijma et al., 2012. It can be seen that the Brown Bank depositional environment was initially present along the entire length of the line.

Middle Weichselian/ Pleniglacial and Late glacial (MIS 4-2)

Estimated age of Pleniglacial: ~71 – 14.7 ka. Estimated age of Late Glacial: 14.7 ka – 11.7 ka

The transition from the Early Glacial (MIS 5d-a) into the Early Pleniglacial (MIS 4) was accompanied by strong climatic cooling and eustatic sea level lowering, that turned the southern North Sea into dry land, until the inundation at the transition into the Holocene (Peeters et al., 2016; Laban & Van der Meer, 2022). Furthermore, the cooling resulted in the development of continuous permafrost. The formation of permafrost in the Rhine-Meuse catchment resulted in an increased peak discharge regime. Which, in combination with the strong base level lowering, resulted in an over ten meters deep incision of the braided Rhine-Meuse river system removing large parts of the Eemian and Early Glacial deposits also along the VLIZ line (view Fig. 3;

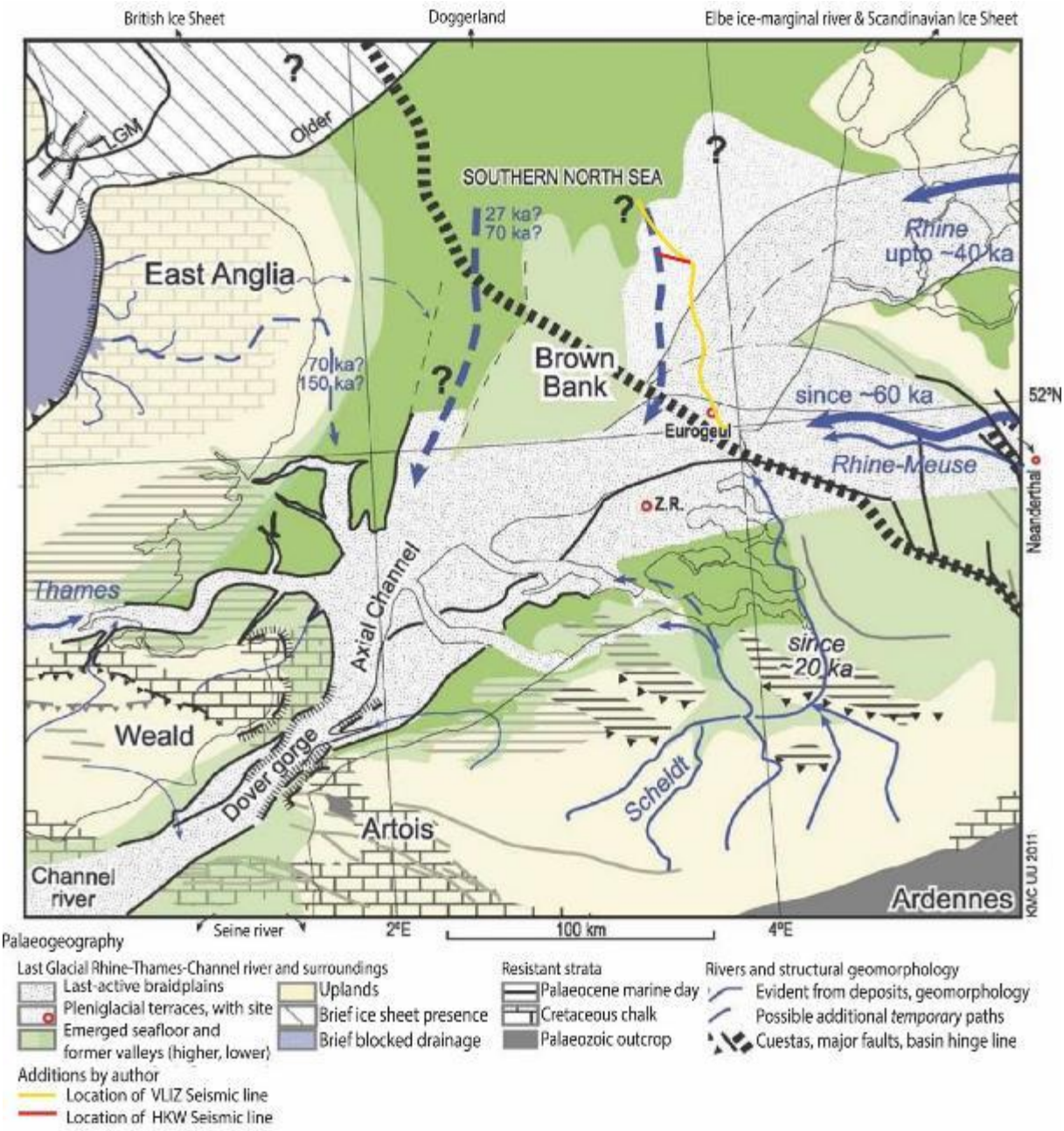

Busschers et al., 2007; Hijma *Figure 3: Paleogeographic reconstruction of Southern North Sea area during the Early Pleniglacial (MIS 4) with addition of the locations of the seismic lines used in this study. Ref: Hijma et al., 2012. It can be seen that the southeast of the VLIZ line was dominated by the fluvial domain and that pleniglacial terraces were present in the northwest of the line.*

et al., 2012; Peeters et al., 2016). These Rhine-Meuse river sediments are part of the Kreftenheye Formation (Cameron et al, 1989; Hijma et al., 2012;).

At the first half of the Middle pleniglacial (MIS 3) the climate became slightly milder. However in the second part of the Middle pleniglacial the climate gradually cooled until the Last Glacial Maximum in the Late Pleniglacial (MIS 2) with prevalence of tundra vegetation or even a lack of vegetation during polar desert conditions (Hijma et al., 2012; Laban & Van der Meer, 2022). Winds transported fine sands from river plains and push-moraines, because of the poor vegetation and were covering the landscape and formed dunes and cover sand ridges (Mathys, 2010; Hijma et al., 2012; Laban & Van der Meer, 2022). These cover sands are part of the

Boxtel Formation and were deposited on the pleniglacial terraces along the VLIZ line (View Fig. 3). In the second part of the Middle Pleniglacial the Rhine river made a major avulsion by changing its flow partly from the Ijssel valley and central Netherlands to the southern Netherlands, merging its flow with the Meuse (Busschers et al., 2007; Peeters et al., 2015; Peeters er al., 2016). Furthermore, the climate became gradually warmer after the Last Glacial Maximum through the Late Glacial into the Holocene (MIS 1).

Holocene (MIS 1)

Estimated age: 11.7 ka - present

From around 9.5 ka onward coastal barriers and barrier islands could form due to sufficient wave working caused by the deepening of the North Sea. Behind these barrier islands salt marshes and tidal flats formed, which are part of the Naaldwijk Formation (Vos & Van Kesteren, 2000; Rijsdijk et al., 2005; Mathys, 2010; TNO-GDN, 2022a). The sea level has risen constantly during the Holocene and therefore, the ground water table has risen as well forming peat bogs across half of the Netherlands. Besides, the earliest deposit dating from the Holocene is the basal peat (Vos & Van Kesteren, 2000; Mathys, 2010; Laban & Van der Meer, 2022). The sea level rise caused the Southern North Sea to deepen which resulted in a gradual increase in the tidal currents. Tidal currents formed elongated tidal ridges on top of the existing seascape relief, while scouring along the sides of the tidal ridges. Since the tidal amplitude is greater in the Southern Bight with respect to the North of the Broad Fourteen basin, more and larger tidal ridges formed in the Southern Bight with respect to the Broad Fourteen basin (Le Bot et al., 2002; Mathys, 2010; Laban & Van der Meer, 2022). After 2.9 ka, the coastal barrier of the eastern southern North Sea coast moved landward, which changed large areas of the peat bogs into salt marshes and tidal flats. This was caused by an increase in river discharge and eroding estuaries, which was the result of climatic changes and possible human activity (Beets & Van der Spek, 2000; Mathys, 2010). Both the Naaldwijk Formation and the Southern Bight Formation can be found along the VLIZ line.

2.2 Geologic setting and stratigraphic units

The North Sea is a semi-enclosed epicontinental sea which is connected to the Baltic Sea trough the Skagerak in the Northeast and to the Atlantic Ocean through the Fair Isle Channel and Norwegian Sea in the North and through the English channel and narrow Strait of Calais (which has a minimum width of 32 km) in the South. The Southern North Sea has a depth of mostly 0-40 m. The seascape and the relevant Pleistocene and Holocene lithostratigraphic units of the Southern North Sea study area are explained below:

Seascape

The seascape or seafloor morphology of the Southern North Sea consist mainly of sands, which are organized in systems of linear sand bank or tidal banks and mobile sand waves or submarine sand dunes. Locally there is gravel, shell and mud deposition and outcrops of early Holocene, Pleistocene and older formations that are eroding and reworked into the Southern Bight and Naaldwijk Formations. Furthermore, channels, swales and glacigenic landforms are part of the Southern North Sea seascape as well (Le Bot et al., 2002; Mathys, 2010; Eaton et al., 2020; Cartelle et al., 2021; Laban & Van der Meer, 2022).

The sand dunes are usually between 2-8 meters high and asymmetrical in shape and move in the dominant residual current direction. However the 10-25 meter high tidal banks are close to stationary over the last 200 years. They are shaped by tidal currents on top of existing submarine relief (e.g. questa's or older tidal ridges). The top part of the tidal banks consists of reworked sediments that are eroded from troughs on the sides (Cameron et al., 1989; Le Bot et al., 2002; Mathys, 2010; Laban & Van der Meer, 2022).

Southern Bight Formation

Code: NUSB
Age: Holocene

The Southern Bight formation consists mainly of shell-rich sands and is deposited in a high-energy marine environment, where sediments are often reworked by waves and tidal currents. (Cameron et al., 1989; Rijsdijk et al., 2005; Stoker et al., 2011; TNO-GDN, 2022b). The Bligh Bank Member (Code: NUSBBL) and the gravelly Buitenbanken Member (Code: NUSBBU) are distinguished in the Southern Bight Formation and are both present in the area around the VLIZ line (Cameron et al. 1989; Rijsdijk et al. 2005; TNO-GDN, 2022c; TNO-GDN, 2022d).

Naaldwijk Formation

Code: NUNA
Age: Holocene

The Naaldwijk Formation comprises all the Holocene coastal plain deposits (Rijsdijk et al., 2005), therefore consisting of sand layers of highly variable grain size with shells and humic silt and clay layers with shells and thin discontinuous peat layers. The Naaldwijk Formation is

locally present around the VLIZ line (Rijsdijk et al., 2005; Missiaen et al., 2021 TNO-GDN, 2022a).

Boxtel Formation

Code: NUBX
Age: Middle Pleistocene – Holocene

The Boxtel Formation is widespread in the southern North Sea, also near the VLIZ line, and consists of periglacial and aeolian sediments and has been deposited in both arid and wet environments, therefore comprising: aeolian cover sands, loess, deflation layers, periglacial lacustrine and small-scale fluvial deposits of streams (including the channels, banks and river basins), deposits of periglacial slopes, alluvial fans, as well as the aeolian deposits from warm periods, such as drifting sand plains and river dunes (Cameron et al., 1989; Rijsdijk et al., 2005; Hijma et al., 2005; TNO-GDN, 2022h). In addition, palaeosols and cryoturbation structures are common in the Boxtel formation. Besides from moderately fine sands, sandy loam, thin peat, gyttja layers and very coarse sands with gravel lags are also sparsely occurring in the Boxtel Formation (TNO-GDN, 2022h).

Kreftenheye Formation

Code: NUKR
Age: late Saalian - Early Holocene

The Kreftenheye Formation comprises fluvial/fluviolacustrine and in some periods a fluvioglacial Late Saalian (MIS 6) to Late Weichselian (MIS 2) deposits from the Rhine river and the lower reaches of the Meuse river. Among which, mainly moderately coarse to very coarse gravelly sand and locally fine to very coarse gravel lags and to a lesser extent silty clay layers and sometimes clayey peat layers. Although the Kreftenheye Formation contains generally very little mollusk remains locally reworked deposits of the Eem Formation do contain significant amounts of shells (TNO-GDN, 2022f). Furthermore, the Kreftenheye Formation is varying greatly in thickness. However, it is mostly about 10 - 25 meters thick in the Southern North Sea area and occurs both on top as well as below the Boxtel and Eem Formations. Figure 4 shows the distribution of the Kreftenheye Formation in the Dutch domain (Cameron et al., 1989; Rijsdijk et al., 2005; Busschers, 2008; TNO-GDN, 2022e). It shows it is also present along large parts of the VLIZ line.

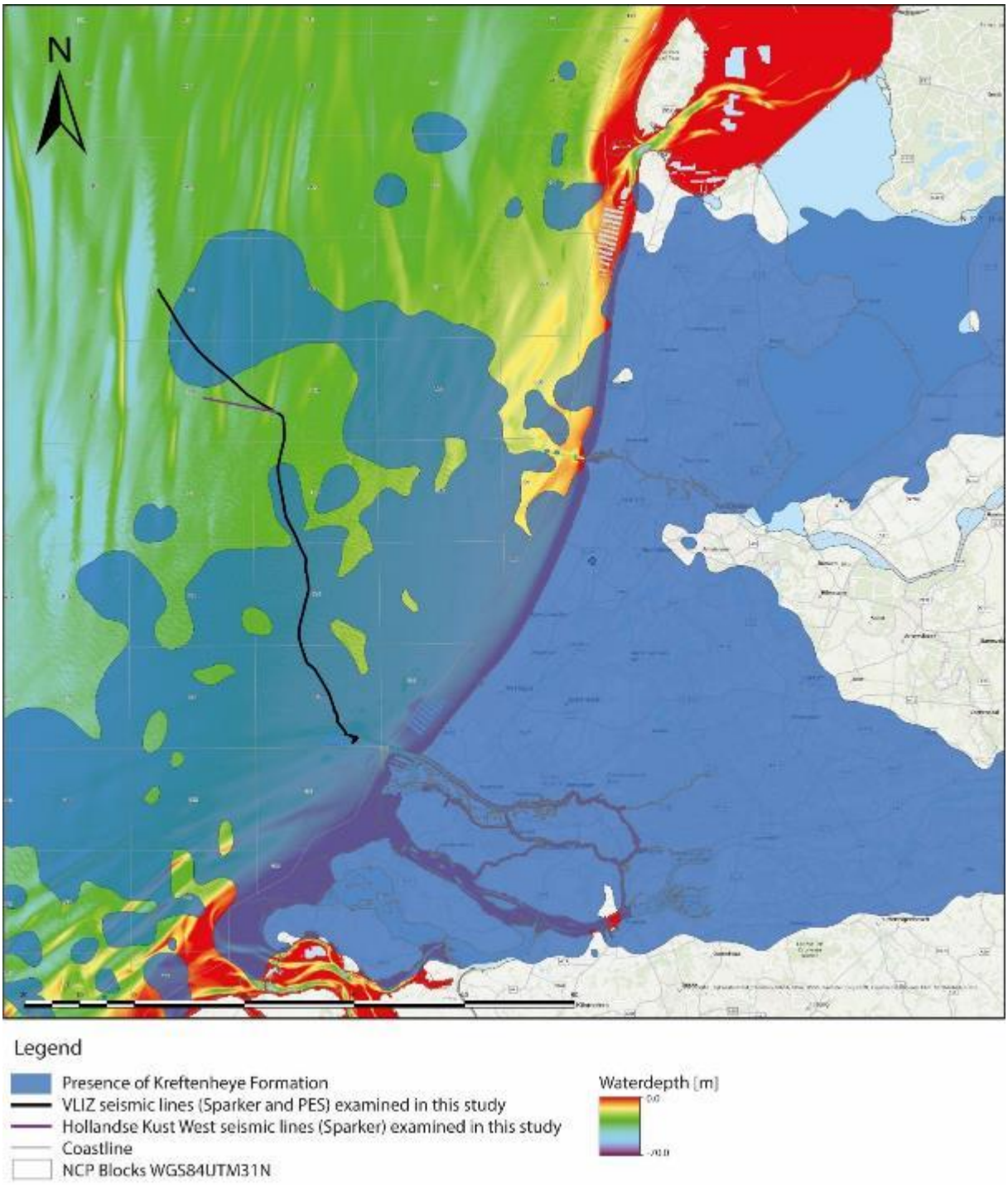

Figure 4: Kreftenheye Formation distribution in the Dutch domain based on presence in sediment core descriptions in the DINOloket database.

Eem Formation

Code: NUEE
Age: Eemian – Early Weichselian

The Eem Formation comprises Eemian coastal and shallow marine, shell rich, often calcareous, sands with clay and silt layers, of which the marine deposits dominate, especially offshore of the Dutch and Flemish coast (Cameron et al., 1989; Rijsdijk et al., 2005; Stoker et al., 2011;

Eaton et al., 2020; TNO-GDN, 2022f). Hijma et al. (2012) mentions the occurrence of local shell-gravel beds. Until recently, the Brown Bank Formation was part of to the Eem Formation when this was viewed as the Brown Bank Member (TNO-GDN, 2022f ; Waajen et al., 2024). The Eem Formation is offshore generally less than 10 meters thick and has an upper contact with the Brown Bank, Boxtel and Kreftenheye Formations. Although the Eem Formation is widely present in the Broad Fourteens Basin and the Southern Bight, the Eem formation is almost absent in the British part of the North Sea (Cameron et al., 1989; TNO-GDN, 2022f).

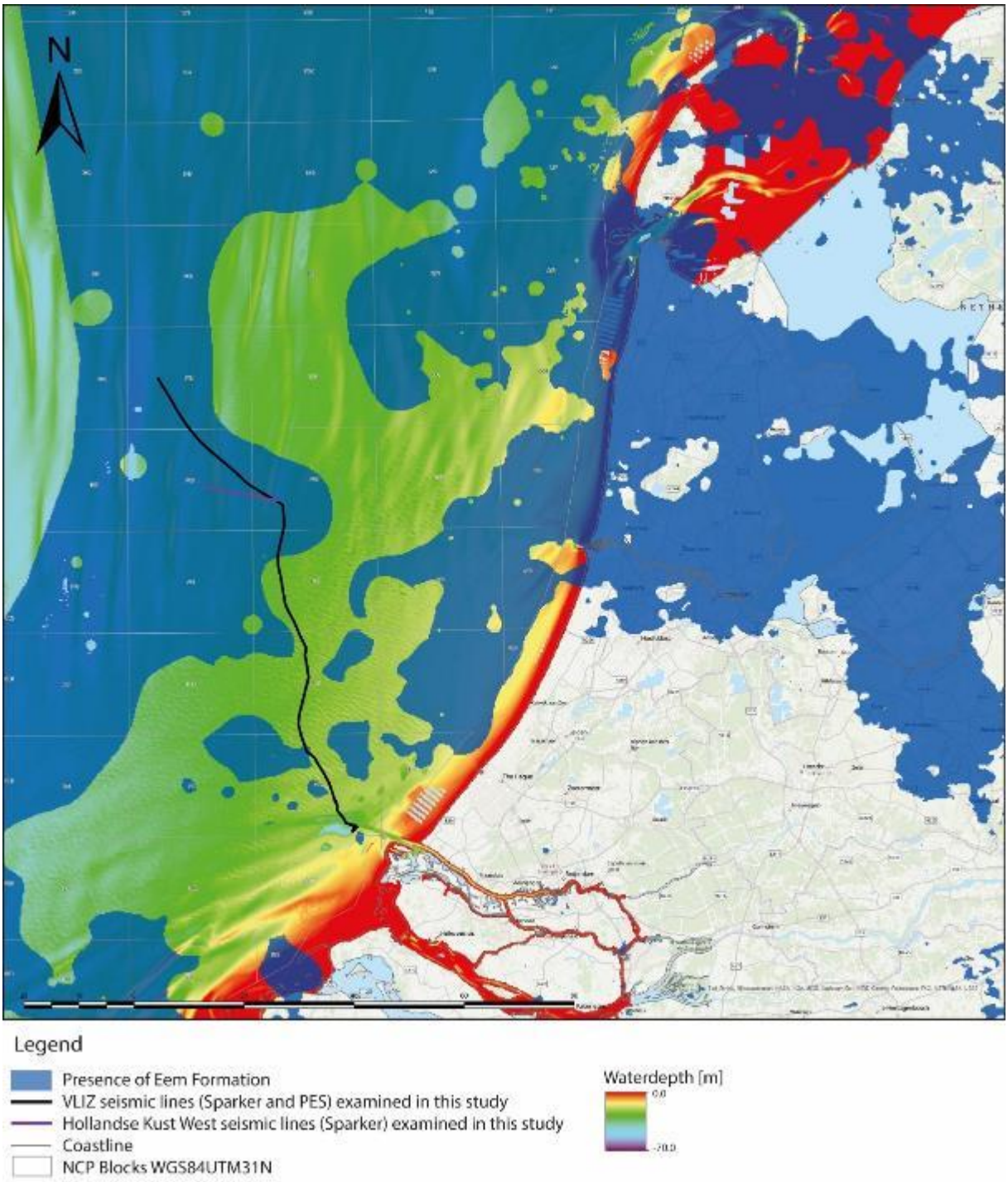

Figure 5 Distribution of the Eem Formation in the Dutch domain based on presence in sediment core descriptions in the DINOloket database.

The distribution of the Eem Formation be viewed in figure 5. It shows the Eem Formation is mainly present along the Northwest of the VLIZ line.

Brown Bank Formation

Code: NUEEBB
Age: Early Weichselian

The Brown bank Formation (formerly known as the Brown Bank Member; Rijsdijk et al., 2005; TNO-GDN, 2022g; Waajen et al., 2024) generally comprises sand, silt and large amounts of clays that are formed in a brackish to marine or lagoonal, estuarine, deltaplain, perhaps even freshwater lacustrine or fluvial, depositional environment (Oele, 1971; Cameron et al.,1992; Eaton et al., 2020; Waajen et al., 2024) Furthermore, the clays are often calcareous and contain layers or lenses of muddy sands and silts. In addition, the clays often contain marine shells or shell layers and are often bioturbated and sometimes cryoturbated or contain dehydration structures or soil horizons and pyrite concretions. Furthermore, local erratic pebbles are found (Cameron et al., 1989; Hijma et al., 2012; Eaton et al., 2020; Missiaen et al., 2021; TNO-GDN, 2022g; Waajen et al., 2024).

The Brown Bank Formation is often subdivided into two or more units, of which the lower unit is often sandier and the upper unit richer in clays which is often linked to a decrease in energy level related to a gradual close off from the sea (Bicket & Tizzard, 2015; Baten, 2019; Eaton et al., 2020; Missiaen et al., 2021; Waajen et al., 2024). The Brown Bank Formation is widespread in the centre of the Southern North Sea and has a more sparse presence closer to coasts. The distribution of the Brown Bank Formation in the Dutch domain can be viewed in Figure 6. Figure 6 shows that the Brown Bank Formation occurs locally along the VLIZ line.

Furthermore, the Brown Bank Formation can be found infilling a series of channels, especially at the British domain (Limpenny et al., 2011; Eaton et al., 2020). Tizzard et al. (2014) mentions the presence of an upper sandier unit of the Brown Bank Formation on top of a lower more clay rich unit within a certain channel, which could represent an increasingly energetic marine influence, contradicting the general environmental change interpretation through the lower and upper unit. Besides, the Brown Bank Formation might locally gradually transition eastwards into the highly energetic fluvial Kreftenheye Formation.

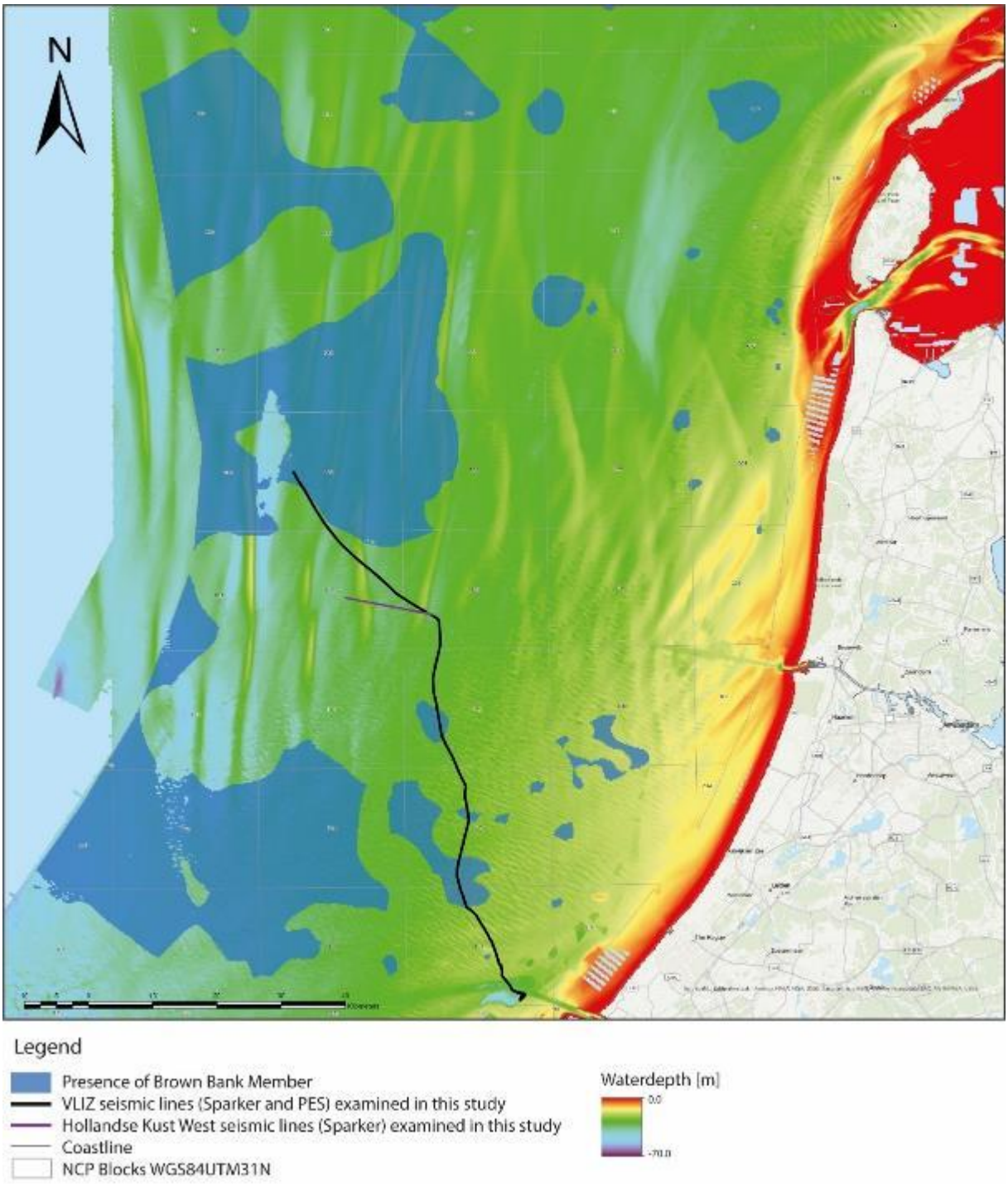

Figure 6: Brown Bank Formation distribution in the Dutch domain based on presence in sediment core descriptions in the DINOloket database.

Egmond Ground Formation

Code: NUEG
Age: Holsteinian (MIS 11)

The Egmond ground formation comprises marine sands (often fine grained) with locally shells and clay layers formed during an interglacial marine incursion. The Egmond ground formation

is up to ten meters thick and occurs locally in the Dutch and British part of the North Sea including along the VLIZ line (Cameron et al., 1989; Rijsdijk et al., 2005; TNO-GDN, 2022i; BGS, 2023a).

Yarmouth Roads Formation

Code: NUYR
Age: Cromerian and older Pleistocene (MIS 62-13)

The Yarmouth Roads formation consists mainly of sand, gravel and clays deposited in open marine, deltaic, delta-top or fluvial sedimentary environments and is widespread in the North Sea (Cameron et al., 1989; Rijsdijk et al., 2005; Stoker et al., 2011; Eaton et al., 2020; TNO-GDN, 2022j; BGS, 2023b). Therefore, the Yarmouth Roads Formation is present along most of the VLIZ line.

3. Reflection Seismology & How to interpret seismic data

Reflection seismology is a geophysical method which uses artificial vibrations or sound waves to visualize the acoustic structure of the subsurface (Schroeder, 2004; Jenny, 2013). A major advantage of reflection seismology is the possibility for large aerial coverage both on land and in the sea where studiable outcropping geology is often minimal.

Sound waves propagate in the subsurface and through water (when shot from a ship) and reflect, refract, split or bend on subsurface structures with an acoustic impedance contrast. These usually occur at the boundaries between lithological bodies with different physical properties (i.e. elasticity, density). The greater the contrast in acoustic impedance, the greater the recorded amplitude of the reflecting wave. In general, the wave speed is higher in bedrock than in unconsolidated sediments. In addition, the wave speed is usually higher in sands than in clay bodies and is even lower in water (Schroeder, 2004; Jenny, 2013).

For the seismic acquisition, use is made of, for example, a seismic source such as a parametric echosounder (PES) or a sparker (Plasma sound source, PSS) and a receiver for which a streamer could be used which is a series of hydrophones connected to a floating cable (Slootweg, 1986; Kluesner et al., 2018; Missiaen et al., 2021). The acquisition equipment of the datasets used in this study together with certain seismic properties are shown in Table 1. After the data is collected, edits or processes can be applied to it to improve the visibility of the geology of interest. This also includes addressing the errors, noise and other artifacts that have arisen from the use of the equipment. Software packages are usually used for editing, processing, displaying and interpreting the seismic data (Jenny, 2013; Kluesner et al., 2018; Hendry et al., 2021).

Table 1: Acquisition equipment and seismic properties of the datatypes examined in this study. Values are determined based on data used in this study.

Seismic datasets	Equipment (seismic acquisition system):	Penetration depth in sea floor	Vertical resolution/ Pulse duration
VLIZ sparker	Plasma sound source (PSS) (Kluesner et al., 2019)	~40 m (deeper strongly influenced by multiple)	~100-150 cm Pulse duration: 2 ms
VLIZ PES	Parametric Echosounder (PES) (Missiaen et al., 2021)	~20 m	~10-15 cm Pulse duration: 0.13 ms
HKW sparker	Fugro Multi level sparker 800 J (Ch. 5.6 in Rijksdienst voor Ondernemend Nederland, 2019)	~60 m	~ 46-53 cm Pulse duration: 1.09 ms

In addition to the amplitude, the Two-way travel time (TWT) is measured which is the duration of the pulse from the source through the media to the recording device (Jenny, 2013). Since the wave speed is varying through the media, the TWT cannot be converted directly to the actual depth. For an accurate time-depth conversion is a time-depth model needed. However, sometimes a simple calculated approximation is sufficient, which is the case for the limited depth range examined in this study. Moreover, since reflection seismology is usually executed

in combination with (sediment) core extraction for providing ground-truthing information, direct depth measurements can be obtained from coring (Rijsdijk et al., 2005). Besides, to correlate a core description stratigraphically with the seismic interpretation, a time-depth conversion is necessary as well.

Since seismic data reflect the geology, reflection configurations (e.g. the shape, thickness, length, presence, absence, termination, expressiveness or the spatial arrangement with respect to other seismic data points or reflections) can be interpreted as stratification patterns or depositional facies (i.e. seismic stratigraphy; Mitchum et al., 1977). However, it must always be taken into account that the seismic data is never a perfect or equal representation of the geology and that the seismic acquisition always involves a certain degree of distortion or noise or the presence of artifacts in the seismic data display (Mitchum et al., 1977; Hendry et al., 2021). Figure 7 summarizes the common reflection configurations and geometries found in sedimentary units rich in sands and clays (as prevails in the Southern North Sea area), as a guide to seismic interpretation following Mitchum et al. (1977), Mellet et al. (2013) and Eaton et al. (2020).

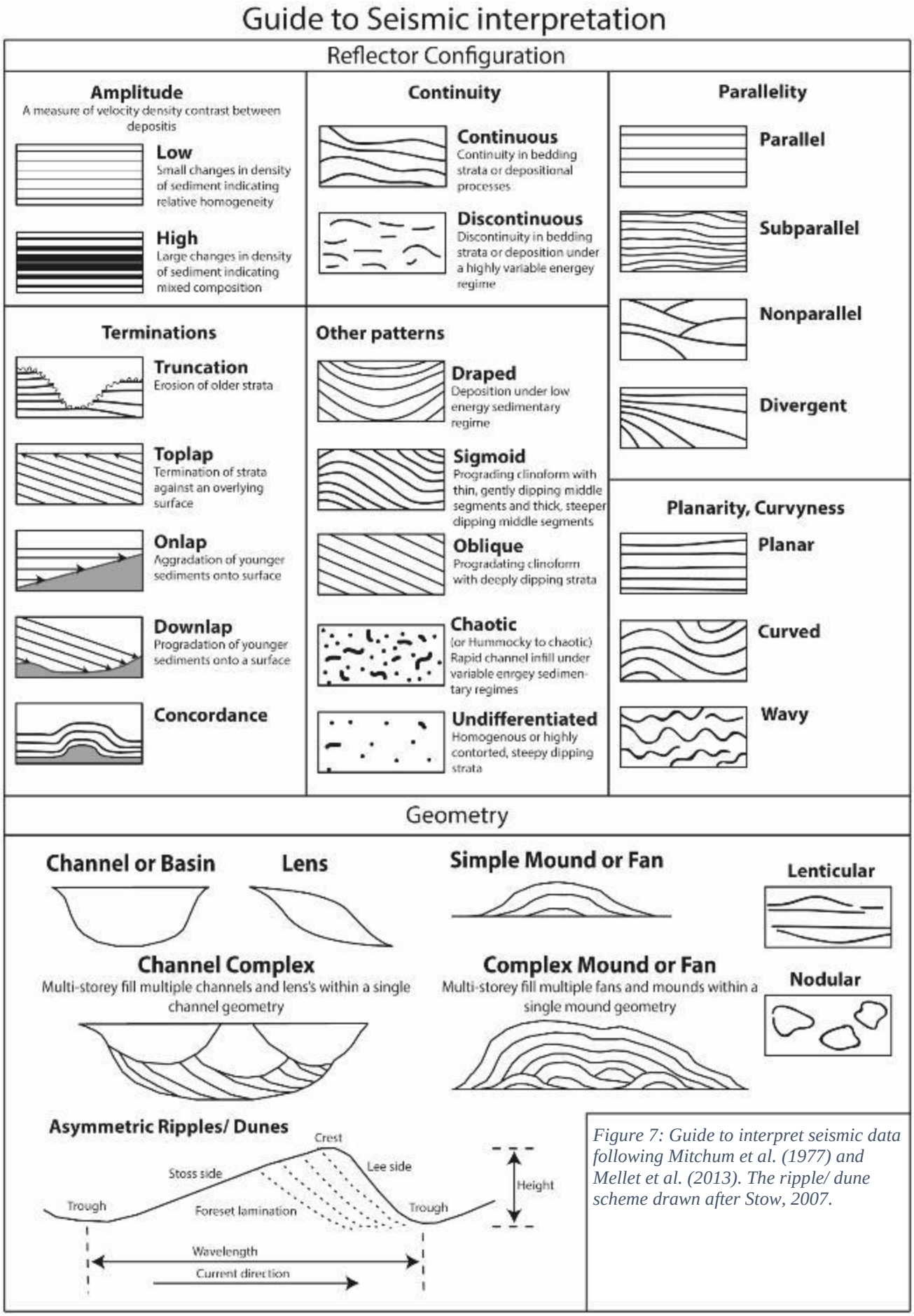

Figure 7: Guide to interpret seismic data following Mitchum et al. (1977) and Mellet et al. (2013). The ripple/ dune scheme drawn after Stow, 2007.

4. Methods, Data & Software

The method consisted of interpreting the seismic data seismostratigraphically (View Fig. 8 for the location of the seismic lines examined in this study), using suitable software packages (Petrel and Delph from respectively Schlumberger and IXBlue, were used with the donated licenses. The choice of these software packages is further explained under the heading 'Used Software').

First, the PES and sparker data of the seismic line were viewed in its entirety and compared with each other and stratigraphically interpreted in little detail. A detailed description of the seismic interpretation process can be found under the heading 'Method of seismic interpretation'. This was followed by a second round of seismic interpretation, in which adjustments and additions were made and in which more attention was paid to the most interesting parts.

The distinction between different layers and units was often better visible in the PES data with respect to the sparker data, which is due to the higher resolution of the PES data. This was especially the case for the parts that contained the specific characteristics of the Brown Bank Member, which were of main interest. Therefore, the PES data were usually interpreted in much more detail than the sparker data. Furthermore, the parts of the PES data that contained the seismic characteristics of the Brown Bank Member or where they suddenly disappeared, were often interpreted in more detail with respect to the parts that lacked the seismofacies of the Brown Bank Member over relatively long distances.

Once the stratigraphy was identified sufficiently, the interpretation was compared with available sediment core data from around the seismic line (view Table 2), that were converted to depth-in-time, which allows for attempts to correlate the sediment core data with the seismic interpretation. For the time-depth conversion, a seismic speed of 1800 m/s was assumed, which was decided based on previous work. This is a constant and average value, which is not a completely correct or realistic assumption. Because it concerns a small number of cores and relatively short cores, this methodology is sufficient to plot information from cores on the seismic profiles, where this model is sufficient to link, identify or validate stratigraphic units and layer transitions with specific reflections with an assumed small margin of error in the vertical scale. This study is not suitable for the development of a detailed velocity model.

Only a handful of data descriptions of the surrounding sediment cores were useful for correlation with the interpreted seismic lines. This was mainly because, sediment cores that were close to 100 meters from the seismic lines were usually already at too great a distance to be of value for stratigraphic correlation. This is because, at this distance significant lithological and stratigraphic differences can already arise due to the typical architectural elements that occur in this area. In addition, many of the sediment core descriptions of relatively close locations, lacked stratigraphic identification.

Furthermore, the PES and sparker interpretations were compared with sparker data from a seismic line of the Hollandse Kust West windfarm construction project (view Fig. 8) (HKW, Rijksdienst voor Ondernemend Nederland, 2019), which was locally parallel to the VLIZ line. These sparker data from HKW have also been interpreted seismostratigraphically in this study.

The results of the seismic interpretation consist of a number of screenshots together with the clean data (view Fig. 13-21) and a map with the location of the shown data segments (view Fig. 12, a diagram with the different units and their seismic facies (view Fig. 10), a schematic cross section of the VLIZ line (view Fig. 22) and a stratigraphic diagram (view Fig. 23).

The seismic data

June 10-11th 2021, seismic data was collected, which we refer to as the VLIZ line (view Fig. 8), during a scientific campaign with the RV Simon Stevin (2021/470). The VLIZ line has a length of about 100 km. Seismics were shot with both a plasma sound source (sparker) and a parametric echosounder (PES) setup. To keep the seismic data workable the sparker data was split into 13 section of each about 7 to 8 km long and the PES data was split into 8 sections of about 12.5 km. The split-up sparker and PES data segments were supplied to the Geological Survey of the Netherlands, part of TNO. The geophysical report and data from the HKW windfarm construction project (Rijksdienst voor Ondernemend Nederland, 2019) are openly available and could therefore be used in this study. Two processed sparker files of the HKW project were chosen to be used to compare with the VLIZ data, on account of their close location and similar orientation. All used data files of the seismic segments, including the PES and sparker segments of the VLIZ line and two processed sparker segments of the HKW project are shown in table 2. Although a selection of interpreted seismic data is discussed in Ch. 5.2 (Figures 13-21), the remaining data are included for Ch. 5.1 and Ch. 6 and for the Figures 22 and 23. Furthermore, all available seismic data from TNO from the surroundings of the VLIZ seismic line are shown in figure 8, to provide context about where other data has been collected. These other data are not used further in this study.

Table 2: The used seismic segments.

Used seismic data segments:	File names:	Example figures added and discussed:
PES 1	TNO1_P1_pes.sgy	
PES 2	TNO2_P1_pes.sgy	Fig. 21
PES 3	TNO3_P1_pes.sgy	
PES 4	TNO4_P1_pes.sgy	
PES 5	TNO5_P1_pes.sgy	Fig. 19
PES 6	TNO6_P1_pes.sgy	Fig. 18
PES 7	TNO7_P1_pes.sgy	Fig. 14
PES 8	TNO8_P1_pes.sgy	Fig. 13
Sparker 1	TNO1_P1_sp_PRC.sgy	
Sparker 2	TNO2_P1_sp_PRC.sgy	
Sparker 3	TNO3_P1_sp_PRC.sgy	
Sparker 4	TNO4_P1_sp_PRC.sgy	
Sparker 5	TNO5_P1_sp_PRC.sgy	Fig. 20
Sparker 6	TNO6_P1_sp_PRC.sgy	
Sparker 7	TNO7_P1_sp_PRC.sgy	
Sparker 8	TNO8_P1_sp_PRC.sgy	
Sparker 9	TNO9_P1_sp_PRC.sgy	
Sparker 10	TNO10_P1_sp_PRC.sgy	Fig. 17

Sparker 11	TNO11_P1_sp_PRC.sgy	Fig. 15
Sparker 12	TNO12_P1_sp_PRC.sgy	
Sparker 13	TNO13_P1_sp_PRC.sgy	
HKW 423	seq423_2X580e_NoMig_Depth_Processed_Stack.segy	Fig. 16
HKW 437	seq437_2X580infb_Mig_Depth_Processed_Stack.segy	

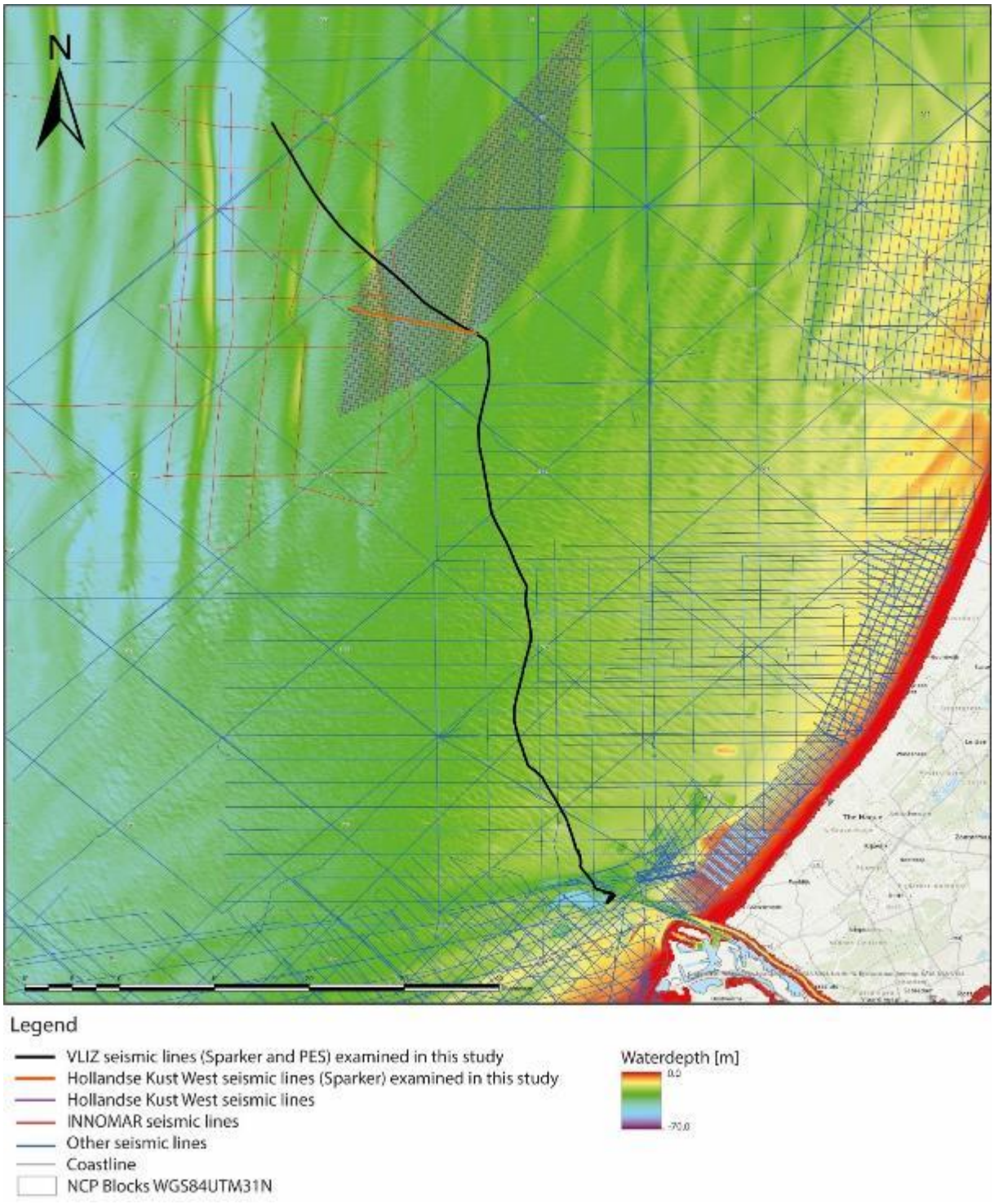

Figure 8: The location of the VLIZ Seismic line and the HKW seismic line together with all other seismic traces done in the area. The scale bar shows 50 km.

Sediment core data

Large numbers of borehole and core descriptions can be found in the TNO archives. This data is largely accessible, allowing sediment core data to be used in this study and compared to the seismic interpretations to ensure a more accurate stratigraphy. All coring locations of sediment core data from the surroundings of the VLIZ seismic line (excluding surface sample cores) are shown in figure 9. A selection of these data were viewed and processed in the Petrel system folder and are shown in Table 2. All cores of Table 2 are taken within 0 – 5 km from the VLIZ seismic line except for the core names that start with BP05, which are 0 – 10 km from the VLIZ seismic line.

Although the data from all of the cores shown in Table 2 have been added to the Petrel System Folder, only a small number of them proved useful to correlate or compare with the seismic interpretation. Because, most of those were not close enough to the VLIZ line, did not penetrate deeply enough or did not have the stratigraphic data. Also some cores could not be projected to the correct location. Furthermore, much attention has been paid for projecting the cores to the correct location as much as possible, by manually adjusting the azimuth.

Sediments from at least three of the cores shown in Table 2 were available in the TNO archives and therefore viewed (BP050004, BP050008 & BP120092) and also to take a closer look at the sediments of the formations in question.

Table 2: The viewed sediment core data.

Well name	Latitude (WGS84 UTM31N):	Longitude (WGS84 UTM31N):	Core pene-tration detph	Water depth	Total vertical depth	Strati-graphic data present	lithologic data present	Sediments from this core were examined
BP050004	528033	5844455	47.5	-29.87	77.37	X	X	X
BP050005	523536	5842163	1.5	-40.93	42.43	X	X	
BP050008	531646	5851060	48.5	-29.85	78.35	X	X	X
BP080004	532673	5834905	3	-29.1	32.1	X	X	
BP080031	543908	5825740	40	-33.5	73.5		X	
BP080047	541876	5823222	19.9	-35	54.9		X	
BP090014	550664	5821122	43.46	-28.88	72.34	X	X	
BP090055	550263	5822762	93	-29.2	122.2	X	X	
BP090080	546408	5824258	1.2	-25	26.2		X	
BP120018	547361	5802362	10	-26.25	36.25	X	X	
BP120019	547388	5807267	10	-24.78	34.78	X	X	
BP120020	547354	5812265	10	-28.92	38.92	X	X	
BP120021	554928	5799766	10	-29.95	39.95	X	X	
BP120041	551624	5806529	81	-24.44	105.44	X	X	X
BP120092	552374	5812384	12	-27.81	39.81	X	X	
BP120093	549900	5809544	12	-28.22	40.22	X	X	
BP120094	552589	5807440	12	-27.71	39.71	X	X	
BP120095	551188	5803174	12	-29.25	41.25	X	X	
BP120096	549931	5798295	12	-26.42	38.42	X	X	
BP150150	552828	5781415	3.9	-29.06	32.96	X	X	
BP150177	554601	5783576	12	-27.69	39.69	X	X	

BP150181	553201	5793290	12	-23.24	35.24	X	X	
BP150227	553557	5781308	7.6	-26.64	34.24	X	X	
BP150229	555264	5790833	16	-27.33	43.33	X	X	
BP150231	554809	5795506	23	-26.89	49.89	X	X	
BP180299	560400	5765748	3.55	-22.87	26.42	X	X	
BP180302	563957	5762699	3.55	-22.98	26.53	X	X	
BP180424	555010	5776693	10	-26.19	36.19	X	X	
BP180508	558558	5771917	25.15	-25.46	50.61	X	X	
BP180526	560536	5765993	21	-23.37	44.37	X	X	
BP180531	561879	5764230	22	-30.61	52.61	X	X	
BP180532	562475	5763046	22	-22.02	44.02	X	X	
BP180533	564273	5762638	22	-21.77	43.77	X	X	
BP180551	559674	5767997	19.5	-22.78	42.28	X	X	
BP180625	560492	5766802	20.5	-23.67	44.17	X	X	
BP180639	562335	5763670	21	-24.62	45.62	X	X	
BP180640	563353	5762504	23	-21.78	44.78	X	X	
BP180649	556541	5775367	25	-24.92	49.92	X	X	
BP180696	563415	5763016	4	-28.8	32.8		X	
BP180697	563407	5762999	4.25	-29	33.25		X	
BP180698	563552	5762983	4.3	-29	33.3		X	
BP180699	563545	5762965	4.9	-29.5	34.4		X	
BP180700	563655	5762943	4.25	-26.6	30.85		X	
BP180701	563643	5762915	4.35	-27	31.35		X	
BP180703	563790	5762953	4.55	-24.04	28.59		X	
BP180707	563776	5762928	4.35	-25.07	29.42		X	
BP180708	563752	5762886	4.8	-27.42	32.22		X	
BP180711	563721	5762834	3.85	-30.72	34.57		X	
BP180712	563716	5762824	4.4	-32.79	37.19		X	
BP180713	563693	5762781	4.55	-34.73	39.28		X	
BP180714	563672	5762748	4.05	-36.39	40.44		X	
BP180715	563661	5762730	4.35	-38.29	42.64		X	
BP180720	563615	5762648	4.9	-42.03	46.93		X	
BP180722	563896	5762863	4.45	-23.3	27.75		X	
BP180723	563882	5762827	4.8	-23	27.8		X	
BP180724	563681	5762938	4.85	-26.4	31.25		X	
BP180725	563718	5762925	4.8	-26.2	31		X	
BP180726	563814	5762893	4.8	-24	28.8		X	
BP180727	563850	5762881	4.85	-23.6	28.45		X	
BP180728	563861	5762658	3.65	-22	25.65		X	

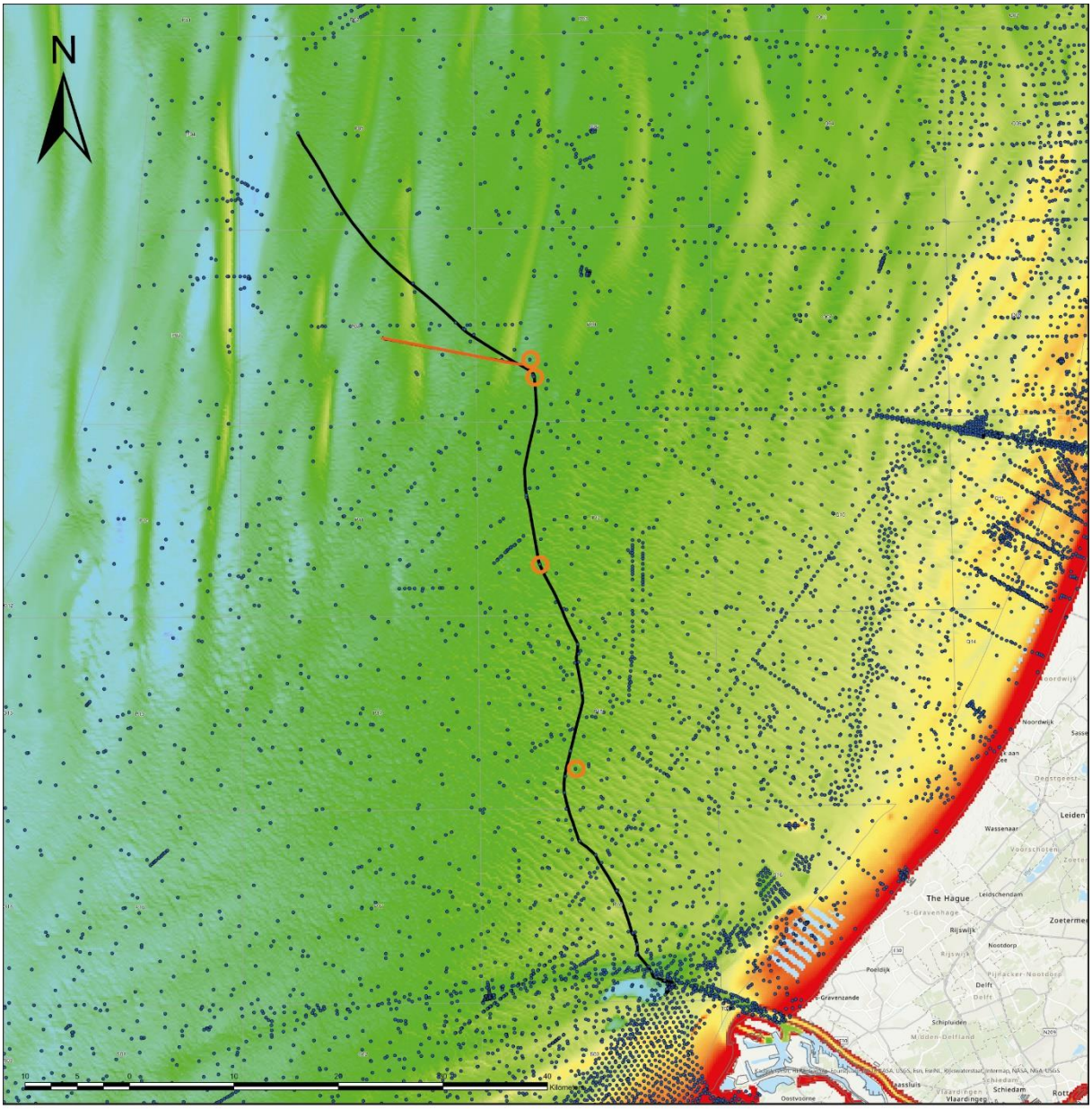

Figure 9: The location of the VLIZ Seismic line and the HKW Seismic line together with all locations where sediment cores have been extracted. The scale bar shows 50 km.

Used software

Since optimal visualization of the seismic data is of major importance, it was decided to use the software packages Petrel and Delph (from respectively Schlumberger and IXBlue) on account of their different benefits. The Delph software was used to execute a number of processing steps

on the sparker data, after which the processed sparker data were interpreted with the Petrel software. The interpretation was mainly done with the help of the Petrel software because it turned out to be more effective, despite the fact that the Delph software had a number of other useful features and that it was able to display the data relatively clearly. However, since the interpretations had started earlier using the Petrel software, the author had become more adept with this program. Besides, multiple seismic horizons had already been identified using the Petrel software, however, many of which could not be properly transferred to the Delph program. This was due to the fact that the maximum number of seismic horizons to be declared, using the Delph software (which was the most recent version at the time), was limited to 18. This would require changing the approach for the seismic interpretation. Furthermore, the Delph software seemed to function too slowly with the entire seismic dataset, however, this was remedied by cutting the dataset into smaller sections of ~3 km when viewing them. All things considered, it seemed more efficient to continue working with the Petrel software, therefore it was decided to continue with the Petrel software for the remaining steps of the seismic interpretation.

Method of seismic interpretation

In order to recognize the reflections of stratigraphic or sedimentary structures as well as possible, the display settings have been adjusted regularly. By changing the color scale or further increasing or decreasing the vertical scale and/ or the horizontal scale of exaggeration, the contrast and the lateral-traceability of certain reflections could be increased.

The seismic interpretation of the VLIZ line was executed in two phases. The first phase of which consisted of interpreting the entire VLIZ line in little detail, from the Northwest to the Southeast and was functioning as an exploration of all the PES and sparker data. Thereafter, the second phase of interpretation followed. Which consisted of improving or refining the interpretations made of the entire line of which significantly more time was spent on the parts that were more interesting for this study.

The seismic interpretation followed the procedure described in Ch. 3. Therefore, first an attempt was made to distinguish between units with different seismic facies. Since it was assumed that certain reflections would represent the top or bottom horizons of certain units (e.g. sand dune complex and brown bank member), an attempt was made to define these boundaries to be traced laterally. The reflections of these identified horizons are accentuated with colored lines. When plotting horizons, attention was paid, to sudden ends of seismic reflections because these often show erosive patterns.

For each data segment (view table 2), work was largely done from left to right and from top to bottom. Furthermore, there has been frequent comparison between the PES and sparker data of the same part of the route. In addition, attention was paid to the location and surrounding topography of the data image to be interpreted at that moment.

After the seismostratigraphy was predominantly identified, the interpretation underwent comparison with the available data of sediment cores from around the VLIZ and HKW seismic lines that penetrated deeply enough, were nearby enough and possessed lithostratigraphic data, which was only the case for a small number of sediment cores. When the seismostratigraphic

interpretation was deviating, it was sometimes decided to adjust the interpretation. This was determined on a case-by-case basis.

5. Results & interpretations

5.1 Facies description

Across all the examined data segments, seven seismic facies units are identified (from top to bottom: Unit A, B, C, D, E, F & G). Although the facies are varying slightly within the seismic units, general facies can be distinguished. Furthermore, similar facies can be recognized between identified seismic units from different seismic data (PES, sparker and HKW-sparker), despite the visual differences between the data types. A description is given of each of the seismic facies units. Furthermore, screenshots of the facies of each of the units are shown in Figure 10 in each of the data types where the units are identified.

Unit A is distinguished from the other units by the fact that it is positioned almost everywhere at the top of the seismic stratigraphy and forms the seabed with characteristic asymmetric dunes. In addition, unit A in the PES data can be recognized by a seismic facies of discontinuous or short-term continuing non-parallel reflections with relatively high amplitudes. The majority contains a chaotic reflection pattern, of which, a significant portion also exhibits oblique reflection patterns, representing the foresets of the dunes. The base of unit A is often characterized by a horizon of high amplitude continuous reflections.

In the sparker data, including those from HKW, the facies of unit A is more chaotic, but the oblique reflection configurations of the foresets can be recognized locally. The dune-shaped surface can also be recognized in these data. A major difference between the seismic facies of unit A in the sparker data of the VLIZ line and those from HKW is that sparker data from VLIZ show high amplitude reflections and the reflections from unit A in HKW show relatively low amplitudes and a facies tending towards acoustic transparency.

Since unit A is located at the top of the stratigraphy it is affected in both the sparker data and the PES data with an artifact of very strong amplitudes and an enhanced seabed reflection, both are caused by a large amount of acoustic energy that is still available at and just below the seafloor. A second artifact that unit A is subject to and that affects the underlying units is the pull-up effect. Which can be seen in the PES data. This can be recognized by a lowered base of unit A beneath the troughs between the sand dunes and a raised base (pull-up) beneath the crests of the sand dunes. This is caused by the acoustic signal moving more slowly through the water column than in the sands and therefore, reaching the base of unit A sooner under the sand dunes than under the troughs.

Unit B can be recognized by the often discontinuous reflections and the chaotic reflection pattern with often relatively high amplitude reflections. Locally, unit B also has shortly continuing oblique reflections and mound and channel or basin geometries. Unit B was only identified in the PES data in some small areas. The unit is distinguished from units A and C in that it is located below the basal horizon of A and usually also forms a clear boundary horizon with unit C. Where this basal horizon could not be recognized as a strong reflection, unit B was distinguishable from unit C on the basis of facies, due to the higher amplitudes, despite the fact

that unit C is often showing a chaotic facies as well. The fact that the unit was not identified in the sparker data may be due to the fact that the unit is sparse and often relatively thin and the facies is sometimes similar to units A and C, which may have caused the unit to be indistinguishable in the sparker data or often overlooked.

Unit C is distinguishable from the other units by mostly acoustically transparent or chaotic facies with mostly low amplitude discontinuous reflections. In addition, unit C is positioned below the contrasting unit A and locally below B and above the contrasting unit D and where unit D is missing, a clear horizon is dividing unit C from the similar, often acoustically transparent unit E. Furthermore, the facies of unit C in the PES data locally exhibits partly continuous subparallel and oblique reflections and channel geometries. The characteristic facies of unit C is also reflected in the sparker data. Parabolas can also be recognized in the HKW sparker data (View Fig. 10, C4).

Unit D consists of the seismic stratigraphic unit that often exhibits the seismic characteristics of the Brown Bank Formation described by Cameron et al. (1989), Eaton et al. (2020) and Waajen et al. (2024). Therefore, unit D can be recognized in the PES data by the relatively high amplitude subparallel continuous subhorizontal reflectors, with locally a more chaotic reflection pattern or with wavy or oblique reflection patterns and fairly acoustically transparent patches, layers or lenses, which can be seen at the bottom of screenshot D2 of Fig. 10.

At the bottom of screenshot D1 of Fig. 10 it can be seen that subparallel oblique reflection configurations also occur, however, subhorizontal reflections predominate. Furthermore, unit D also often shows draping patterns, which is not clearly visible in Fig. 10. The top and bottom of unit D can often be well distinguished by prominent reflections, which are caused by the fact that unit D is strongly contrasting with the fairly acoustically transparent upper and lower units C and E. In the VLIZ sparker data and HKW sparker data, unit D has a similar facies with relatively high amplitude subparallel continuous reflections and local lenses with a facies tending towards acoustically transparency.

Although units C and E often consist of fairly acoustically transparent and chaotic facies in the PES data, unit E does have a more diverse facies with respect to unit C. Because, unit E consists of horizontal subparallel continuous reflections as well as discontinuous chaotic and oblique reflections. However, unit E often has an acoustically transparent facies in the PES data, which is due to the fact that significant acoustic energy loss has already occurred at this seismic depth during the PES data acquisition. In the sparker data, unit E consist of relatively low amplitudes and often discontinuous chaotic or short continuous oblique reflections between the relatively high amplitude reflection facies of Unit D and F. In the HKW sparker data the facies of unit E is similar to the other sparker data, however, it contains diffraction parabola and hyperbola structures (both positive and negative parabolas) as shown in screenshot E4 of Fig. 10.

Unit F can be recognized by relatively high amplitude reflections, often chaotic or noncontinuous reflections or continuous, sub-parallel reflections of which, in addition to horizontal reflections (View Fig. 10, F1) also oblique reflections occur (View Fig. 10, F2) in the HKW sparker data. Furthermore, unit F can be seen as sequences with varying facies between internal horizons, in the HKW data.

Initially unit F was only distinguished in the sparker data, including the HKW sparker, because unit F was thought to be at too great a depth to be included in the PES data, the same holds for

Unit G. However, later unit E in a PES data image was redefined as unit F, because the occurrence of deposits of the Yarmouth Roads Formation was identified at this place according to the description of core BP120095. However, this redefinition is disputable, because facies characteristics were not decisive here. Furthermore, this redefinition happened too late to update Figure 10 with a PES data image of unit F. Although, this single occurrence may not be suitable to show the characteristic appearance, as was intended with the other units.

Unit G is only distinguished in the HKW sparker as the unit below a horizon with a very high amplitude reflection, below which, subparallel discontinuous reflections with low amplitudes are alternating with medium-high amplitude continuous reflections.

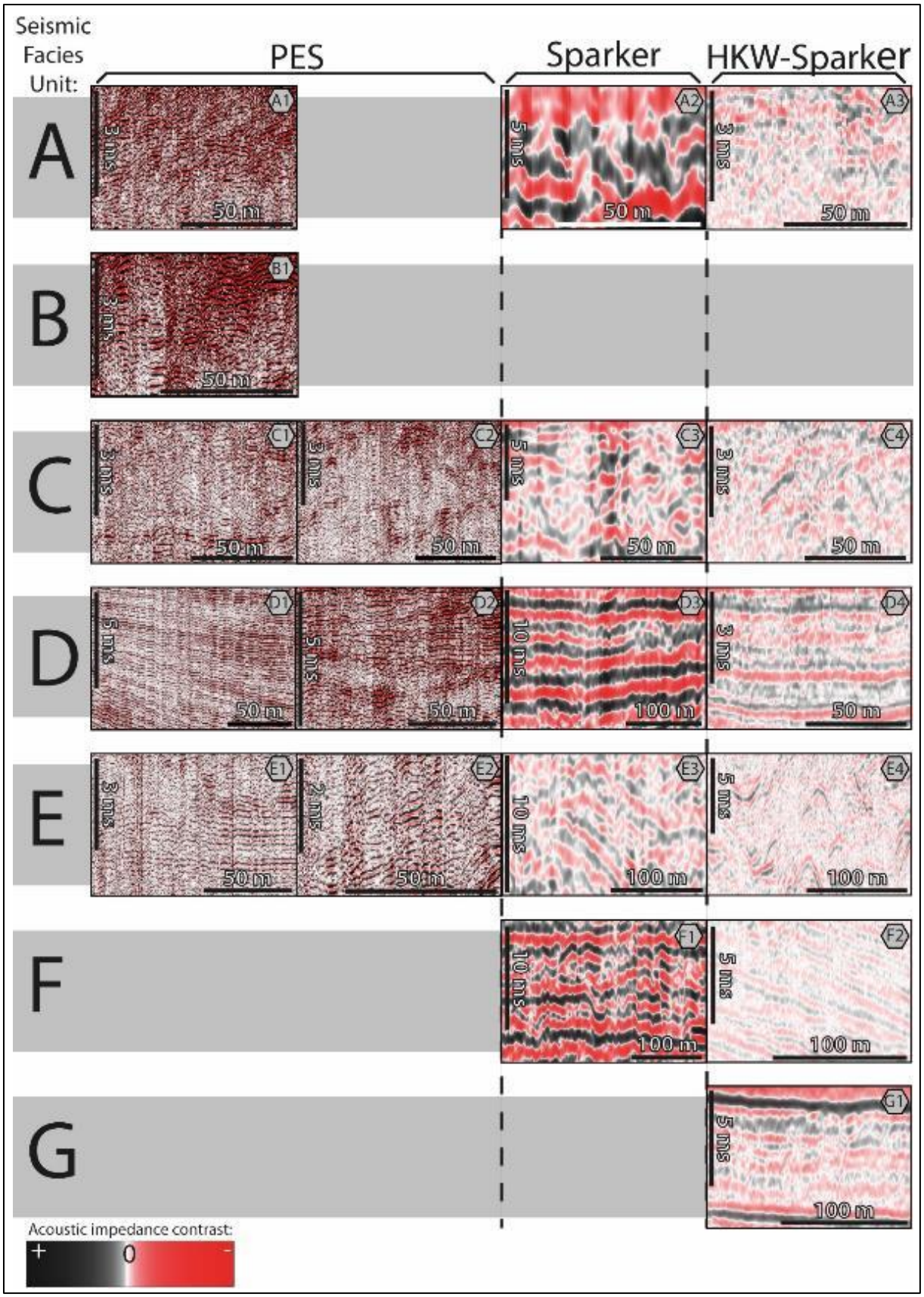

Figure 10: Seismic facies of identified seismic units: A-G across seismic data types (PES, VLIZ-Sparker, HKW-Sparker). Note that the vertical and horizontal scales vary.

5.2 Seismic interpretations

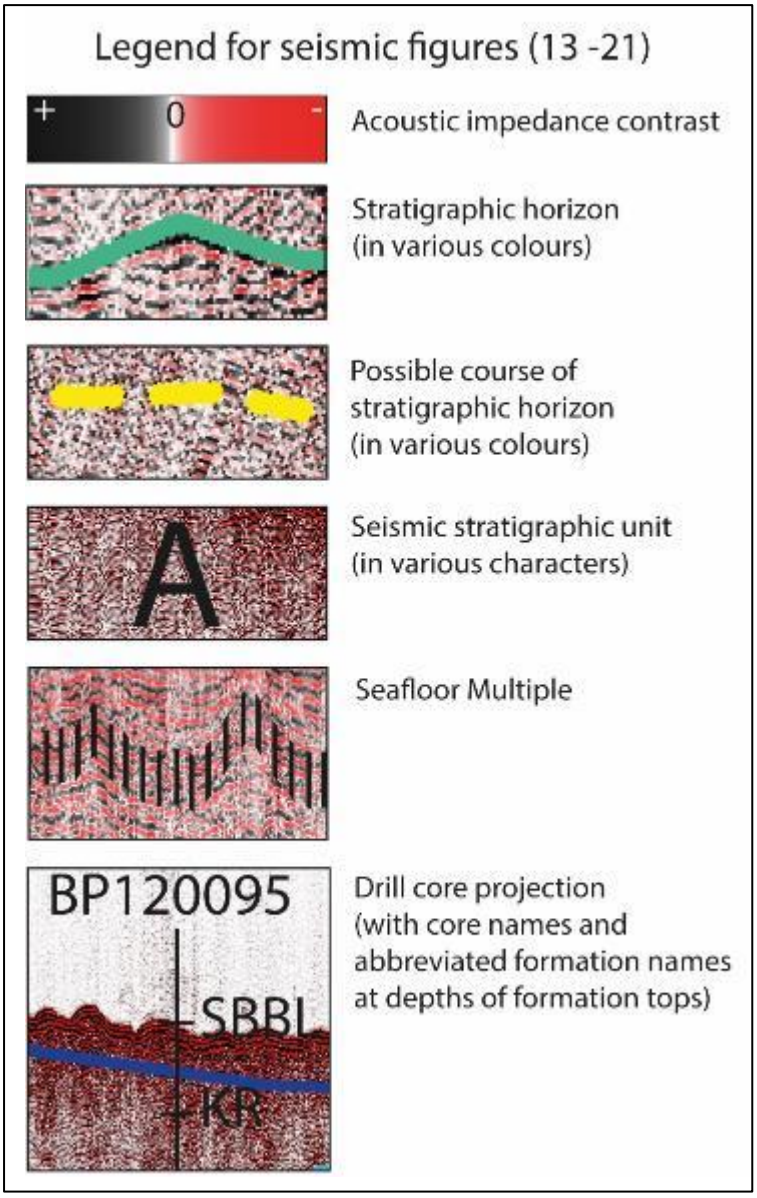

Figure 11: Legend for seismic figures (13-21).

In this section nine key figures (Fig. 13 – 21) of interpreted seismic data (both PES and sparker data) are presented together with their descriptions, all followed by an initial interpretation. It concerns both characteristic examples of the seismic stratigraphy and more deviating, but significant images of seismic profiles. Note that these seismic profiles can be visualized better with the use of the software then in screenshot images as published in this report. Furthermore, note that the scale varies per figure and the horizontal and vertical scales differ greatly.

The interpretations of the entire VLIZ line and the HKW lines can be viewed in the Petrel system folder (Appendix 2). The locations of the presented sections of figures 13 – 21 as well as the projected sediment cores are shown in Figure 12. Figure 11 provides a legend with explanations to the colours, lines and the recurring symbols of figures 13 – 21.

The nine key figures (Fig. 13 – 21), equal to all other seismic stratigraphy (Table 1), have been interpreted and subdivided into seismic facies units (Unit A, B, C, D, E, F & G), which were introduced in Ch. 5.1. However, it was sometimes not possible to link certain seismic facies to a single facies unit. A more accurate identification was sometimes not done due to lower seismic resolution (difference between PES and sparker) or because possible boundary horizons were missing. Therefore, when several units could not be distinguished from each other, they were combined. For example, units A, B, and C are sometimes merged into A-C. In addition, sometimes units are subdivided. However, subunits with the same name in different figures are then not necessary the same subunit. For example, subunits are indicated in several figures with D_1 and these cannot be directly correlated to each other. Nevertheless, both are part of seismo-stratigraphic unit D.

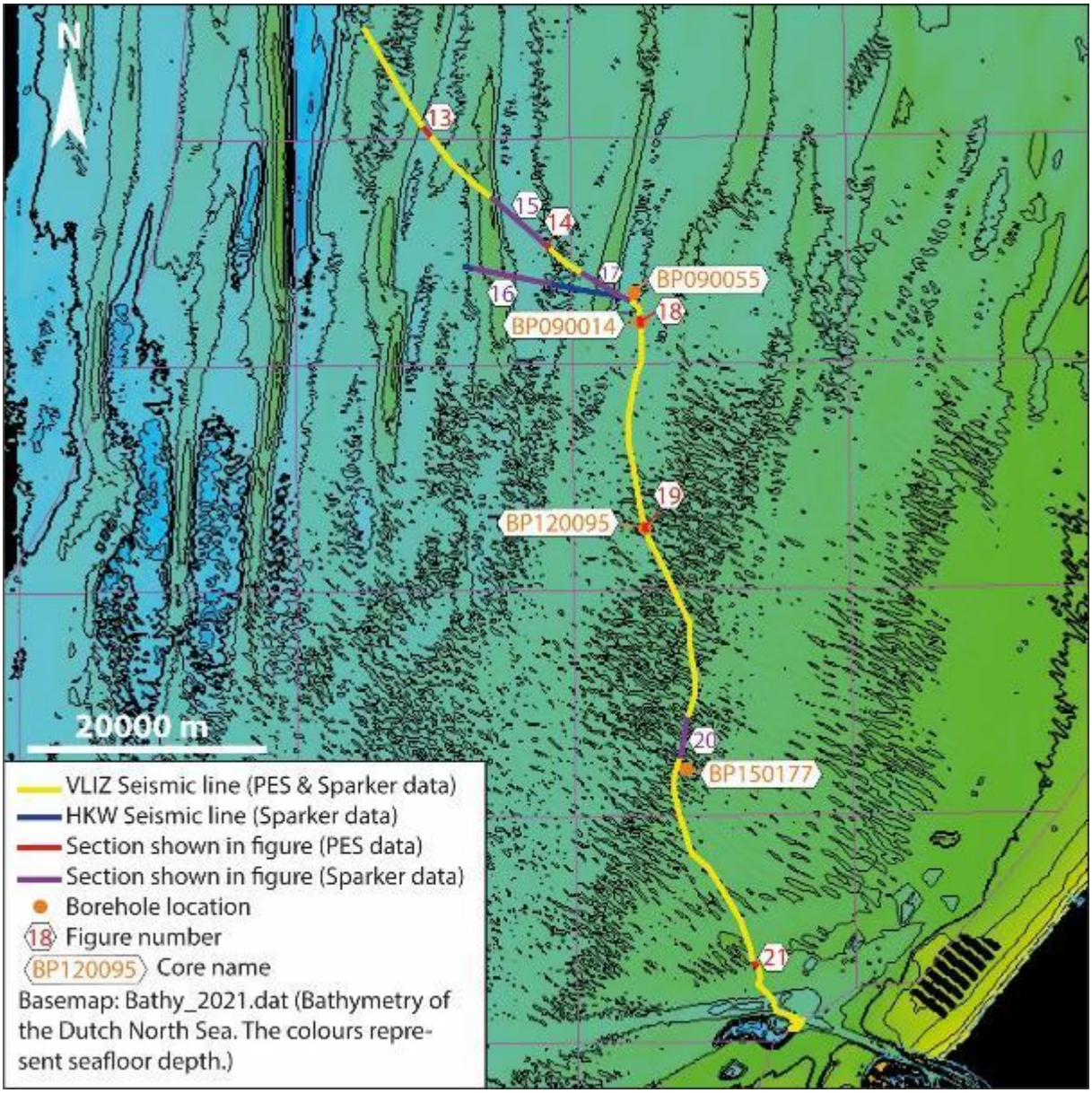

Figure 12: Overview map of seismic figures and projected sediment cores shown in this report, with respect to the seismic lines.

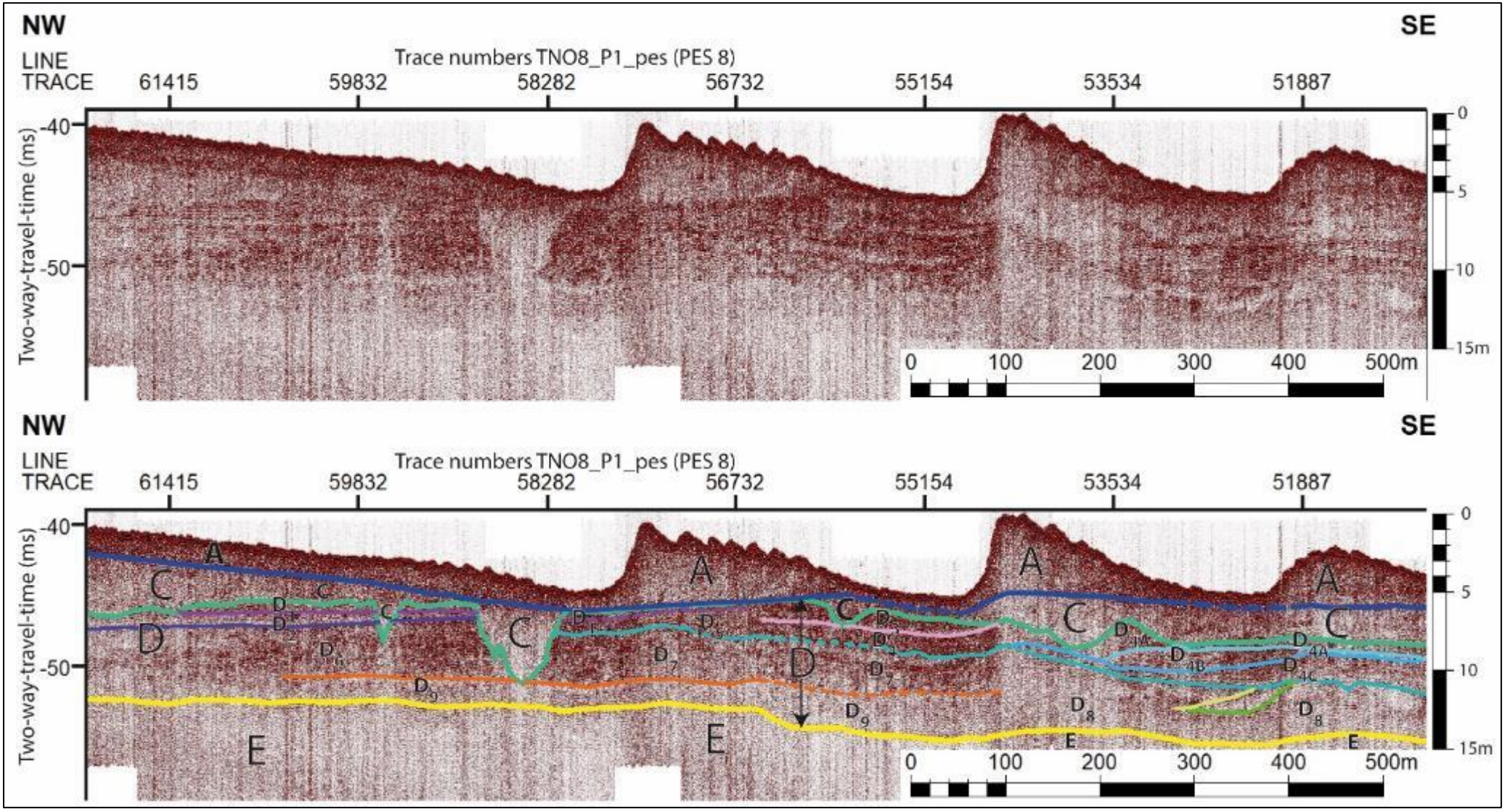

Figure 13: PES seismic data from segment TNO8_P1_PES. Approximately 15 meters below the seabed are shown over a horizontal distance of approximately 1.5 km. Top panel: clean seismic data. Lower panel: interpretation. View fig. 12 for the location of shown section.

Description figure 13

The seismic data of figure 13 are divided into four units (A, C, D and E). These are bounded by 3 horizons (Dark blue, green and yellow). The characteristics of each of the seismic units and boundary horizons, which served as the main reason for this layout, are written below. In addition, seismic artifacts are discussed.

Due to the strong relief of the sea floor some distortion and amplitude-variation artifacts can be seen in Figure 13. Beneath the crests of the mega ripple structures or sand dunes the reflection amplitudes are relatively lower and higher beneath the troughs, resulting in a colour shading as between trace 55154 and 53534, which does not reflect the sediment type. In addition, vertical striations can be seen, which are artifacts as a result of either the method of data acquisition used or the processing that followed. Furthermore, around these same traces a striking upward and downward shift can be seen of the basal horizon of unit A beneath the crest and through of the sand wave, which is due to a pull-up effect. In reality, this horizon has a flatter arrangement.

Unit A comprises the sand waves or sand dunes at the top and only the upper part of the dunal body on the left (obliquely arranged sheet deposit on top of wedge shaped deposit of unit C), which is because this ‘dunal body’ is a actually a tidal bank instead of a sand dune. These mega ripples consist of shortly continuing or discontinuous obliquely arranged reflections, with relatively moderate to high amplitudes, that represent internal foreset laminations. These sand waves exhibit smaller scale ripples at their top margin. Furthermore, the Facies of unit A in Fig. 13 is not deviating from the described general facies of unit A in Ch. 5.1.

Unit C has an undifferentiated or acoustic transparent to chaotic seismic facies with mainly discontinuous reflection configurations and is therefore consistent with the facies description in Ch. 5.1. The boundary horizon (thick green line) between unit C and unit D has an erosive pattern, following multiple incisions in unit D. The infills of the incisions in unit D are part of unit C as well as the wedge shaped deposit on the NW as mentioned in the paragraph above.

Unit D is located between the green and yellow horizons, between which many internal horizons are distinguished with limited lateral traceability. These sub-horizons are drawn to display the internal structure better. The facies of unit D in Fig. 13 is similar to the facies described in Ch. 5.1 and shown in Fig. 10, D_2, however at this section the facies is relatively diverse. Unit D has generally a high amplitude facies, nevertheless in Fig. 13 it is downwards decreasing in amplitude. This is partly due to the fact that acoustic energy is decreasing with depth. However, the sharper transitions in amplitude such as those between D_9 and D_7/D_6 show that this amplitude gradient is not only artificial, but also reflects sedimentation. Although there is quite some internal variation in unit D, it should be noted that it contains relatively many laterally continuous reflections, some of which have a subparallel configuration. Subparallel-continuous reflections can be seen in particular at the top left, at D_1 and D_2 and at the bottom at D_9. Locally unit D is somewhat more chaotic, has more discontinuous, wavy and, or nonparallel reflections or is tending to a moderate acoustically transparent facies. The facies changes appear gradually. It can be seen that D_{4A}, D_7 and D_8, relatively speaking, have a more chaotic facies compared to D_1, D_2 and D_9. An example of where the facies tends to be acoustically transparent, can be seen in D_8, in particular in the lenticular body (with the light green boundary lines). The internal structure of unit D is complex and even in the subunits changes in thickness, geometry and facies can be recognized. For example, note the gradient of D_5 (between the turquoise colored horizon and the green upper boundary of unit D) between trace 58282 and the right

flank of the frame. Moreover, the parallel subhorizons that occlude subunit D_2 on the left side of the frame, are dipping slightly Northwestward. Furthermore, around trace 55154 and between traces 53534 and 51887 there seem to be two channel shapes that are separated from each other by a small mound This geometry is probably enhanced as seabed-relief artefact, however, it is probably still sedimentary in nature.

Unit E largely has an acoustically transparent facies with locally low-amplitude subparallel discontinuous reflections. The low amplitude facies is partly due to the reduced acoustic energy level at depth, which is called acoustic blanking, next to reflecting the sedimentation.

Interpretation figure 13

Unit A in figure 13 consist of still moving submarine sand dunes. A northwestward sediment transport direction can be deducted on account of their asymmetry and orientation (Stow, 2005; view figure 7). Unit A is probably an expression of the Bligh Bank Member of the Southern Bight Formation, which is omnipresent at the seafloor surface in this area. The obliquely arranged sheet deposit of unit A on top of the wedge deposit (or actually a mound in half) of unit C is discordant. The deposit of unit C is part of a N-S oriented tidal bank which is thought to be part of a sedimentary plateau or cuesta, which was eroded on the flanks into the troughs and raised on the top, which is the deposit part of unit A (Le Bot et al., 2002 and Mathys, 2010; read 'Seascape', Ch. 2.2).

In addition to the aforementioned 'positive' topographic deposit, Unit C consists of infill deposits of similar acoustic characteristics and patterns. From this facies it can be deduced that unit C consists of relatively homogeneous sandy deposits. This suggests unit C here is either part of the Boxtel or the Kreftenheye Formation. However, a Holocene age (Naaldwijk Formation) cannot be completely excluded. Figure 4 shows that the edge of the Kreftenheye formation is close to the location of the seismic profile of Fig. 13. However, the small-scale filled-up incisions into unit D are probably indicative for small-scale streams, which fits with the theory about the Boxtel Formation. On the contrary, the Kreftenheye Formation is characterized by large scale fluvial deposits. In addition, the distribution of the Kreftenheye Formation in Fig. 4 might not be exactly right, since it is based on extrapolation of sediment core descriptions. Therefore, unit C in Fig. 13 is probably an expression of the Boxtel Formation, which consist mainly of aeolian fine sands together with small-scale fluvial deposits.

The subparallel continuous, high amplitude seismic facies of unit D in Fig. 13 suggests a clayey or silty laminated deposit and is characteristic of the Brown Bank Formation. Where the facies are relatively more chaotic and transparent, the sediments are probably sandier. Unit D appears to be a layered deposit of fine and relatively coarser sediments, of which the coarser sediments locally form thicker lenses and interfinger with the thin-layered fine sediments. The thinly layered deposit of fine material is probably deposited in a low-energy environment, reminiscent of a (partly closed) lake or lagoon where multiple (regular or irregular) pulses with more current bring in coarser sediment. The relatively more transparent or chaotic seismic facies (e.g. D_9) compared to the high amplitude facies (e.g. D_6) could indicate an average higher energy level, which could be explained by a more opened depositional environment. Therefore resembling a lagoon that is gaining and losing influence from the open sea. The sandy lenses could be channels along which both fine and coarse material was transported, of which however, only

the coarser fraction was deposited due to the current velocity. There are two channels of about 200 meters width, which one is around trace 55154, through the subunits D_3, D_4 and D_7 and the second channel between traces 53534 and 51887, in subunits D_4 and D_8. These two channels appear to have sandy lenses at the bottom and more clayey deposits near the top of the infills. At the base in between these two channels is a mound located (part of subunit D_8), although amplified by the pull-up effect. This mound might be deposited during a phase of stronger current velocity. However, because of the artificial colour shading, it is difficult to determine whether this mound is made up of similar clayey deposits as found in D_7 and D_4 or whether it has a more sandy content. However, it can be hypothesized that this mound is the result of slightly higher energetic processes than most of the layered clays, silts and sands. Perhaps this mound is the result of storm-like event. Moreover, it is more common for remnants of sand dunes to be found in the Brown Bank Formation (Eaton et al., 2020) or at the base of the Brown Bank Formation (Waajen et al., 2024). Perhaps, a second mound or dune could be found at 51887 in the same subunit D_8. Furthermore, it is questionable whether the northwestward dipping deposits at the left of the frame (D_1 and D_2) are deposited obliquely or has (partially) sunk. It can be expected that compaction of clay have occurred locally in this clay rich unit.

The acoustic transparent facies of unit E in Fig. 13 is probably an indication for a homogenous deposit which will probably consist of sand. Although this interpretation might be hindered due to acoustic blanking at this level, which could have resulted in reduced amplitudes. The local subparallel reflections might indicate layers of smaller grainsizes alternating with sands. Unit E is probably part of the Eem Formation. Similar to unit D, unit E consist partly of alternations of sand and finer sediments. Possibly unit E and D existed in relatively similar environments, however in the depositional environment of unit E the phases with stronger currents were present to a greater extent, relative to the phases with weaker currents that deposited the finer sediments. In the environment that deposited unit D it probably was the other way around: The weaker current phases were dominating with respect to the stronger current phases.

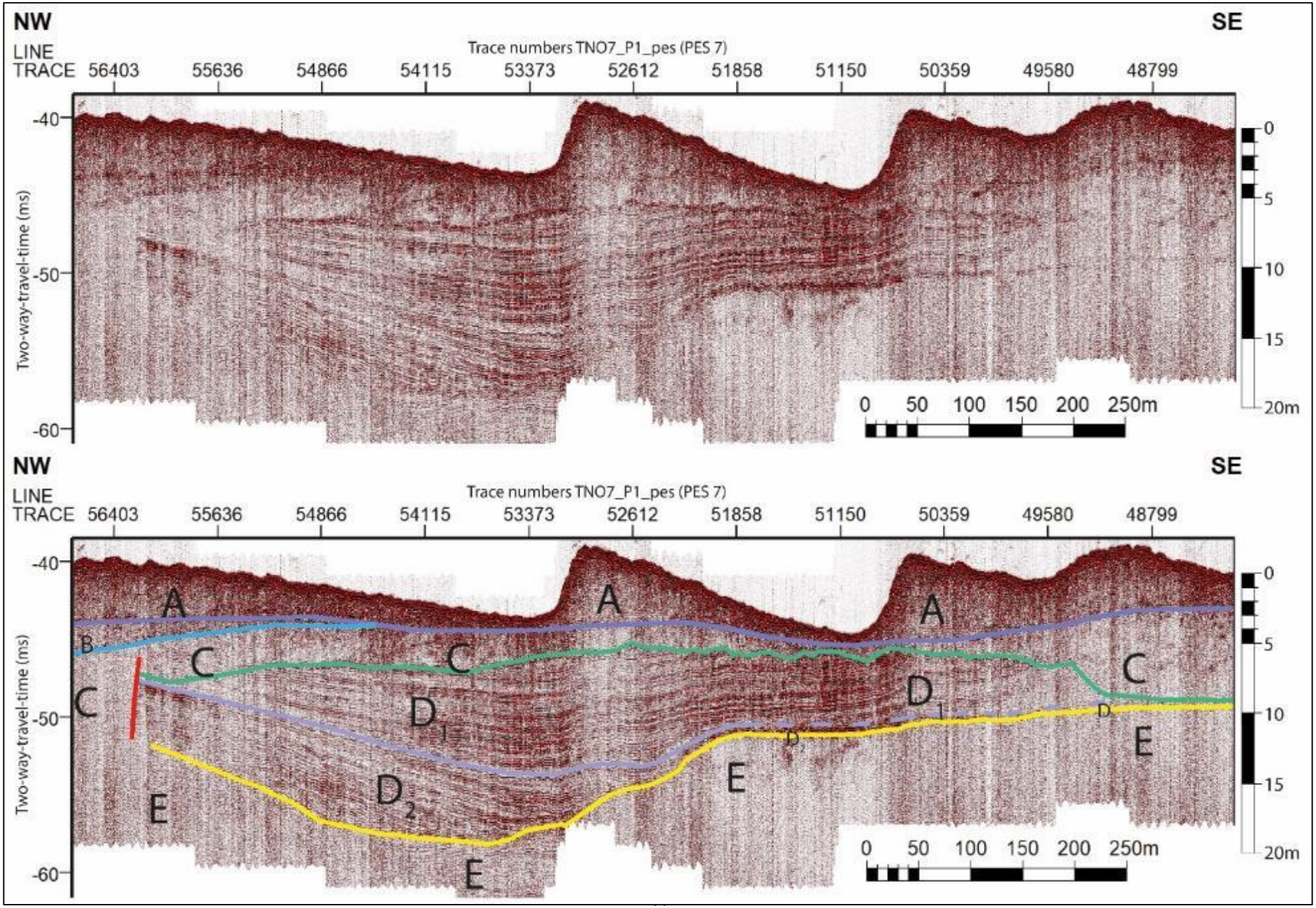

Figure 14: PES seismic data from segment TNO7_P1_PES. Approximately 20 meters below the seabed are shown over a horizontal distance of approximately 1 km. Top panel: clean seismic data. Lower panel: interpretation. View fig. 12 for the location of shown section.

Description figure 14

Figure 14 shows a PES seismic profile, which is subdivided into five units (A, B, C, D, and E, with unit D being subdivided into D_1 and D_2) bounded by four horizons. The main feature of Fig. 14 is the 500-900 m wide channel body (depending on what width is measured), of which the intersection was almost perpendicular to the channel direction. Furthermore, this channel body is part of unit D.

Unit A is placed between the seafloor and the upper purple horizon, because it generally exhibits the visual characteristics consistent with the description of unit A in Ch 5.1. More precise, unit A in Fig. 14 contains mega-ripple structures superimposed on sand waves with relatively high amplitude and discontinuous reflections which form a pattern of internal cross-lamination. The base (upper purple horizon) is oriented subhorizontally. However, this base is shifting up underneath the dunes and is shifting down, underneath the troughs which is probably partly due to a type of seismic distortion called a pull-up effect. This is caused by the difference in seismic velocity between the sand dunes and the water column. Due to the seabed relief and because, the seismic velocity is higher in the sandy deposit than in seawater, with the same arrival time, the pulse penetrates deeper into and below the sand dunes than below the troughs. This creates an artifact of slightly pulled-up or pulled-down reflections. Furthermore, the darker colours or high amplitude reflections at this top unit do not fully reflect acoustic impedance increases, and are partially an artifact as well.

Unit B is placed between the upper purple horizon and the blue horizon and is only present at the left side of the image. The lower boundary horizon is not parallel to the upper purple horizon which might indicate that unit B is part of an older formation, which is a reason to classify unit B as a separate unit. Unit B consist of partly continuous, nonparallel or oblique reflections, which might indicate forest structures. Furthermore, unit B has a moderately chaotic facies with an average amplitude lower than unit A and higher than large parts of unit C.

Unit C is placed below the upper purple horizon and above the green horizon. At the left there is an undifferentiated transition into unit E. Unit C has no unambiguous facies. In some parts reflections are still recognizable, however, they are partly traceable or show chaotic patterns. However, these partly traceable reflections form cross-laminations indicating foresets of a northwestern transport direction. No reflections are distinguishable in the northwestern part where unit D is missing. Below the troughs of the sand dunes, the amplitudes of the reflections in unit C are significantly higher with respect to below the peaks of the dunes. This colour shading artefact is due to the fact that acoustic energy is lost with depth and more energy is preserved below the troughs. In addition, this artefact has also affected unit D. Furthermore, as in Fig. 13, vertical striations have also distorted the seismics of Fig. 14 and are present in all units.

In the middle of the frame is unit D placed at a relatively large body with a channel-shaped geometry with relatively homogeneous internal facies of high amplitude reflections with a pattern of subparallel continuous laminations, which seem to demonstrate the characteristic seismic facies of the Brown Bank Formation as described in Ch. 5.1. Unit D has the green horizon as upper boundary. Reflection terminations indicate truncation at this boundary. The lower boundary of unit D is marked by the yellow horizon, which is truncating unit E. Some reflections of unit E show terminations at this horizon. Unit D is subdivided into D_1 and D_2, because, the continuous reflections of D_1 are more parallel to each other than to the continuous

reflections of D_2 which are also more parallel to each other than to those of D_1. The purple horizon dividing unit D_1 and D_2 is placed at the boundary between these sets of similar reflection configurations. Furthermore unit D_2 has a parallel-oblique reflection pattern in the left part. D_2 is thinning towards the right and seems to have a parallel-drape reflection pattern. The purple boundary horizon is less distinguishable near the right of unit D. Unit D is significantly thinner at the right of the panel. Unit D and even part of unit C seem to be truncated at the left of the panel, which is indicated by the red line.

Unit E is placed below the yellow horizon. This unit has a mainly undifferentiated facies which is due to the fact that at this depth significant amount of acoustic energy has lost which hinders accurate distinguishments. Nevertheless was recognized that unit E is consisting of subparallel continuous reflections underneath the deepest part of the yellow horizon, similar to the local occurrence of unit E in Fig. 13.

Interpretation figure 14

Unit A here has a strong similarity to unit A in Fig. 13 and is therefore probably an expression of the Bligh Bank Member of the Southern Bight Formation. The mega ripples, or sand dunes are presumably still moving in Northwestern direction as can be deduced from their asymmetry (View Fig. 7; Stow, 2007).

Unit B probably consist of sands and might be part of the Naaldwijk Formation. In that case, these sands would have been deposited as beach deposits or near-coastal marine deposits. However, preservation of these relatively high situated deposits is somewhat rare. Another option could be that this unit is also part of the Southern Bight Formation, although it might be an older unit than A. The generally large amplitudes of unit B compared to unit C (which contains local high amplitude reflections as well) could be explained by more grainsize contrasting layers with finer sediments in between coarser sediments. Which could be explained by unit B being composed of silt or clay layers in a general sandy matrix formed at or near tidal flats or creeks, which are common in the Naaldwijk Formation. Unit C on the other hand, might be composed of more homogeneous sands (except for the areas were unit C is showing stronger amplitude reflections). However, unit C does contain similar foreset structures that seem to be in the same orientation as unit B. This could mean that unit B is not that much younger with respect to unit C and part of the same formation which is prograding towards the NW.

Furthermore, the sharp colour transition between the darker data of unit A/B and general lighter, low amplitude data of unit C is reflecting a decrease in the abundance of density contrasts as well. The chaotic to undifferentiated reflection patterns of unit C are probably indicating relatively homogenous sandy sediments. Since the Kreftenheye Formation has not been found to date around this part of the seismic line (as seen in fig. 4), it is more likely that this sandy unit is part of the Boxtel Formation. The more chaotic, high-amplitude facies is partially an artefact, caused by the thinning unit A on top (the troughs between the sand dunes). However, it might be an expression of small scale fluviatile deposits or periglacial soil deposits containing clay or loam layers. Moreover, the cross lamination or foreset structures in unit C might be the result of windblown dunes developing towards the NW. Furthermore, unit C is noticeably more deeply incised on either side of the channel body. This channel body may have been an erosion-resistant structure in the landscape.

Unit D is part of the Brown Bank Formation on account of the characteristic facies. Moreover, the subparallel continuous laminations and drape pattern of unit D are presumably an indication for fine sediments and a largely low-energy environment. However, in combination with high amplitude reflections, there might be large variation in the grainsizes. This could indicate that unit D is a succession of clays and sands and could have been deposited by pulses of higher and lower current velocity. The channel geometry could also have been formed as a remnant of a lake, however, the HKW project has shed light on this by analysis of their geophysical data and discovered that this channel continues for at least ten km towards the North and the South (RVO, 2024) . The parallel-oblique or sigmoid to oblique reflection pattern of unit D_2 is an indication for lateral progradation into a deeper basin (Mitchum, 1977; Mitchum et al., 1977 and Mellett et al., 2013; view Fig. 7). The basin is first filled in by D_2 with most of the sediments being transported from the West. Thereafter filled in by D_1. It is unlikely that the same processes and magnitudes of the rather low energy environment that deposited unit D, cut the 500 to 900 meter wide trench into the underlying unit E. It is more plausible that the erosive base of unit D may be a relict that was later filled in by unit D.

Unit E in Fig. 14 shows similarly varied facies as in Fig. 13 and is probably part of the Eem Formation. The acoustically transparent facies is probably indicating homogeneous sands. Due to the local occurrence subparallel continuous reflections, it is plausible that the acoustic transparent facies is reflecting the sedimentology and not an artefact of limited seismic penetration. The subparallel continuous reflections with weak amplitudes indicate alternating layers of fine and slightly coarser sediments that could have been deposited in an environment that experienced periodic energy changes, similar to the environment that formed unit D, with however, relatively higher energy levels and more coarse grained (sandy) sedimentation.

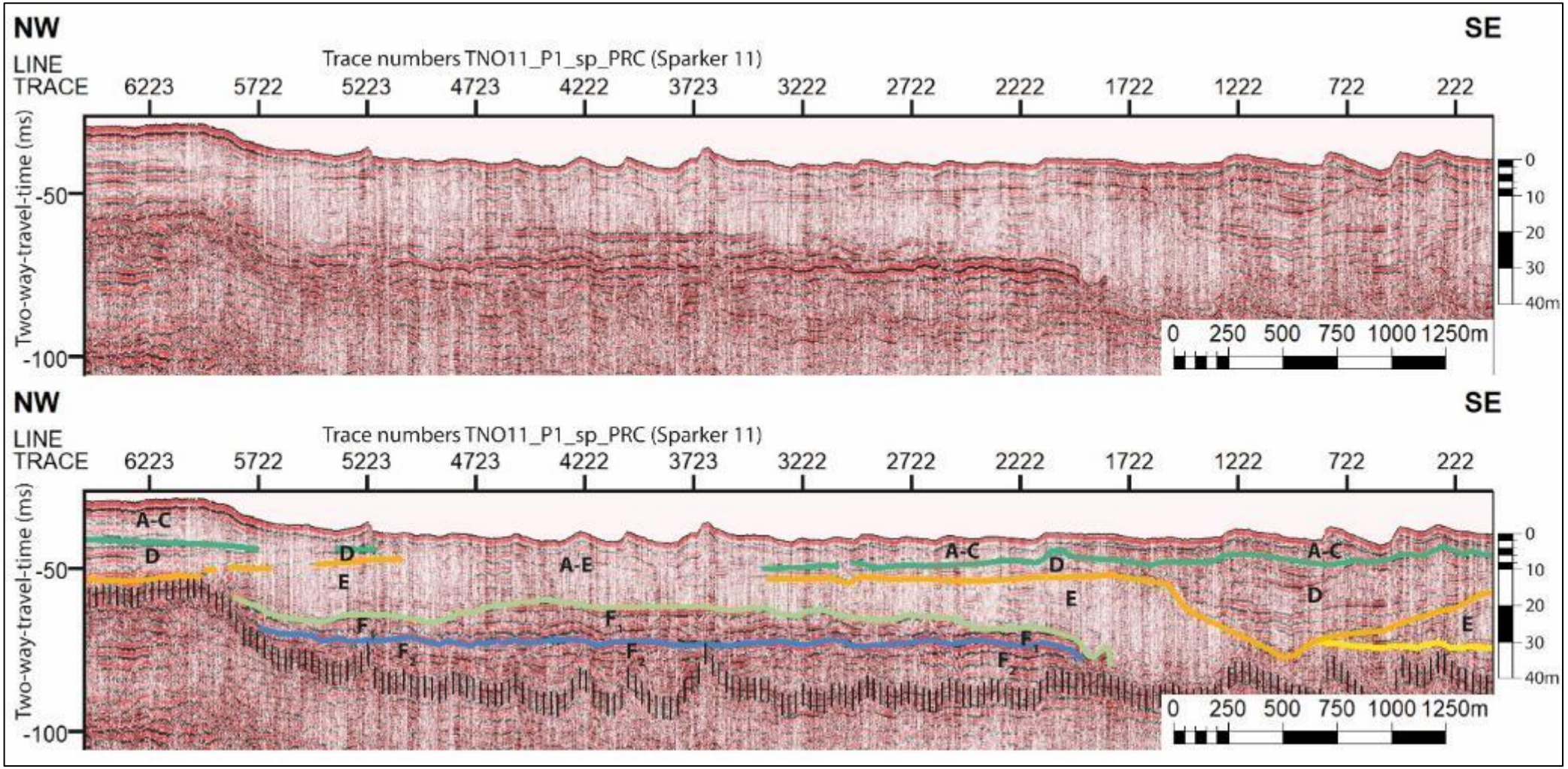

Figure 15: Sparker seismic data from segment TNO11_P1_sp_PRC. Approximately 50 meters below the seabed are shown over a horizontal distance of approximately 5 km. Top panel: clean seismic data. Lower panel: interpretation. View fig. 12 for the location of shown section.

Description figure 15

The interpretated sparker seismics of figure 15 are divided into up to four units where they are all identifiable. The second and fourth or bottom units (resp. D and F) have a higher amplitude with respect to the first or upper unit (A-C) and the third unit (E). In the middle of the frame, unit D is absent and because of the lack of reflections and facial change to mark the boundary between unit A-C and E, these have been combined into unit A-E.

Other than in the PES seismics of figure 15 and 16, no separate unit A, B or C as described in Ch. 5.1 was identified in this sparker seismic image. Therefore, these are here lumped into the single seismic unit A-C. This unit is affected by a strong seabed reflection together with an artifact of contouring reflections underneath. The amplitudes decrease downwards while the facies becomes acoustically transparent locally, in particular on the left part (around trace 6223).

The channel-shaped structure of figure 14 is also visible in the sparker seismics of figure 15, on the right, between the green and orange horizons. However, unit D seem to continue to the northwest of the channel structure, instead of being cut off as seemed to be the case in figure 14. Unit D consists of high amplitude lateral continuous reflections. Where unit D is thinner, planar reflections can be seen. Furthermore, curved subparallel reflections or draping reflection patterns can be seen in the channel body.

Unit D cuts into unit E, which can be seen in particular with the channel body. Locally where unit D is missing, unit A-C is merging undifferentiated into unit E. Both on the left side (around trace 6223) and on the right side (around traces 222 – 1722) is unit E partly disturbed by the seabed multiple, causing the base of unit E to be locally unrecognizable. Except for the part where unit F is located above the multiple. Likewise, the lower limit and the further course of unit F are unclear as a result of the multiple artifact as well. Unit E has a relatively acoustically transparent to chaotic facies. Unit E contains parts where low amplitude discontinuous reflections prevail (e.g. around traces 1722 and 4222) and parts where relatively higher amplitude and more continuous reflections can be found (e.g. around traces 222 and 4723).

Furthermore, unit F has a similar facies as unit D, with fairly continuous reflections, with often however, even higher amplitudes and appears locally somewhat chaotic. Terminating reflections at the top boundary of unit F are indicative for an erosive horizon. Unit F is subdivided into F_1 and F_2, because of the presence of a pronounced internal reflection of higher amplitude. However, there is no clear difference between the seismic facies of these subunits.

Interpretation figure 15

The general low amplitude reflections and presence of acoustic transparency of unit A-C are an indication for sandy deposits. Therefore, this is presumably a succession of the sand-rich Bligh Bank Member of the Southern Bight Formation with the Boxtel Formation below. Furthermore, a possible occurrence of the Naaldwijk Formation cannot be excluded. In addition, the Kreftenheye Formation could also be present on the northwestern part, as can be seen in figure 4. In the left edge of Fig. 15, a N-S oriented tidal bank can be seen, with a core of sandy sediment.

Unit D contains the characteristic seismic facies of the Brown Bank Formation. The returning subparallel reflections of unit D are indicating a layered deposit with alternating grain sizes, which are probably alternations of fine sediments such as clays and silts and thin layers of relatively coarser sediments (e.g. sands).

The acoustically transparent facies of unit E is probably reflecting a homogeneous sandy deposit. The fact that this acoustically transparent facies of unit E is again seen in these sparker data shows that it was not an artifact of seismic energy loss as was suspected as a possible cause in Figures 13 and 14. The local high-amplitude continuous reflections that are present around trace 222 might indicate the presence of finer or coarser layers between the sands. Unit E is probably the Eem Formation here.

The high-amplitude continuous reflections of unit F, locally sub-parallel in character, suggest an alternating fine and coarse stratified deposit that is likely part of the Egmond grounds (Cameron et al., 1989; Rijsdijk et al., 2005 and TNO-GDN, 2022i) or Yarmouth Roads Formation (Cameron et al., 1989; Rijsdijk et al., 2005; Eaton et al., 2020 and TNO-GDN, 2022k). Layers of finer sediments can be found occasionally in both formations. The close resemblance between the seismic facies of unit D and unit F in the sparker data of Fig. 15 might suggest that unit F is deposited in a similar environment as unit D, however, from an older glacial period.

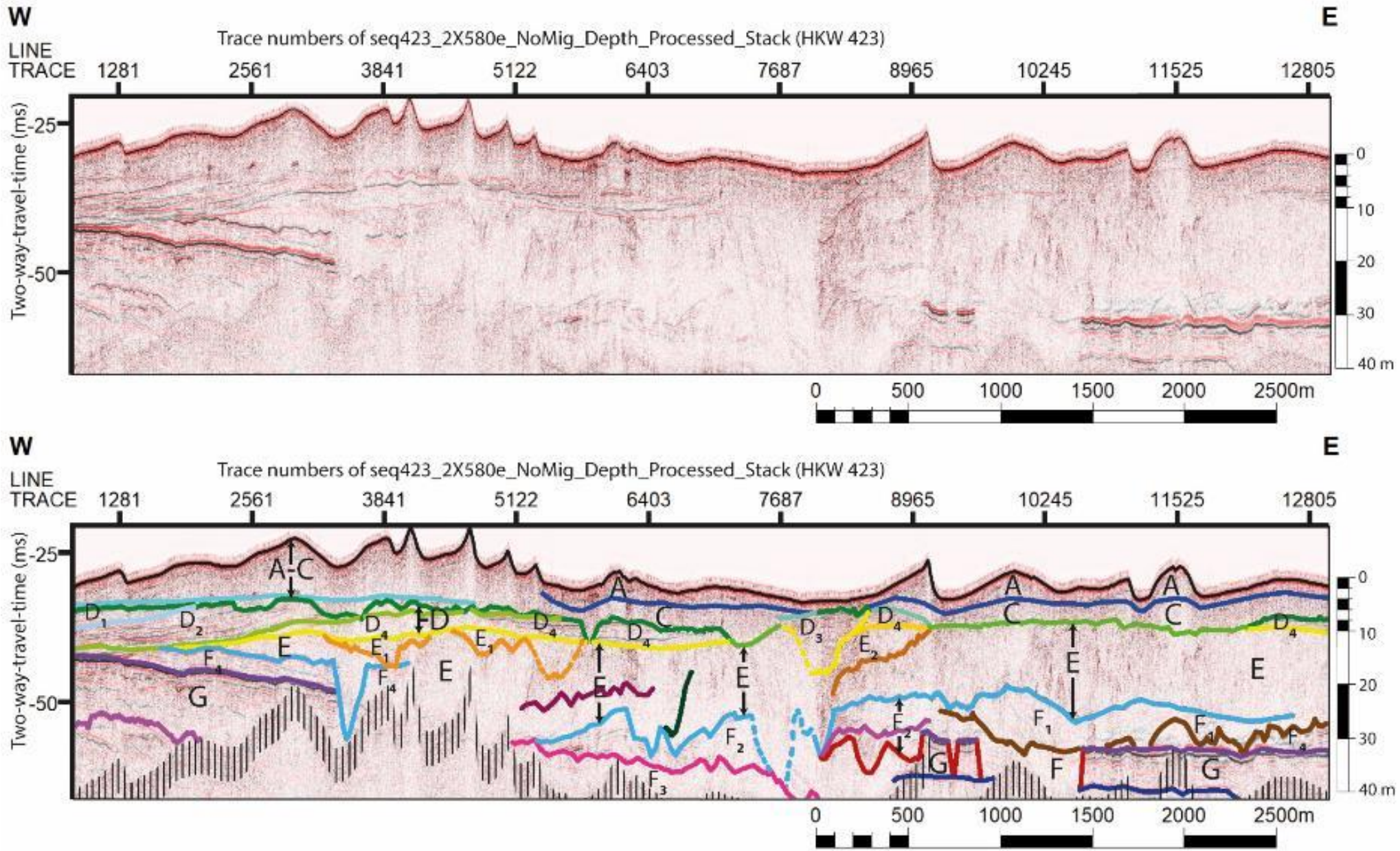

Figure 16: Sparker seismic data (HKW-sparker) from segment seq423_2X580e_NoMig_Depth_Processed_Stack. Approximately 40 meters below the seabed are shown over a horizontal distance of approximately 6 km. Top panel: clean seismic data. Lower panel: interpretation. View fig. 12 for the location of shown section.

Description figure 16

From top to bottom, the seismic image of Figure 16 is organized as follows: Units A, C and A-C (which is on the left side where these two units are indistinguishable). Underneath is unit D placed, which is bounded by the top green line and is divided into several subunits and beneath is unit E placed below the yellow line. Notably on the right side unit E sits directly below unit C, here unit D is absent on either side of the channel structure (around trace 7687 and between traces 8965 and 11525). This channel is the same as seen in Figures 14 and 15. Unit E is absent on the left side, here unit D lies directly on the oldest subunit of unit F (F_4) with unit G below, which is bounded by the purple line. The border between unit E and F is indicated with the lower light blue line. Unit F is present almost over the entire width, although the course of units F and G is locally unclear due to disturbance of the seabed multiple. Unit G is absent in the center and returns locally to the right at a greater depth. Where unit G is missing is the thickness of unit F increased.

Unit A comprises the sand dunes similar to the previous figures. However, here are both asymmetrical sand dunes (at trace 8965) as well as symmetrical sand dunes (at trace 11525 and left from trace 10245). This might be the result of local changes in the current direction in between the tidal ridges, however, it is more plausible that this is just the result of the way the dunes are broached in the seismic data. The horizon dividing unit A and C (upper blue line) is probably flatter in reality, the contouring curviness of this line is an artefact. On the left where a N-S oriented tidal bank is located with sand dunes on top, this line is not distinguishable. Presumably, this is because unit A is thinning on top of the tidal bank. However, another horizon within unit A-C is identified around a series of high amplitude spots. All three, unit A, C and A-C, have discontinuous, fairly acoustically transparent reflections. Within unit A the reflections are contouring, while in unit C the reflections have a more chaotic or oblique pattern.

The oldest subunit of unit D is D_4, which is present underneath trace 12805, 8965, 6403 and is covered by D_2 below traces 2561-5122. Also unit D_3 (which is the aforementioned channel) is cutting into D_4 and unit E. Subunit D_1 is only present at the left side of the figure and sits on top of D_2, both subunits are deepening towards the West. The upper boundary of unit D (upper green layer) has an erosive character, unit C has incised into and through unit D on multiple locations. The Seismic facies of unit D consist of relatively high amplitude, laterally continuous subparallel reflections with local occurrences of lower amplitude reflections where the facies is also tending towards transparency. For example, subunit D_1 has, compared to D_2, a more transparent facies. In subunit D_4 lower amplitude reflections also occur towards the West. In contrast, towards the east of D_4 and also in D_2 and D_3 recognizable high amplitude laterally continuous reflections are common. Subunit D_3 in particular consist also of the subparallel reflection configuration. In D_2 the reflection horizons are partly oblique with a draping pattern below trace 2561 as well. In D_2, lenses with lower amplitude reflections can also be recognized. A processing artifact can be seen on the left side of D_3, where many reflections are ending. What processes caused this artifact are unknown. The course of the channel body on the left side is therefore drawn in dotted lines. In general, unit D has the visual characteristics of the Brown Bank Formation.

The lower boundary of unit E is strongly erosive. Therefore, unit E has locally deeply incised into unit F and even into unit G. Unit E has a relatively more undifferentiated facies compared to the units D, F and G. However, some internal horizons are identified that often follow an erosive pattern. These internal horizons are defined as subunit boundaries. Nevertheless, the

subunits are little different in facies compared to the general facies of unit E. Unit E contains low amplitude, discontinuous reflections in particular and is locally chaotic or nearly reflection free. Particularly characteristic of the seismic facies of unit E are the point diffractions (the arrow or parabola shaped noise) that are omnipresent in only this unit.

Unit G and subunit F_4 are lost in the middle part of figure 16. Also beneath trace 10245 is a big incision into unit G. The lost parts of unit G and F_4 are infilled with younger subunits of F (F_1, F_2, F_3) and E. The top of unit G is located up to 15 meters deeper in the East compared to the West. The top of unit F is also significantly deeper in the eastern part. The subunits of F are varying strongly in facies. High-amplitude continuous reflections are present in most subunits, with the exception of F_3, which facies is almost undifferentiated with low untraceable reflections. F_1 and F_2 contain subhorizontal, wavy and strongly oblique subparallel reflections. In F_2 (in between traces 6403 and 7687 and in between traces 7687 and 8965) the tilting subparallel reflections dip to the West and in F_1 (at trace 10245) they are tilting to the East. Subunit F_4 and unit G contain tilted subparallel reflections as well, which are dipping towards the East. However, they are dipping with lower angles compared to subunit F1. Furthermore, unit G contains high amplitude continuous reflections in general. However, the eastern part contains reflections that are more horizontal or wavy configurated or are partly discontinuous and have relatively lower amplitudes. The lower amplitudes are probably a result of the greater depth and loss of acoustic energy.

Interpretation figure 16

Unit A is probably part of the Bligh Bank Member of the Southern Bight Formation (Cameron et al., 1989; Rijsdijk et al., 2005; Stoker et al., 2011 and TNO-GDN, 2022b), while unit C is probably mainly composed of the Boxtel Formation (Cameron et al., 1989; Rijsdijk et al., 2005 and TNO-GDN, 2022h). The fact that the boundary horizon between unit A and C is slightly below the base of the sand waves, might indicate that there are older deposits of the Southern Bight Formation or of the Naaldwijk Formation below the sand waves. However, the lack of an upper horizon and facies difference do not suggest that the Naaldwijk Formation is located below the sand waves of unit A. Furthermore, there is no indication that deposits of the Naaldwijk Formation are located at the top of unit C or in the middle of unit A-C, but it cannot be excluded either. There could be some deposits that are part of the Kreftenheye Formation around the western part, because this formation would be present here according to Fig. 4. However, because there is little seismic variation within units C and A-C, it is expected that mainly homogeneous sand deposits of the Boxtel formation are shown here (below those of the Southern Bight Formation). However, the spots of high amplitude reflections on the left where the light blue horizon is drawn is a facial anomaly. These spots might indicate gas bubbles.

Unit D is probably an expression of the Brown Bank Formation. It is striking that there is a greater variation in facies and thus depositional environment than was seen in previous figures. Low amplitude reflections or more transparent facies indicate little grainsize variation and probably sandy deposits. These are, as it seems in subunits D_1 and D_4, also part of the Brown Bank Formation. The variation in sediment type means that it is not correct here to identify these deposits as the ‘Brown Bank Member’. However, since the term ‘Brown Bank Formation’ has come back into use and is fitting for a greater variety of sediments, it is recommendable to classify unit D of Fig. 16 as a succession of the Brown Bank Formation. The way units D_2 and

D_4 and also D_1 and D_2 are arranged vertically and laterally indicates a progradational system. Foresets of the Brown Bank Formation have formed in (North)Western direction during a sea level regression. It is not clear whether subunit D_3 (the channel) is older than subunits D_1 and D_2, however it is younger than D_4, because the internal reflectors truncate on the base of D_3. In addition, D_3 could be formed at roughly the same time as D_1 or D_2. The more transparent facies of D_1 compared to D_2 is probably reflecting a more sandy content. Therefore the transition from D_2 into D_1 expresses a transition into a general higher energetic environment. This means the phases of sand deposition increased in magnitude and/or duration. Furthermore, the possible gas bubbles in unit A-C might originate from the Brown Bank Formation clays. Because, these clays probably have a relatively high organic content.

Unit E consist mainly of sandy deposits. The erosive boundaries of the subunits show a sedimentary history of multiple phases of accumulation and truncation. These phases are expected to have been relatively short and local in nature. Unit E is probably an expression of the Eem Formation with shallow marine to coastal sandy deposits. The point diffraction parabolas indicate relatively hard reflective material such as gravel, dropstones, ice rafting debris, perhaps coarse shell material. Very coarse sands or fine gravel beds and/or shell beds might be expected within the Eem Formation. However, theses point diffractions seem fairly homogeneously distributed. This could be a consequence of the scale, which would mean that, in reality, there are multiple gravel or shell beds present. Gravel beds also occur in the Kreftenheye Formation, however, the occurrence of Kreftenheye Formation right below the Brown Bank Formation is not known, despite the fact that the Kreftenheye Formation has been active since the late Saalian. Therefore, it seems unlikely that (part of) unit E in Fig. 16 is reflecting the Kreftenheye Formation, however, interfingering cannot be excluded.

High amplitude reflections in unit F and G indicate deposits with alternating grainsizes. Furthermore, both units show high amplitude subparallel reflections at some parts similar to those of unit D. Possibly this could indicate that these deposits originate from a similar depositional environment as the Brown Bank Formation. Thus a largely calm, shallow, partly closed basin, where weak currents have deposited clays and were alternated with moments of stronger current that deposit layers of sand. Especially subunit F_3 contains acoustic transparent facies as well, indicating homogenous sandy deposits. The Yarmouth Roads Formation and the Egmond Ground Formation both contain a wide variety of sandy and clay deposits. Therefore, one or both of these formations are probably present in unit F and G. It is striking that unit F is located over 10 meters deeper right next to the channel as can be seen in figure 15, however further west, unit F is at a similar depth as in figure 15. Furthermore, presumably the depth difference of about 10 meters of unit G between the eastern and western part is not the result of subsidence, because the distance of about 10 km is too little for that. It is more probable that unit G has been deposited with this depth profile. The obliquely oriented reflections in subunits F_1 and F_2 could indicate that these tilted deposits were deposited at the edge of a relatively deep or growing basin. Note that the slope of these reflections and deposits are in reality significantly smaller due to the vertical exaggeration. Furthermore, the fact that these oblique deposits are located directly above the parts where unit G is missing and has been eroded in between the depositions of F_3 and F_4, resulting in the formation of valleys or depressions with significant space for accumulation, is consistent with this theory. However, these tilted sediments could also be deformed by glaciotectonic forces during the Saalian glaciation, which would be an alternative theory.

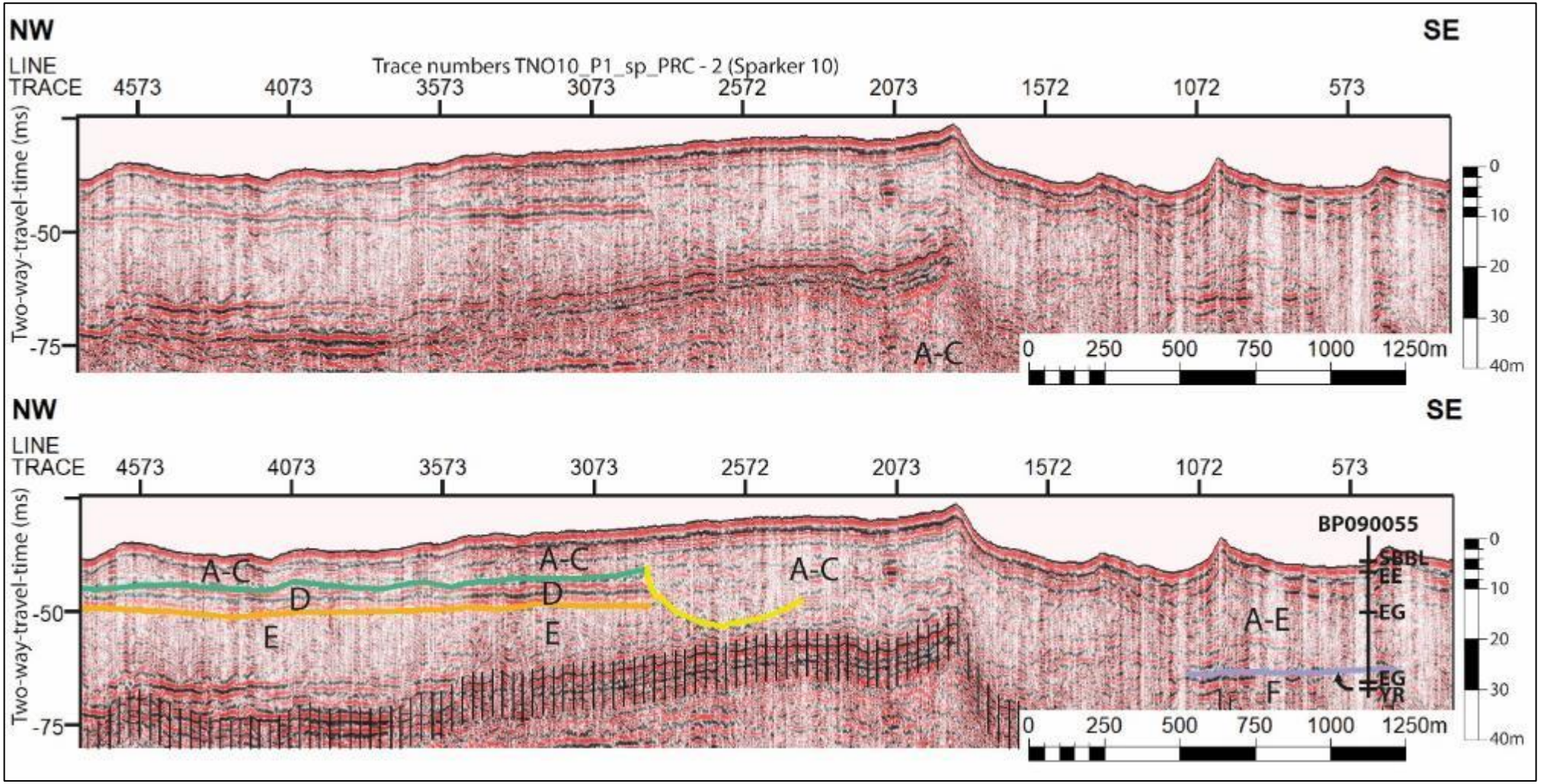

Figure 17: Sparker seismic data from segment TNO10_P1_sp_PRC - 2. Approximately 30 meters below the seabed are shown over a horizontal distance of approximately 5 km. Top panel: clean seismic data. Lower panel: interpretation with a sediment core projected on the profile with the tops of various lithostratigraphic units: SBBL (Southern Bight Formation, Bligh Bank Member), EE (Eem Formation), EG (Egmond Ground Formation), YR (Yarmouth Roads Formation). View fig. 12 for the location of shown section.

Description figure 17

The left part of Figure 17 is divided into three units, mainly on the basis of the explicit presence of unit D. This unit does not seem to return in the right part. However, on the right part high amplitude reflections, indicative of a horizon, are occurring at a greater depth relative to unit D. This is why the right part is only divided into two units (A-E and F) and the left part into three (A-C, D and E). On the left part at the bottom of unit E, some high amplitude reflections appear that should be part of unit F as well. However this is not made clear in Figure 17.

As in the previous sparker figures, this seismic image of figure 17 is influenced by a strong seabed reflection with high-amplitude contouring reflections below and a strong seafloor multiple at depth. There are also pronounced vertical striations, especially on the right side.

Unit A-C is influenced by the strong seabed reflection, which limits the visibility of the natural structure of this unit. At the bottom, that natural structure is more present and a chaotic, relatively transparent facies can be seen. The base of unit A-C is indicated by the green and yellow horizons. An erosive surface appears to be present where the reflections of units D and E terminate. Laterally, towards the Southeast, no horizon is identified between units A-C and E. Unit A-E is facially very similar to that of unit A-C, although towards the lower boundary (purple horizon) there are reflections with a higher amplitude and a laterally more continuous character.

Unit D contains high amplitude subparallel continuous reflections that are truncating on the yellow erosive horizon. Unit D seems to return around trace 2073, however, this is unclear. These local higher amplitudes around this trace could be the result of free gas, but then the amplitude would have to be even higher and the polarity would have to be reversed. It is more likely that here is a relatively small deposit with contrasting lithology. Therefore a remnant of unit D with a width of approximately 50 meter cannot be excluded.

Unit E often has an acoustically transparent facies and locally a more chaotic character where reflections have slightly higher amplitudes.

A high amplitude reflection in the right part of figure 17 has been interpreted as the boundary between units A-E and F. Since the surrounding reflections have a relatively high amplitude as well, this part appears similar to unit D. However, these reflections are at a significant greater depth, which makes it unlikely. The lateral course and base of unit F is not or only partially visible due to the intersecting seabed multiple. In the part of unit F above the multiple, relatively slightly higher amplitudes can be seen with respect to those in unit E and A-E. Despite the higher amplitudes, a rather chaotic facies is present in unit F.

Interpretation figure 17

The fairly acoustic transparent facies of unit A-C and A-E are indicating a sandy deposit. The more continuous reflections of unit A-E suggest a relatively layered deposit with fluctuating grainsize. Unit A-C is probably an expression of the Bligh Bank Member of the Southern Bight Formation on top of the Boxtel Formation, with perhaps also the Naaldwijk Formation in between. Unit A-E is probably a similar succession and expressing the Eem and, or the Egmond Ground Formation in the lower part. Assuming that the stratigraphy corresponds to that of the described core BP090055 (view fig. 17 for projection), this would suggest that both the

Naaldwijk and Boxtel Formations are absent in the southwestern part, however, the Eem and Egmond Ground Formations are present here. It is striking to see the Eem and Egmond Ground Formations so close beneath the surface and directly underneath the Bligh Bank Member of the Southern Bight Formation.

Unit D contains the distinctive facies of the Brown Bank Formation as described in Ch. 5.1, which makes this identification very plausible.

Because of the general low amplitudes and acoustic transparent facies, unit E is probably consisting of mainly sandy sediments and because of its stratigraphic position probably part of the Eem Formation. However, given that borehole BP090055 contained a 12 meter-thick silt deposit of the Egmond Ground Formation and was taken only 100-200 meters away, it is likely that part of unit E belongs to the this silt deposit of the Egmond Ground Formation. Note that it is unknown what the decisive reasons were for the identification of Egmond Ground Formation of this deposit.

Unit F appears to have a sedimentary composition varying relatively more in grain size with respect to unit E and unit A-E due to the local high amplitude reflections. Observing the projection of core BP090055, the boundary between unit E and F appears to be the boundary between the Egmond Ground Formation and the Yarmouth Roads Formation, despite the fact that the core Formation boundary projection does not quite match. However, in BP090055 is a meter-thick clay layer described at the bottom of what was identified as the Egmond Ground Formation. Therefore, it is more plausible that this horizon dividing units E and F correlates to this bottom layer of the Egmond Ground Formation. The rest of unit F is probably an expression of the Yarmouth Roads Formation.

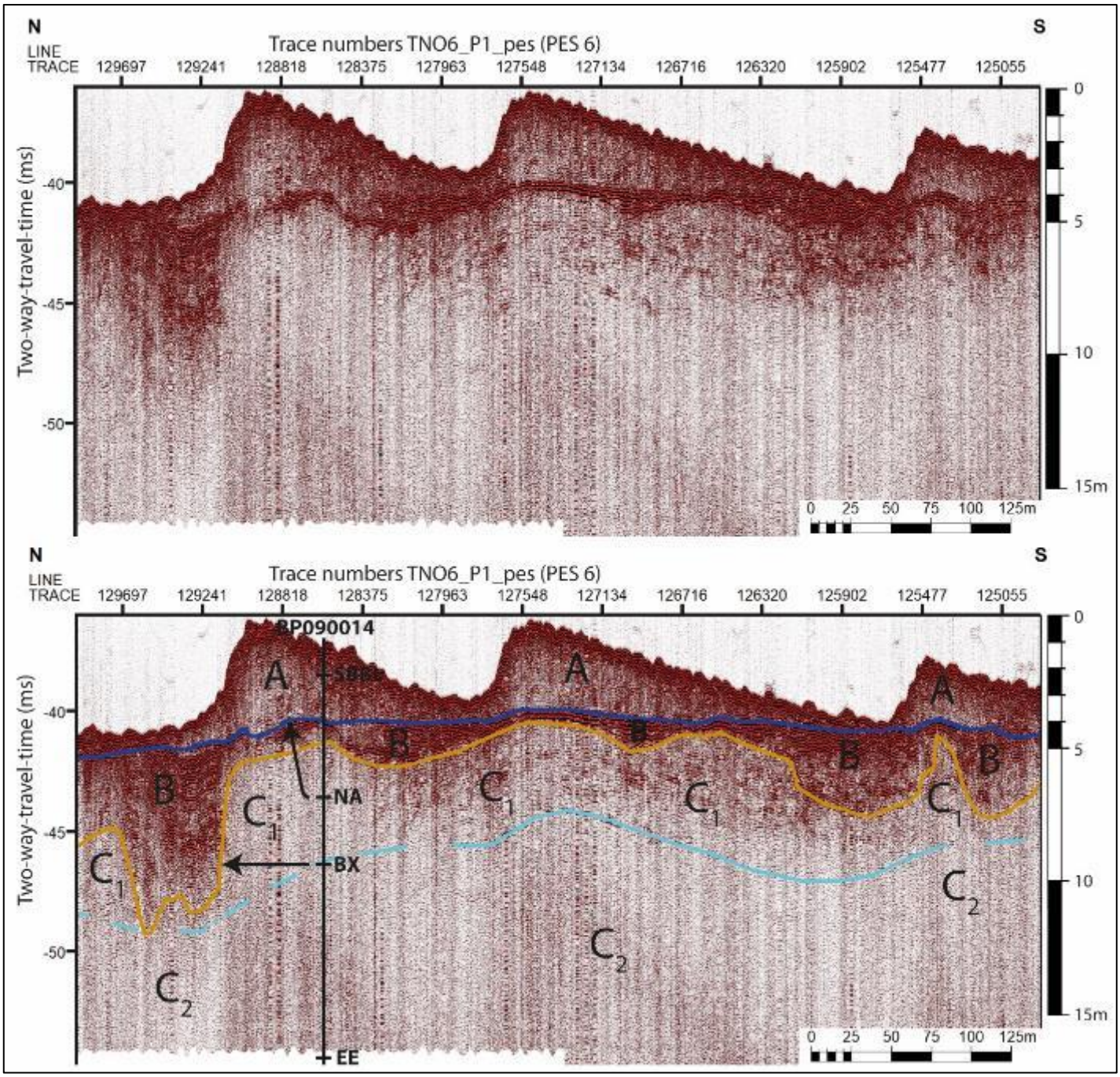

Figure 18: PES seismic data from segment TNO6_P1_PES. Approximately 13 meters below the seabed are shown over a horizontal distance of approximately 0.5 km. Top panel: clean seismic data. Lower panel: interpretation with a sediment core projected on the profile with the tops of various lithostratigraphic units: SBBL (Southern Bight Formation, Bligh Bank Member), NA (Naaldwijk Formation), EE (Eem Formation). View fig. 12 for the location of shown section.

Description figure 18

The seismic profile of figure 18 is divided into three units (A, B and C), of which unit C is subdivided into C_1 and C_2. Unit A comprises the asymmetric mega ripple structures or sand dunes with internal cross lamination, at the top and is bordering unit B by the dark blue horizon. Unit B consist of relatively continuous high amplitude reflections and local wavy reflections and multiple channel-like bodies. At first glance, it might seem that colour shading heavily impacted the image right where unit B is located, due to the high amplitudes beneath the troughs. However, the reflections continue beneath the crests of the dunes, where otherwise acoustic blanking would be expected, which demonstrates that the high amplitude facies is natural in origin. The border between unit B and unit C is marked by a pronounced horizon, except for north of trace 129241 and south of 125902 where unit B is transitioning diffusively into unit C. Where this horizon between units B and C is absent is the border only drawn on the basis of facial differences. Subunits C_1 and C_2 show some facial similarities, such as overall low amplitudes or a relatively transparent character, however some differences as well. For example, subunit C_1 contains more relatively continuous reflections of higher amplitude with respect to C_2 which has a clear homogeneously acoustically transparent facies. The light blue boundary between subunits C_1 and C_2 is put on a curving horizon and is extended to the North and South where the course of this horizon is less pronounced. The continuous reflections of subunit C_1 follow the curving horizon concordantly. To the North and South, the facies of subunit C_1 is more chaotic and locally diffuses into unit B.

Interpretation figure 18

Unit A in Figure 18 has the characteristic facies and morphology of the Southern Bight Formation as described in Ch, 5.1 and shown in Fig. 13 and 14. The orientation of the asymmetrical sand dunes suggests a transport direction to the North (View Fig. 7; Stow, 2007).

Unit B contains high amplitude reflections that could indicate peat, clay or coarse shell material. However, Holocene peat, clay or shell deposits are not known from described cores from the nearby area. Clay or shell deposits could have formed at mudflats or other near-coastal environments of for example the Naaldwijk Formation (Rijsdijk et al., 2005; TNO-GDN, 2022a), which is identified in core BP090014, albeit at about 3 meters greater depth. The Core BP090014 was cored relatively close to the seismic line (approximately 100 metres), yet the depths of the identified formations do not completely match the interpretation in Fig. 18. The incisions from unit B into unit C are probably cut by channel systems that are present in near-coastal environments. Taking all aforementioned into account, it is probable that unit B here is an expression of the Naaldwijk Formation.

The low amplitude facies of unit C suggest a sandy deposit, of which subunit C_1 is probably more stratified with layers of varying grain sizes and subunit C_2 consists of a nearly homogeneous sand deposit. The Kreftenheye Formation does occur around this part of the seismic line, however it has probably only been identified in a few neighboring cores. It is unclear whether unit C or one of its subunits could be an expression of the Kreftenheye Formation. Core BP090014 shows the Boxtel Formation being present here. Despite the top of the Naaldwijk Formation being too deep, the depth of the top of the Boxtel Formation does correspond to the boundary between unit B and C. However it does correspond to the depth of the border between subunits C_1 and C_2 as well, which makes it debatable whether unit B and

C_1 are not both part of the Naaldwijk Formation. In addition, sandy deposits are a large part of the Naaldwijk Formation as well. Considering the depth profile of the units, the deviation between the lithostratigraphy of core BP090014 is understandable. If the core had been 100 meters further from its current projected spot, large lithological differences could have occurred. Furthermore, the upper limit of the Eem Formation, which is also distinguished in BP090014, is at too great a dept for this PES seismic section or not visible at depth.

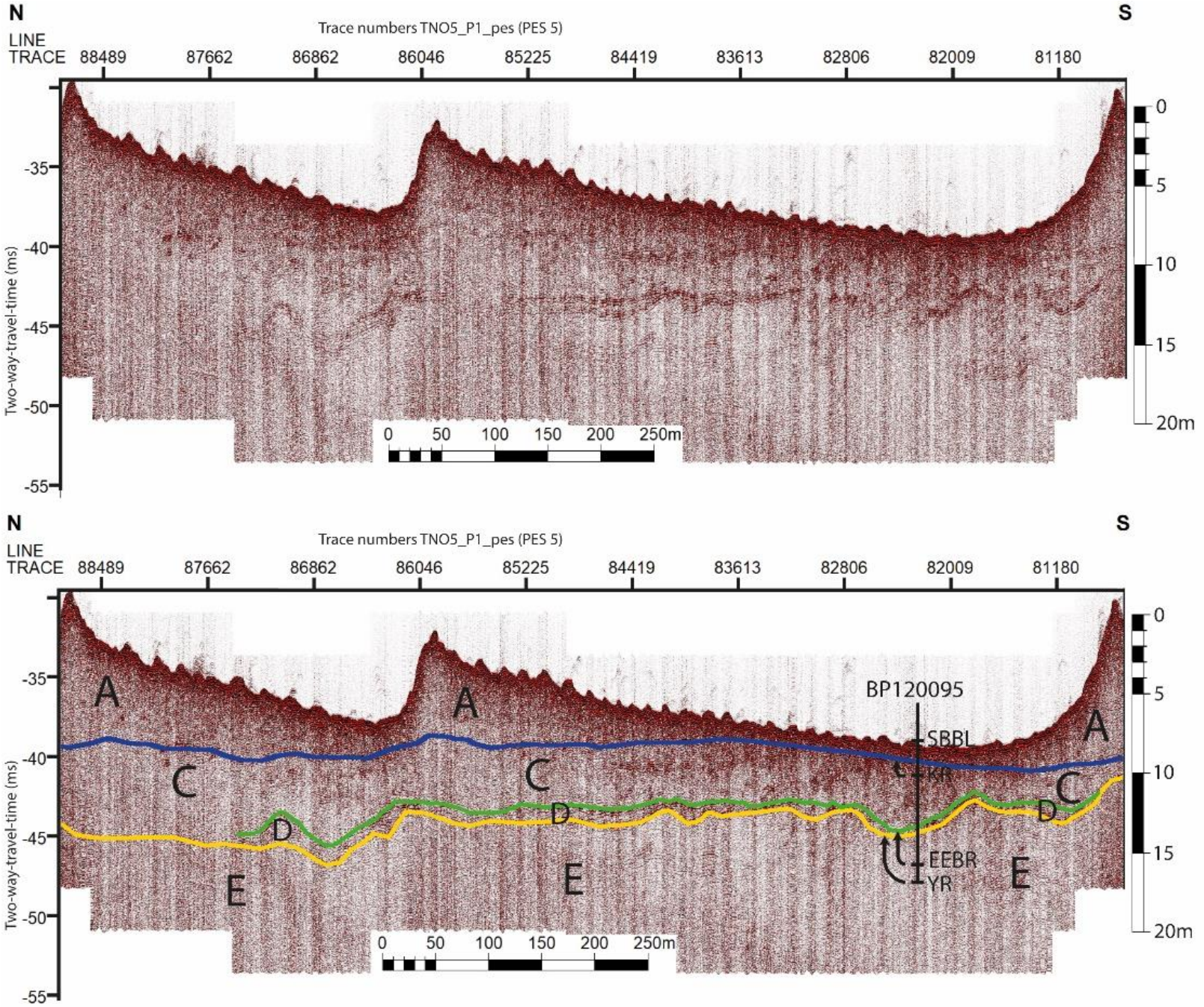

Figure 19: PES seismic data from segment TNO5_P1_PES. Approximately 15 meters below the seabed are shown over a horizontal distance of approximately 1 km. Top panel: clean seismic data. Lower panel: interpretation with a sediment core projected on the profile with the tops of various lithostratigraphic units: SBBL (Southern Bight Formation, Bligh Bank Member), KR (Kreftenheye Formation), EEBR (Eem Formation, Brown Bank Member), YR (Yarmouth Roads Formation). View fig. 12 for the location of shown section.

Description figure 19

In figure 19 four seismostratigraphic units are identified (A, C, D and E) which are bounded by three horizons (blue, green and yellow). The visible relief in the dark blue horizon is a pull-up effect as seen in previous PES figures. The horizon appears to be shallower below the crests of the dunes and appears deeper below the troughs. However, this curved horizon is in reality probably almost flat, horizontal. Furthermore, the sediment core BP120095 with its lithostratigraphic interpretation is projected on top of the seismic data in figure 19.

Unit A is characterized by the sand waves with internal foreset laminations and smaller scale ripples on their stoss side. Unit C has a varying facies with more chaotic higher amplitude facies between traces 83613 and 81180 and more transparent facies on the left. Furthermore, it seems that the amplitudes of unit C have been reduced by seismic blanking below the crests of the sand dunes. Unit D is put on an area with more continuous reflections that disappear at both the northern and southern side of the profile. Note that unit D and the green horizon are perfectly concordant to the yellow horizon, even in its depressions and highs. Therefore, it is not clear whether unit D is a thin draping deposit that follows the existing topography of the yellow horizon or if unit D is a base layer of unit C with different facies and therefore a sedimentologically different content. The yellow horizon which forms the upper limit of unit E, has an erosive character. Unit E shows in general a relatively transparent facies with locally some chaotic low amplitude reflection patterns.

Interpretation figure 19

Unit A is probably part of the Southern Bight Formation and consist of sand dunes pointing to a northbound transport. Unit C, given the chaotic seismic facies, is a sandy unit and probably part of the Kreftenheye Formation, which also occurs in this area (view figure 4). In addition, this is supported by the identification of the Kreftenheye Formation in core BP120095. Considering the fact that the Kreftenheye often has an erosional base, it would not be expected (however, not impossible) to find a perfectly concordant deposit of unit D at the base of the Kreftenheye Formation. Therefore, if unit D is in fact a bottom part of the Kreftenheye Formation, the incision into unit E has occurred prior to deposition or partially during deposition of the Kreftenheye Formation. Unit D could then be a coarse sedimentary base of the Kreftenheye Formation. However, since BP120095 contains a thin silty clay deposit at similar depth that is identified as the Brown Bank Member, unit D is more likely to be an expression of the Brown Bank Formation. Furthermore, its facial resemblance to previously described unit D (Brown Bank Formation) with clay-sand or silt intervals, suggests that unit D has a similar content and supports this latter interpretation. In addition, the Kreftenheye Formation contains virtually no clayey deposits.

Furthermore, the relatively transparent facies of unit E would suggest that this unit contains a relatively homogenous sandy deposit and may be part of the Eem Formation. However, in the sediment core BP120095, the Yarmouth Roads Formation is identified Since the Yarmouth Roads Formation does contain all kinds of sandy deposits (e.g. marine, coastal, deltatop, fluvial etc.) it is plausible that unit E here is indeed the Yarmouth Roads Formation. Furthermore, The Eem formation would be absent at this area based on its distribution shown in figure 5.

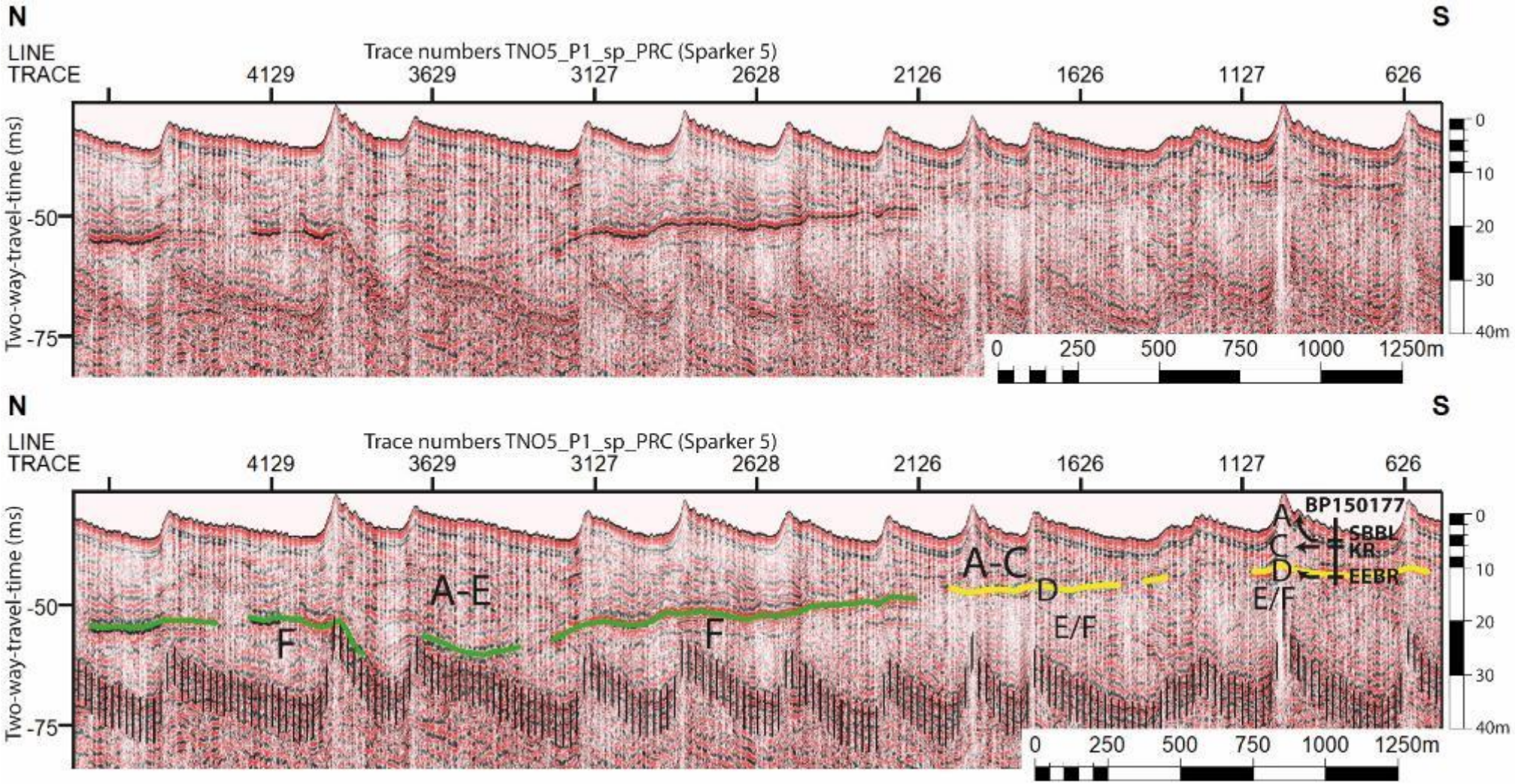

Figure 20: Sparker seismic data from segment TNO5_P1_sp_PRC. Approximately 40 meters below the seabed are shown over a horizontal distance of approximately 5 km. Top panel: clean seismic data. Lower panel: interpretation with a sediment core projected on the profile with the tops of various lithostratigraphic units: SBBL (Southern Bight Formation, Bligh Bank Member), KR (Kreftenheye Formation), EEBR (Eem Formation, Brown Bank Member). View fig. 12 for the location of shown section.

Description figure 20

The seismic data of figure 20 are divided into two units in both the North and the South. The upper unit is, as in previous sparker images, somewhat affected by a strong seafloor reflection. The seismic facies below is chaotic with non-parallel usually short-traceable reflections. The lower unit, beneath the green and yellow horizons, has also a chaotic facies and is however, more transparent with respect to the upper unit. There seems to be one horizon that is marked with the green line in the northern part and with the yellow line in the southern part. However, it is more likely that these are two different horizons reflecting different stratigraphic boundaries. Consequently, the northern part is divided into unit A-E and unit F and the southern part into unit A-C and unit E/F with the yellow horizon presenting unit D (top and base together). Furthermore, the sediment core description BP150177 is projected on top of the seismic data in figure 20.

Interpretation figure 20

The green horizon on the left is possibly a relatively old surface that caused a high amplitude reflection due to a strong acoustic contrast. With the relatively transparent facies below the green horizon possibly representing more sandy deposits and relatively higher amplitudes above the green horizon representing layers of finer sediments within sandy deposits. Unit F might be an expression of the Yarmouth Roads Formation (which comprises a wide variety of deposits including sands), although this cannot be substantiated with evidence from the BP150177 core because it penetrated not deep enough.

The top of unit F is varying greatly in depth. Notably this is also the case in figures 15 and 16 where unit F is locally partly at the same depth as unit D. Unit A-E on top of that is probably consisting of the Southern Bight Formation and the Kreftenheye Formation with presumably no deposit of the Eem Formation since no deposits have been identified in this exact area (view fig. 5;), although Eem Formation deposits may have been preserved locally. Unit A-C at the right probably consists of the Southern Bight Formation on top of the Kreftenheye Formation. Unit D is probably a thin but acoustically pronounced layered fine sedimentary deposit and probably an expression of the Brown Bank Formation. Which is consistent with the presence of the Brown Bank Formation in core BP150177 at about the right depth. Furthermore, Unit E-F is probably consisting of a sandy deposit that can be part of an Eem Formation remnant, despite the fact that it is still unidentified in this area (view figure 5). Another option could be that unit E/F here is the Egmond Ground Formation, however, its distribution is sparse and unclear and it is therefore not expected to be present at unit E/F. Besides, unit E/F could be entirely composed of the sedimentary diverse Yarmouth Roads Formation. In the end, there is no very clear variation in seismic facies in the units A-C, A-E and E-F, that can provide hard evidence about the sedimentological diversity

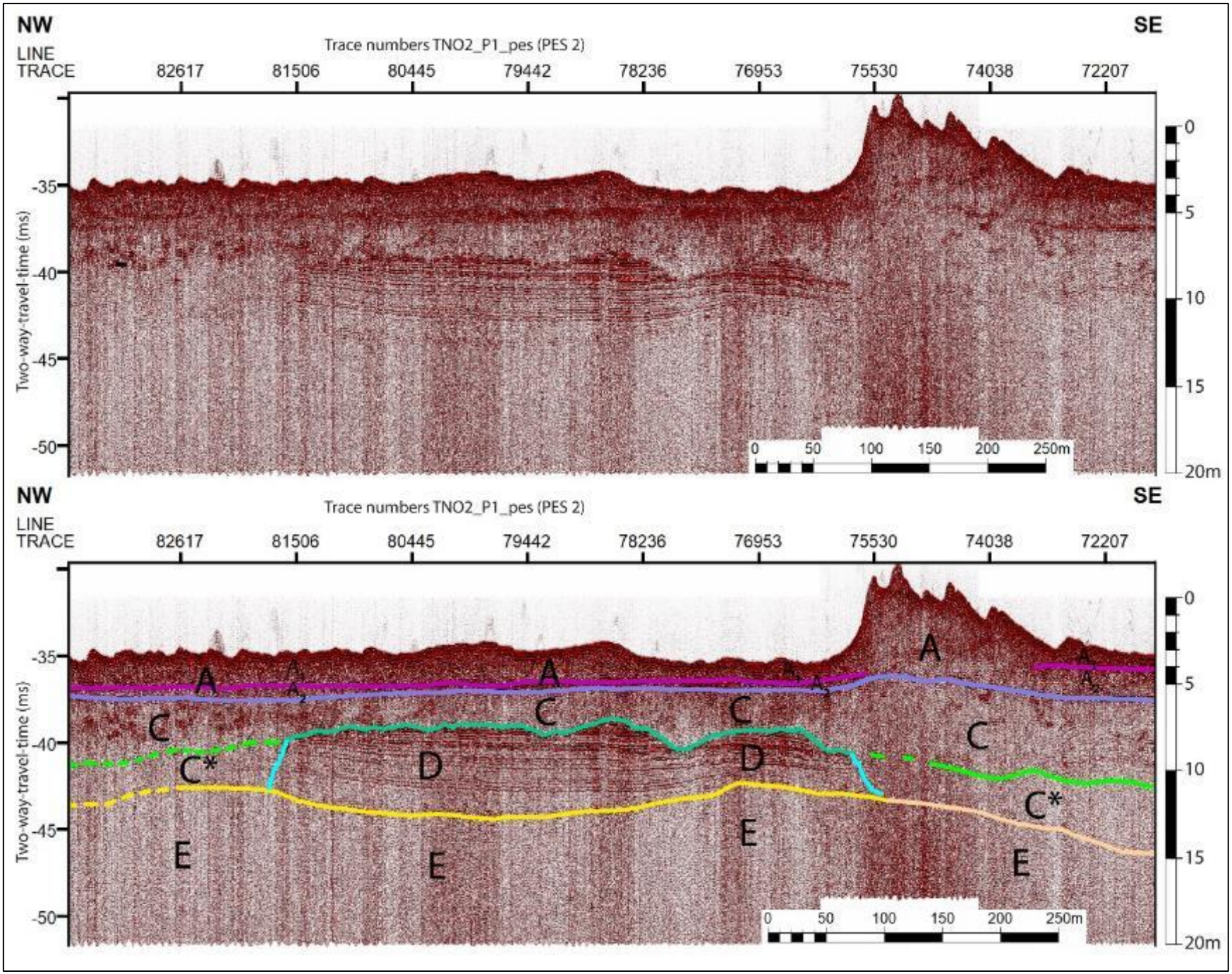

Figure 21: PES seismic data from segment TNO2_P1_PES. Approximately 15 meters below the seabed are shown over a horizontal distance of approximately 1 km. Top panel: clean seismic data. Lower panel: interpretation. View fig. 12 for the location of shown section.

Description figure 21

In figure 21 four units are distinguished (A,C,D,E). Notable is the subparallel laminated deposit in the center, which is defined as unit D and is truncated at the top and at its left and right sides.The boundary horizon between units A and C is indicated with the lilac coloured line. Furthermore, the boundary horizon between unit C (including C*) and D is indicated with the dark green and light blue lines and besides, the bounding horizon between unit E and units D and C* is indicated with the yellow line.

Below the sand dune (between traces 75530 and 74038) the seismic data have local higher amplitudes. This is striking, because relative acoustic energy loss usually occurs when it has to pass through a thicker deposit, which often result in seismic blanking as seen in previous figures. Therefore this is probably an artifact that caused by initial data processing. Furthermore, the horizon that forms the boundary between units A and C (lilac coloured line) is a somewhat flat horizon except for the hump in this horizon exactly beneath the sand dune at the right of the frame, This hump is presumably a pull-up effect as seen in the previous PES seismic images.

An internal horizon is indicated with the fuchsia-pink coloured line which divides unit A into unit A_1 and A_2. Unit A contained in the previous PES data figures some oblique reflection patterns or cross lamination, that indicated the forests of the sand dunes. However, in figure 21 this is not really visible. The facies of unit A here generally contains high amplitude discontinuous reflections in a chaotic pattern.

The upper part of unit C has a chaotic facies with locally higher amplitudes and locally continuous reflections with mediocre amplitudes. Subunit C* is placed were unit C contained an acoustic transparent facies with low amplitude reflections.

Unit D consist of high amplitude, subparallel continuous reflections. From the top to the bottom do high amplitude thin spaced reflections gradually change into relatively lower amplitude reflections spaced by thicker lenses of low amplitudes. Reflections terminate on the top, right and left unit boundaries. Furthermore, unit D is draped onto unit E.

Unit E has an acoustic transparent facies and shows no clear distinguishable reflections, however, the seismic facies is dominated by noise (e.g. vertical striations and colour shading).

Interpretation figure 21

Unit A is probably part of the Bligh Bank Member of the Southern Bight Formation. Considering the asymmetry of the sand dune, the dominant sediment transport is in a northwesterly direction (view figure 7; Stow, 2007). Notable is the subhorizon in unit A, which might be formed due to an upward shift of the base layer of the moving sand dunes, which resulted in burial of the lower horizons and basal horizon of unit A. Therefore unit A_2 is just an older remnant of the Southern Bight Formation

Since there is a facies difference between upper unit C and C*, it was considered that unit C* was not part of unit C and could be its own unit or be part of unit D. That the upper boundary of unit C seem to be the extension of the erosive upper horizon lies between units C and D is speaking for the last theory. However, the facial difference between unit C* and unit D is even

greater. Moreover, there could have been a truncation phase after deposition of C* and before deposition of the upper part of unit C. The chaotic character of the upper part of unit C might indicate local coarse grained river beds of the Kreftenheye Formation. The occurrence of the Kreftenheye Formation is supported by the distribution map of figure 4. The acoustic transparent facies of the lower subunit C* are probably reflecting a homogenous sandy deposit, which suggests this is an aeolian deposit of the Boxtel Formation. However, it is unlikely that the truncation of unit D has occurred in the same environment as the deposition of subunit C*. The truncation probably happened before the aeolian deposition.

Unit D consist of a layered deposit of clay, silts and sand intervals and is probably part of the Brown Bank Formation, because it shows the characteristic features as previously described in Ch. 5.1. Note the facies transition with the relatively acoustically transparent lenses, representing sandy intervals, becoming less and thinner upwards. Presumably, this shows that the environment was subject to recurrent pulses of stronger current bringing coarser sediment in a predominantly low current environment with deposition of fine material. From the bottom to the top of unit D the strong current periods or moments have become shorter and or weaker. The Brown Bank Formation is not known to be present at this exact location, however, relatively small and isolated remnants of the Brown Bank Formation have been found nearby (view fig. 5).

The acoustic transparent facies of unit E indicates a homogenous sandy deposit. That could be part of the Eem Formation, Egmond Ground Formation or the Yarmouth Roads Formation. Despite the fact that the Eem Formation is not known from this exact area, several remnants of the Eem Formation have been identified in the area (view Figure 5). Therefore, it is plausible that the Eem Formation is preserved here as well. In addition, with the Brown Bank Formation on top, which is usually on top of the Eem Formation in the northwestern part of the VLIZ line, it is likely that unit E here expresses the Eem Formation. Nevertheless, it cannot be excluded that (part of) the homogeneous sandy succession shown here in unit E is the Yarmouth Roads or Egmond Grounds Formation.

6. Overarching discussion

In this section the questions concerning the stratigraphical extent and depositional environment of the Brown Bank Formation, which were introduced in Chapter 1, are being discussed through an outline of the depositional history of the southern North Sea study area. The results and interpretations of the other seismostratigraphic units are also discussed alongside. However, the stratigraphic architecture and integrated stratigraphy of the VLIZ line are being discussed first.

6. 1 Stratigraphic architecture

In this section the vertical and lateral distribution and succession of the seismostratigraphic units, as identified in this study, are discussed. View figure 22 for the schematic profile of the entire VLIZ seismic line.

Unit A is almost everywhere at the surface. However, unit A has not been identified around the Eurogeul and the Maasvlakte extraction pit and is probably partly excavated. In addition, unit A is also not identified at some parts of the tidal ridges. However, unit A is presumably covering the tidal banks almost completely as well, but it was not distinguishable everywhere. Unit A is generally less than 4 meters thick (hight of sand dunes). Furthermore, unit A is interpreted to be the Bligh Bank Member of the Southern Bight Formation (Cameron et al. 1989; Rijsdijk et al. 2005; TNO-GDN, 2022c). Although the gravelly Buitenbanken Member might be present at the surface locally, no different seismic facies was identified that would indicate the presence of the Buitenbanken Member (TNO-GDN, 2022d).

Unit B is only at a few places identified, namely at the Northwest (view figure 14) representing a sandy facies with foresets near the centre of the VLIZ line (view Fig. 18), where it represented a transition of sandy deposits to muddy intertidal, coastal plain or salt marsh deposits. It is almost certain that unit B at the latter area is representing the Naaldwijk Formation. However, on the northwestern location it is debatable whether unit B here is part of the Naaldwijk formation or should rather have been included in unit C and is representing the Boxtel Formation. It is probable that unit B has often been overlooked, due to the resemblance of the sandy facies of unit B with respect to units A and C. It is therefore likely that the Naaldwijk formation is present in more places that are now mapped as unit A or C.

Unit C is present at almost the entire length of the VLIZ seismic line, although unit C is relatively thin in some northwestern places where a thin deposit of the Boxtel Formation is preserved on top of the Brown Bank Formation (unit D) and where it is also truncated by the Southern Bight Formation (unit A) on top. Only at the single location found where the Eem Formation (unit E) is located directly beneath the Southern Bight Formation (view Fig. 17),

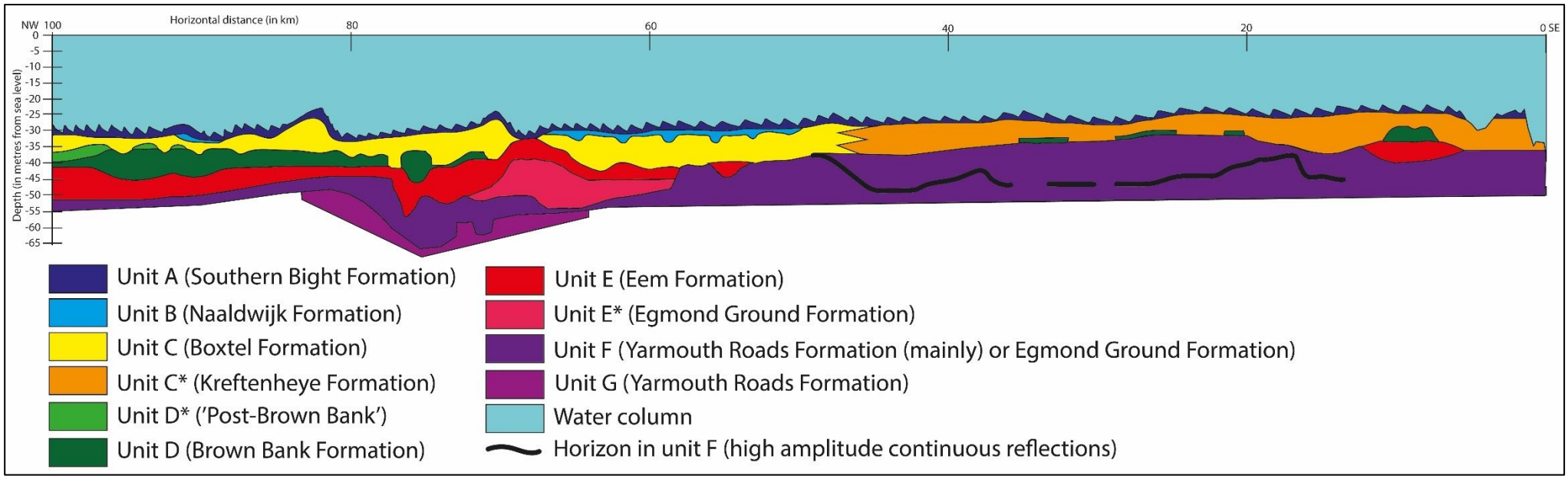

Figure 22: Schematic profile of the entire VLIZ seismic line with combined interpretations of PES and sparker data and the HKW sparker segments.

was unit C missing from the succession, which was identified due to the sediment core descriptions of BP090055. Furthermore, in the northwestern part is unit C almost completely represented by the Boxtel Formation, because indications for the presence of Kreftenheye Formation in this area were barely found. Relatively small-scale incisions of unit C into unit D were found (view Fig. 13), which were linked to small scale streams, which fall within the set of depositional environments of the Boxtel Formation. Contrary, unit C in the southeastern area consist mainly of deposits of the Kreftenheye Formation and comprises locally deposits of both formations. It is to be expected that deposition of the Boxtel Formation (and associated local small scale erosion) in the Northwest and erosion and deposition of the braided rivers (that are part of the Kreftenheye Formation) in the Southeast, occurred at least partly simultaneously. However, most of the Kreftenheye Formation deposits are expected to be younger compared to the Boxtel Formation deposits that are found in the southeastern part. However, a more detailed analysis is needed to confirm this theory.

At every location where unit D is identified is the Brown Bank Formation shown, which can be determined with great certainty due to the unique horizontally laminated high amplitude seismic facies. Except for the upper part of unit D in the northwest which is indicated with D* in figure 22, which deposit is probably of similar fine grained composition (clays, silts and sands) as the Brown Bank Formation and is presumably a younger unit and the same unit as the one Waajen referred to as the ‘post-Brown Bank’ (I. M. Waajen-Labee, personal communication, May 10, 2024).

Unit D generally has substantially thicker deposits in the northwestern part and is however, also missing locally, or is strongly eroded, leaving only thin deposits preserved. Unit D has completely disappeared in the middle of the seismic line (view Fig. 22), due to erosion of the Meuse-Rhine (Kreftenheye Formation, unit C). In the eastern part, however, very thin deposits (less than 1 meter) of unit D have locally been preserved (view Fig. 19 and 20). However, in the far east a thicker deposit is preserved (view Fig. 21).

It is striking to see that unit D at this southeasternmost location contains almost identical facies compared to its facial presence in the Northwest. This means that the Brown Bank Formation in the Southeast is reflecting a similar environmental succession as in the Northwest. This insight can provide more clarity as to whether the Brown Bank Formation would landward gradually transition into the Kreftenheye Formation. This does not seem to be the case. Despite the shallower presence (approximately 6 meters) of unit D in Figure 21.

This difference in depth between the northwestern part and the southeastern part is presumably just the result of slightly faster subsidence in the Northwest. The stronger subsidence can be inferred from the fact that the base of the Quaternary deposits lies about 150 meters deeper in the Northwest compared to the Southeast of the VLIZ line as can be observed in Figure 12.14 of Knox et al. (2010). In addition, the Brown Bank Formation is often deposited in existing depressions such as the pronounced channel (view figures 14-16) and the undulating base at the far northwest. Waajen et al. (2024) reported buried sand dunes at the base of the Brown Bank Formation from seismic interpretations of a more eastern location (Het Gat). Furthermore, Eaton et al. (2020) reported buried dune-scale bedforms in a sandy layer in between the characteristic subhorizontal laminated Brown Bank Formation seismic facies at a more northwestern location in the British domain. However, no buried sand dunes have been observed in or at the base of the Brown Bank Formation in the VLIZ and HKW seismic lines.

Although the base of the Brown Bank Formation appears to be highly embossed, this appears to be primarily an erosive pattern. Still, to be sure, there should be looked at the possible occurrence of buried sand dunes.

Furthermore, it seemed as if a second, often deeper Brown-Bank like unit could be seen in the sparker data as several stacked high amplitude reflections. However, this has been interpreted as an older surface within unit F and the Yarmouth Roads Formation instead of unit D.

Unit D was subdivided in multiple subunits in the interpreted HKW seismics (view figure 16), that seemed to prograde to the West or Northwest. The youngest of these subunits (D_1) probably has a sandier composition, indicating a more energetic environment. This could be a fluviatile environment or a coastal to marine environment. When the transition trough subunits D_2 to D_1 in figure 16 reflects the same transition as reported by Tizzard et al. (2014) it would point towards the latter option.

The seismic facies unit E is present in the northwestern part below unit C and D and on top of unit F. In addition, it is found at a relatively small section in the Southeast. This was probably a remnant. Therefore, unit E was initially deposited almost everywhere along the VLIZ line, but subsequently largely eroded. Furthermore, in the HKW sparker data (view Fig. 16) is unit E locally lost and truncated by unit D, which was deposited directly on top of unit F. This is not shown in Figure 22, because this figure presents the profile along the VLIZ line.

Unit E is most often representing the Eem Formation. However, around kilometre 60-70 unit E is split with the upper part representing the Eem Formation and the lower part the Egmond Ground Formation. Striking is the fact that both formations seem to form a stack of mount deposits, which seems unnatural. Therefore, their morphology will probably be slightly different in reality. The placement of these formation boundaries was determined based on information from core BP090055 (view figure 17).

The transition from the Eem Formation to the Egmond Ground Formation was not characterised by a sharp facies change. In fact the transition appeared diffuse with fairly transparent facies above and below the level of the presumed formation boundary. Due to the similarity of the often transparent facies of the Eem Formation and the Egmond Ground Formation, they are difficult to distinguish from each other in the sparker data. Because, both consist largely of interglacial marine sands (Rijsdijk et al. 2005). In addition, the Egmond Ground Formation is not identified in the PES data at all, however this is mostly due to the Egmond Ground Formation being relatively rare or occurring at greater depth.

Furthermore there has also been doubt between unit E or the Eem Formation on the one hand and unit F or the Yarmouth Roads Formation on the other hand: Note that in Figure 19 unit E was identified on the basis of fairly acoustic transparent facies with few low amplitude continuous reflections beneath facies zones that were identified as unit D and C. However, due to the indication of Yarmouth Roads Formation at this depth (as was identified in the sediment core BP120095), it was decided to show this part in the profile as unit F. Because unit F should represent the facies of the Yarmouth Roads Formation. However, at this location (view Fig. 12) the facies fits better in unit E, while these deposits are probably part of the Yarmouth Roads Formation. Which, by the way, consists of a great diversity of low energy marine, deltaic, delta-top and fluvial deposits (TNO-GDN, 2022j; BGS, 2023b). Yet, this choice is debatable.

There could also be local Rhine-Meuse sediments from the Saalian (MIS 6) and earlier (MIS 11-7) underlying the Eem Formation. However, these could also have been eroded with the sediments of the Eem Formation. Indications for the presence of these (older) Rhine-Meuse sediments could be found in the sparker data. However, these have not been identified. Unless, unit E in the HKW sparker data (view Fig. 10, E4), which contained hyperbolic structures in the seismic facies, which are indicative of gravel deposits, are in fact reflecting these Rhine-Meuse sediments instead of the Eem Formation. However, the facies E4 (Fig. 10) shows a more uniform occurrence of gravel, while in the Eem and Kreftenheye Formations gravel mainly occurs in lags or channel floor deposits (TNO-GDN, 2022e).

Unit F is present along the entire VLIZ line and the majority is probably representing the Yarmouth Road Formation. Despite the fact that the Egmond Ground Formation is not identified in unit F, it is plausible that local occurrences have been missed in the central and southeastern part. In both formations, in addition to sands, clay (and silt) layers also occur, making the seismic facies difficult to distinguish.

A sharp horizon in unit F (view Figure 22) is locally distinguishable along the VLIZ line by high amplitude relatively continuous reflections. This makes unit F locally facially similar to unit D in the sparker data (view Figure 15 and 20). As mentioned previously, the high amplitude continuous reflections of unit F in Figure 20 were interpreted as a buried surface, which is part of the Yarmouth Roads Formation. It is striking that this surface is relatively strongly embossed. Furthermore, the fact that this horizon is only visible in the sparker data and absent in the PES data even at the places where it should be shallow enough to be detected is striking. This probably means that this horizon consists of a relatively gradual sedimentary transition that appears homogeneous and contrastless in small scale resolution of the PES data and forms however, a strong acoustic contrast in the sparker data. Furthermore, despite the fact that this horizon or old surface is recognizable at multiple places around the centre and the southeast of the line, it is absent in more places. This is probably because, it has partly been eroded.

Other internal structures in unit F are not visible in the VLIZ sparker data, however, they can fortunately be identified in the HKW sparker data (view Fig. 16). Furthermore, unit G is only distinguished in the HKW data. The sequence of unit G and F (including the subunits) reflect multiple phases of deposition of mostly sand-clay intervals and erosion in a delta plain environment. Substantial erosion occurred between deposition of subunit F_4 and F_3 resulting in a canyon that was filled in with younger subunits of unit F and unit E. Strikingly, the channel of unit D (view Fig. 14 and 16) is located above this deeply buried canyon. This could show that this area was relatively unstable and/ or relatively stronger subsidence was occurring (perhaps due to compaction of clay layers), which allowed the channel to have formed here.

Furthermore, no glacial deposits have been identified along the seismic line in accordance with expectations (Cartelle et al., 2021). However, possible glacio-tectonic structures might have been found in unit F (view figure 16). However, the local oblique reflections in unit F are probably not pushed sediments and are nonetheless dipping layered deposits that appear steeper than they actually are due to the vertical scale exaggeration.

Unit G is only recognized in the HKW sparker seismic. A broader distribution is likely, however, cannot be determined. Unit G is probably also part of the Yarmouth Roads Formation. It is debatable whether unit G should have been classified as a separate unit and not as an older subunit of unit F.

6.2 Integrated stratigraphy & depositional history

An integrated stratigraphic interpretation of the entire length of the VLIZ and HKW seismic lines and the seismic facies units distinguished therein, is summarized in a single stratigraphic diagram (view Fig. 23). This stratigraphic diagram provides the chronological guideline for the depositional and climatic history of the southern North Sea study area, which is elaborated below:

During the Cromerian (MIS 19-13) there have been many transgressions and regressions in which the coastline has shifted across the study area. During the highest highstands, approximately the entire study area was under the influence of the sea, i.e. a shallow marine depositional environment. However, often the coastline was placed further north, causing coastal deposits and deltatop depositional environments to prevail in the area. During the lowstands, terraces were formed that were subject to erosion (Hijma et al., 2012; Eaton et al., 2020). Furthermore, rivers flowed that left their deposits behind (Eaton et al., 2020). These truncation phases are reflected in the multiple sequences of infilled incisions of mainly relatively high amplitude facies in the (sub)units F and G of figure 16, reflecting alternating clay and sand layers of the Yarmouth Roads Formation. Furthermore, the pronounced horizon that can be found in large parts of the Sparker data (view Fig. 18), may reflect subaerial exposure during one of these lowstand episodes.

During the Elsterian (MIS 12) periglacial continental conditions prevailed until the basin was flooded with the proglacial lake, bringing lacustrine conditions. These lacustrine deposits were probably eroded directly, first when the lake emptied and associated channel erosion and then by wave and tidal action during the multiple transgressions and regressions that have occurred during the Holsteinian interglacial (MIS 11). The shell-rich sands and clays of the Egmond Ground Formation have their origin in the coastal zone where shallow marine conditions prevailed at that time.

During the Saalian Complex (MIS 10-6) there were times when the Meuse and later the Rhine-Meuse flowed through part of the study area. Although they mostly flowed northwards because the Strait of Dover was closed again (Peeters et al., 2015; Peeters et al., 2016). The truncation phase that took place before deposition of the Eem Formation, might be due to relatively small-scale fluviatile erosion of the subaerial North Sea terrace. Which could have occurred during times when the surface was not or incompletely frozen. During the Saalian glaciation (MIS 6), periglacial conditions prevailed until he southern North Sea area flooded again by the proglacial lake (Peeters et al., 2015; Peeters et al., 2016). Later, after this lake had drained, the Meuse probably flowed through the southernmost part of the study area and possibly also the Rhine flowed in the Northwest. Although, it is not known whether the deposits of the Saalian Rhine and Meuse have been preserved around the study area. Nevertheless, the fact that these deposits have not been identified in the VLIZ seismics might point to complete erosion in this area. In this case these deposits were eroded by wave and tidal action during the Eemian transgression (MIS 5e).

During the Eemian (MIS 5e) the study area was flooded by the sea during a transgression. During the climate optimum, higher temperatures prevailed than are known from the Holocene (Laban & Van der Meer, 2022). The fairly transparent seismic facies of unit E were identified as sands of the Eem Formation, which were deposited in a shallow marine environment during

Figure 23: Stratigraphic diagram of all seismic facies units (A-G) and their interpretation.

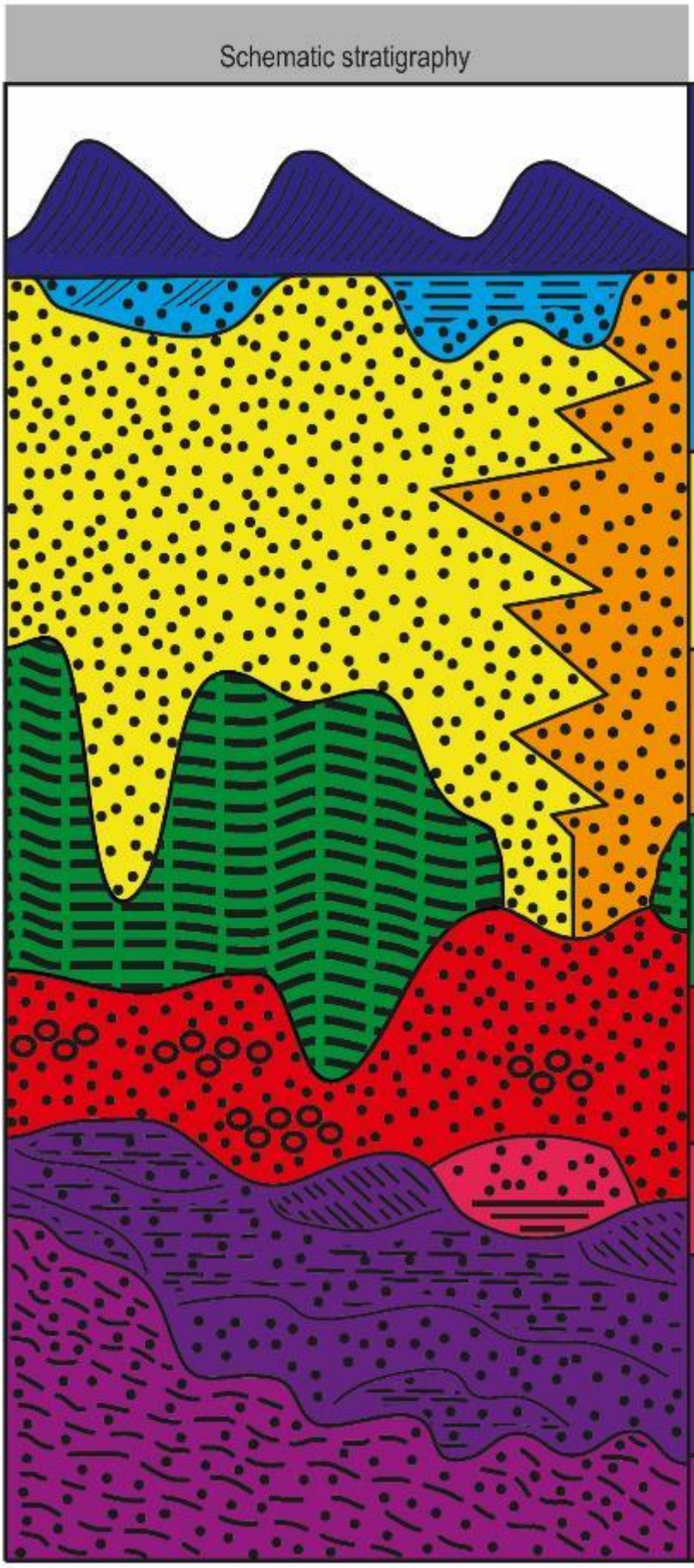

Seismic Facies Unit	Seismic signature	Sedimentology	Depositional setting	Formation (and Member)	Estimated age
A	High amplitudes, oblique reflection patters (forsets) & megaripples	Sands	High energy open marine	Bligh Bank Member of Southern Bight Formation	MIS 1, Holocene
B	Relatively High amplitudes, local continuous refl., oblique reflection patters & channels	Sands & clays	Coastal, shoreface, beaches, tidal basin to shallow marine	Naaldwijk Formation	MIS 1, Holocene
C	Acoustic transparent to chaotic, medium high ampl. refl. & local continuous oblique refl., parabola's	Sands	periglacial aeolian and small-scale fuvlial	Boxtel Formation	MIS 4-2, Weich-selian Plenigla-cial
C	Acoustic transparent to chaotic, medium high ampl. refl. & local channels	Sands	Braided and meander-ing fluviogla-cial	Kreften-heye Formation	MIS 4-2 Weichseli an-Plenigla-cial
D	Subparallel continuous, high amplitude reflections, draping patterns, lensen with low ampl.	clay or silt and fine sand inter-vals	Regressive lagoonal to lacustrine	Brown Bank Formation	MIS 5a, Odderade Interstadi-al
E	Acoustic transparent, local low ampl. continuous subparallel refl., hyperbola's	Sands and local coarse shell or gravel	Coastal to shallow marine	Eem Formation	MIS 5e, Eemian
E	Chaotic facies, continuous and discontinuous reflections	Sands and clays	Coastal to shallow marine	Egmond Ground Formation	MIS 11 Holsteini-an (?)
F	High amplitudes, continuous reflections, local oblique configuration, local acoustic-transparent	Sands and clays	low energy open-ma-rine deltaic, deltatop and fluvial	Mainly Yarmouth Roads Formation, also Egmond Ground Formation	MIS 13,11 Cromerian (?), Holsteini-an (?)
G	Rel. High amplitudes, continuous, wavy reflections	Sands and clays	low energy open-marine deltaic, deltatop and fluvial	Yarmouth Roads Formation	MIS 13, Cromeri-an (?)

the Eemian and the first part of the Herning stadial (MIS 5d). The subparallel continuous reflections that are shown locally at the top of unit E of the northwestern part of the VLIZ line (view Fig. 13 and Fig. 14), possibly show alternating layers of sand and finer material that could be deposited in a relatively low energetic environment (for example from a shallow, partly closed bay or lagoon) from the Herning The hyperbolic structures in the facies of unit E in the HKW sparker data (view Fig. 10) are presumably showing local gravel or shell beds from high energetic phases in a shallow marine environment. Hijma et al. (2012) mentions the local occurrence of gravel-shell beds in the Eem Formation as well.

With some uncertainty the following can be stated about the Weichselian Early Glacial: The transition from the Eemian to the Herning stadial (MIS 5d) was probably accompanied by a regression that turned the study area subaerial. In the following Brørup interstadial (MIS 5c) and the Rederstall stadial (MIS 5b), the study area probably experienced a transgression and regression that inundated the area with the sea followed by aerial exposure with probable additional erosion. The water depth changes just mentioned during the Early Glacial in the study area can be stated with relatively more certainty (Eaton et al., 2020; Waajen et al., 2024 and references therein: Spratt & Lisiecki, 2016). The erosion that occurred between deposition of the Eem Formation and before the deposition of the Brown Bank Formation probably occurred mainly during the regressions and lowstands of the Herning and Rederstall. This truncation phase formed the surface on which part of the Brown Bank Formation was deposited. However, because subunit D_4 is truncated by D_3 in figure 16, it has become known that at least one local truncation phase occurred during the accumulation period of the Brown Bank Formation. This could have been a submarine truncation, for example due to wave action.

Most of the Brown Bank Formation was probably deposited during the transition from the Odderade interstadial (MIS 5d) to the Middle Weichselian/ Pleniglacial (MIS 4; Waajen et al., 2024). A low-energy pro-deltaic environment formed with relatively little tidal flow. Eaton et al., (2020) showed that small scale sealevel variation in a few meters deep sea can probably cause relatively large topographical changes such as the creation of peninsulas, islands, semi-enclosed lagoons and fully-closed lakes, thereby reducing the influence of the open sea to a greater or lesser extent. Presumably the depositional environment of the characteristic facies (the subparallel continuous high amplitude reflections) of the Brown Bank Formation (unit D), originated in a pro-deltaic environment and/or in shallow bays or lagoon(s) with probably weak tidal activity and relatively little influence from the open sea, where clay deposition predominated, however, regular (possibly seasonal) episodes supplied sands and silts, which created the alternating clay-sand layers. The sandy lenses are the result of local channels that were formed either during these slightly higher energetic episodes. Or slightly stronger currents prevailed here constantly, resulting in sandy deposition.

Furthermore, the occurrence of cryoturbation and desiccation cracks and soil horizons indicate local subaerial episodes (Cameron et al., 1989). This suggests that brackish water lakes and lagoons also existed, because the environment was at least sometimes and at some places around sea level (Peeters et al., 2015; Peeters et al., 2016). Furthermore, the occurrence of local erratic pebbles, indicate the (episodal) presence of ice flows (Cameron et al., 1989).

The channel shown in figures 14, 15 and 16, has a fill showing the characteristic facies indicative of the low-energy pro-deltaic or lagoonal environment described above, however, with more oblique reflection patterns that are due to sedimentation into the relatively deep

depression. It is therefore unlikely that the deep incisive channel was formed under the influence of these low-energy flow velocities. Therefore, this is probably not a channel, it is however, a gradually filled depression with low-energy pro-deltaic deposits that originated as a channel. Since the base of the channel or depression is truncating older deposits of the Brown Bank Formation (view Fig. 16, note subunits D_3 and D_4), the base of the channel or depression was formed during the accumulation phase of the Brown Bank Formation and not before. Which means that this depression is formed near the presence of the Brown Bank Formation environment. Therefore, this depression was probably a main channel of the delta and carved by erosion. Because there was probably little tidal flow, this channel will have been eroded by drainage currents. After which this channel fell into disuse due to an avulsion. Whereafter, the resulting depression gradually filled up with the low-energy lagoonal pro-deltaic deposits.

The influence of the sea seemed to have generally decreased. Because, the general decreasing amount and thickness of sand layers upwards in unit D in most figures, is indicative of a decreasing extent of the higher energy pulses, that provide the deposition of sand. Contrarily the general energy level seem to increase again later, which can be deduced from the more transparent facies in D_1 of figure 16 relative to the other subunits of D, which is indicative of a more sandy deposit. This may indicate a transgression or the local opening of the lagoon and increasing influence of the sea, or a transition to more fluvial sands. Furthermore, the 'Post-Brown Bank' (View Fig. 22, D*) might represent a re-entry of the partly-closed submerged delta plain environment. Furthermore, the subunits of unit D distinguished in figure 16 show a progradational clinoform pattern indicating the Brown Bank Formation was prograding towards the Northwest. Moreover, no clear binary division has been found in the Brown Bank Formation, with the lower Brown Bank unit having a higher sandy content and the upper Brown Bank unit having a more clayey content as previously described by many authors (Bicket & Tizzard, 2015; Baten, 2019; Eaton et al., 2020; Missiaen et al., 2021; Waajen et al., 2024). However, several subunits have been found with slightly varying facies.

When the sea level fell further during the Middle Weichselian or Pleniglacial (MIS 4-3), the study area turned into dry land again. This was accompanied by soil formation and the formation of small-scale streams that cut into the underlying Brown Bank Formation and Eem Formation (view Fig. 13) and also left their deposits that are part of the Boxtel Formation. In the southeastern part, the braided river system of the Rhine-Meuse dominated, which largely eroded the deposits of the Brown Bank Formation and the Eem Formation and replaced them with mostly sands and gravel, that is part of the Kreftenheye Formation. Presumably deposits of the Yarmouth Roads Formation (and Egmond Grounds Formation) were also removed locally. Moreover, local remnants of the Brown Bank Formation and the underlying Eem Formation have been preserved as islands between the intersecting braided rivers (view Fig. 21). Because of continued climate cooling, permafrost and drifting sand deposits formed due to the scarcer becoming vegetation. The drifting sand deposits are part of the Boxtel Formation and are mainly preserved in the northwestern and central part of the study area. Furthermore, local drifting sand deposits of the Boxtel Formation could be present underneath or between the deposits of the Kreftenheye Formation. However, these deposits or the transition between these formations has not been found in the VLIZ seismics. Deposits of the Boxtel Formation and the Kreftenheye Formation formed largely simultaneously and both dominated part of the study area. The erosive base of the formations is formed by many moments of local truncation within the Kreftenheye Formation and Boxtel Formation and concurrent with lateral accumulation.

During the Holocene (MIS 1) transgression, the coastline was briefly located in the study area. This led to the formation of coastal deposits, such as clay rich tidal plains, salt marshes and beach deposits, that are all part of the Naaldwijk Formation. These have largely been eroded due to the ongoing transgression. However, local deposits have been found (view Fig. 18). Furthermore, during the early Holocene, local channels and tidal creeks made incisions into the underlying Weichselian deposits and were subsequently filled with deposits of the Naaldwijk Formation. After which rising sea levels gradually transformed the coastal plain of the study area into a high-energy shallow marine environment accompanied by sandy deposits part of the Southern Bight Formation (mainly Bligh Bank Member and locally Buitenbanken Member), in which sand dunes formed and moved and tidal banks formed and were carved from the subsurface. The deepening tidal basin caused by continued sea level rise, resulted in stronger tides and the creation of new and higher tidal banks and more erosion in the adjacent troughs (Le Bot et al., 2002; Mathys, 2010). Truncation of the underlying Naaldwijk Formation, Kreftenheye Formation and Boxtel Formation occurred in the high-energy marine environment where the Southern Bight Formation was deposited, where erosion occurs at the base of the moving sand dunes. This results in the flattened basal horizon that can be seen in most figures (view Fig. 13, 14, 19 & 21).

6.3 Methodological evaluation & recommendations for future research

This section reflects on the method used and provides some suggestions for similar studies involving seismic interpretation. In addition, several starting points and unresolved or new questions for future research are raised regarding the Brown Bank Formation and the surrounding Formations.

It worked reasonably well to first view the VLIZ line as a whole and interpret it in little detail, whereafter the line was interpret in great detail from side to side, while the scale and amplitude scale were changed regularly for optimal visualization. However, this working method could have been much stricter, which may have resulted in missing out of certain horizons or certain insights. For example, each segment should have first been captured in one screen wide image, to help it become clearer quickly how certain sections were put together stratigraphically. This has been done sometimes for this study, however it has not happened structurally in every segment from the start. Furthermore, horizon interpretations could also have been drawn when fully zoomed out, that could possibly be replaced or adjusted later with a detailed line. Furthermore, it is useful to name or number seismic horizons, because, this helps to discuss these horizons more structurally. In this study, horizons were only referred to on the basis of colour, however, codes were used in the Petrel workbook to organize the horizons.

Furthermore, this study helped identifying interesting locations to acquire sediment cores that contain the Brown Bank Formation. Which have led to cores being extracted that contain the top part of the Brown Bank 'Channel', that is viewed in figure 14 (I. M. Waajen-Labee, personal communication, May 10, 2024). Because there are only a small amount of sediment cores taken around the northwestern part and therefore little reference material to compare seismic interpretations with, while this part could offer many important stratigraphic insights, obtaining new sediment cores from this region is extra valuable.

Unit D (the Brown Bank Formation) shows relatively high internal variation despite clear recurring features. In the PES data, unit D is locally more chaotic and shows sandy lenses and mounds (view Fig. 13). In other places the Brown Bank Formation shows more homogeneous lamination and draping patterns (view Fig. 14 and Fig. 21). It may be valuable to undertake a more detailed study of the internal variation of the Brown Bank Formation to gain further insight into the range of depositional environments in which it formed. Furthermore, the more acoustically transparent (sandy) subunit D_1 in figure 16 is interesting to discover whether the energetic change that led to a more sandy deposit has a fluvial or marine origin (Tizzard et al., 2024). Nevertheless, it should be considered whether small-scale environmental changes, which can be detected with detailed facies studies, are as valuable as large-scale seismic interpretations that can provide broader insights into Early glacial development and climatic history of the southern North Sea area.

Due to uncertainty about the distribution of the Egmond Ground Formation, uncertainty has also arisen in the interpretation of the mainly acoustically transparent facies of unit E. In addition, the Eem Formation and the transparent facies of the varying Yarmouth Roads Formation are indistinguishable without information from sediment cores. The ambiguity regarding the interpretation of unit E may also mean that older sandy deposits (often with acoustically transparent facies as in unit C) of the Saalian Kreftenheye Formation (MIS 6) have been overlooked. For example, there is the striking occurrence of hyperbolic structures in the

seismic facies of unit E in the HKW sparker data (view Fig. 10), which indicate the occurrence of gravel deposits. Could this perhaps be an older Rhine-Meuse deposit? This might be worth looking into. Furthermore, more insight into the distribution and variation of the Egmond Ground Formation and the Yarmouth Roads Formations is desirable, not only to learn more about these Formations and the environments and periods in which they were deposited, however, also to better distinguish between these formations and the Eem Formation.

7. Main conclusions

Seven facies units are recognized in the VLIZ and HKW seismic lines. Unit A represents the Bligh Bank Member of the Southern Bight Formation and unit B the Naaldwijk Formation. Unit C represents the Boxtel Formation in the northwestern part of the VLIZ line while unit C in the southeastern part generally represents the Kreftenheye Formation. Unit D represents the Brown Bank Formation, which was, based on the seismic facies, formed in a low-energy, pro-deltaic or lagoonal setting. This environment was dominated by clay deposition, with periodic higher energy pulses leading to sand deposition. Unit E represents the Eem Formation and locally the Egmond Ground Formation. Unit F represents the Yarmouth Roads Formation and possibly the Egmond Ground Formation locally. Unit G represents the Yarmouth Roads Formation as well.

The question whether the Brown Bank Formation transitions laterally along the VLIZ line into the fluviatile domain can be answered with a no. Due to the discovery of a remnant of the Brown Bank Formation near the southeastern end of the line that possessed no particularly anomalous facies from the Brown Bank Formation deposits in the Northeast, it can be deduced that the Brown Bank Formation does not transition gradually into a fluvial facies laterally along the VLIZ line. In addition, the Brown Bank Formation comprises erosional contacts with the Boxtel and Kreftenheye Formations everywhere.

A 500-900 meter broad deposit in the Brown Bank Formation with a channel morphology is probably not a channel. Because, it is unlikely that the relatively deep, incisive channel was formed in a low-energy environment, suggesting it is not a true channel. However, rather a gradually filled depression that was once a main delta channel that was abandoned due to an avulsion.

Acknowledgements

First and foremost, I would like to thank my supervisors, Dr. Timme Donders, Dr. Bart Meijninger, Dr. Sytze van Heteren, Dr. Freek Busschers and Irene Waajen-Labee MSc., for all the help, the useful input during the meetings, for the fun coffee chats (especially Irene), for their goodwill, for the strictness when I needed it and for providing me the opportunity to finish this thesis. I would also like to express my gratitude to Ina Vissinga-Schalkwijk for, among other things, arranging my contract and the rest of the geomodeling department for the good atmosphere, which made it a great time and for the amazing excursion to the Boulonnais. At last I would like to thank my intern-colleagues for the fun coffee chats and for making this this time enjoyable (especially: Marius Valk, Noémi Brunschwiler, Alessia Corbetta, Jeroen Carmiggelt and Martijn van Isselt).

References

- Amkreutz, L., Niekus, M., Schiltmans, D., & Smit, B. (2022). 'Beyond bycatch. The prehistoric archaeology of Doggerland.' *Grondboor & Hamer, Staringia 17*, 76(3/4), 167-187.

- Baten, A. (2019). The Late Pleistocene to Early Holocene Geology of the Brown Bank Are a in the Dutch North Sea. *Unpublished MSc Dissertation, Ghent University, Belgium*.

- Beets, D. J., & van der Spek, A. J. (2000). The Holocene evolution of the barrier and the back-barrier basins of Belgium and the Netherlands as a function of late Weichselian morphology, relative sea-level rise and sediment supply. *Netherlands Journal of Geosciences*, *79*(1), 3-16.

- Berton, F. & Vesely, F. F. (2016). 'Seismic expression of depositional elements associated with a strongly progradational shelf margin: northern Santos Basin, southeastern Brazil.' *Brazilian Journal of Geology*, *46*, 585-603.

- BGS (2024a). Tea Kettle Hole Formation. In: BGS Linked Open Data – *British Geological Survey*. Accessed on March 27, 2024 via https://data.bgs.ac.uk/id/Lexicon/NamedRockUnit/TKH

- BGS (2024b). Cleaverbank Formation. In: BGS Linked Open Data – *British Geological Survey*. Accessed on March 27, 2024 via https://data.bgs.ac.uk/id/Lexicon/NamedRockUnit/CLBK

- Bicket, A., & Tizzard, L. (2015). A review of the submerged prehistory and palaeolandscapes of the British Isles. *Proceedings of the Geologists' Association*, 126(6), 643-663.

- Bohncke, S., & Wijmstra, L. (1988). Reconstruction of Late-Glacial lake-level fluctuations in The Netherlands based on palaeobotanical analyses, geochemical results and pollen-density data. *Boreas*, 17(3), 403-425.

- Le Bot, S., Van Lancker, V., Deleu, S., De Batist, M., & Henriet, J. P. (2003). 'Tertiary and quaternary geology of the Belgian Continental Shelf.' *PPS Science policy/Science Policy Office of Belgium*: Brussel.

- Busschers, F. S., Kasse, C., Van Balen, R. T., Vandenberghe, J., Cohen, K. M., Weerts, H. J. T., Wallinga, J., Johns., C., Cleveringa., P. & Bunnik, F. P. M. (2007). 'Late Pleistocene evolution of the Rhine-Meuse system in the southern North Sea basin: imprints of climate change, sea-level oscillation and glacio-isostacy.' *Quaternary Science Reviews*, 26(25-28), 3216-3248.

- Cai, Y., Cheng, H., An, Z., Edwards, R. L., Wang, X., Tan, L., & Wang, J. (2010). Large variations of oxygen isotopes in precipitation over south-central Tibet during Marine Isotope Stage 5. *Geology*, *38*(3), 243-246.

- Cameron, T.D.J., Schüttenhelm, R.T.E., Laban, C. (1989). 'Middle and Upper Pleistocene and Holocene stratigraphy in the southern North Sea between 52° and 54° N, 2° to 4° E.' *The Quaternary and Tertiary Geology of the Southern Bight, North Sea*. By Henriet, J. P., De Moor, G., & De Batist, M. (1989).

- Cartelle, V., Barlow, N. L., Hodgson, D. M., Busschers, F. S., Cohen, K. M., Meijninger, B. M., & van Kesteren, W. P. (2021). 'Sedimentary architecture and landforms of the late Saalian (MIS 6) ice sheet margin offshore of the Netherlands.' *Earth Surface Dynamics*, 9(6), 1399-1421.

- Cohen, K. M., Cartelle, V., Barnett, R., Busschers, F. S., & Barlow, N. L. (2022). 'Last Interglacial sea-level data points from Northwest Europe.' *Earth System Science Data*, 14(6), 2895-2937.

- Eaton, S.J., Hodgson, D.M., Barlow, N.L., Mortimer, E.E. and Mellett, C.L., 2020. 'Palaeogeographical changes in response to glacial–interglacial cycles, as recorded in Middle and Late Pleistocene seismic stratigraphy, southern North Sea'. *Journal of Quaternary Science* 35(6), 760-775.

- Fagan, B. (2009) Ijstijd het Complete verhaal. Nederlandse editie, *Waanders*. Zwolle.

- Van Geel, B. (2022). 'Weichselien and Holocene lake sediments, Peat deposits and molar folds as environmental archives in the North Sea area.' *Grondboor & Hamer, Staringia 17*, 76(3/4), 188-199.

- Van Ginkel, E., Reumer, J., Van der Valk, B. (2014) Schatten van het mammoetstrand. *Havenbedrijf Rotterdam.*

- Hendry, J., Burgess, P., Hunt, D., Janson, X., & Zampetti, V. (2021). 'Seismic characterization of carbonate platforms and reservoirs: an introduction and review.' *Geological Society, London, Special Publications*, 509(1), 1-28.

- Hijma, M. P., Cohen, K. M., Roebroeks, W., Westerhoff, W. E., & Busschers, F. S. (2012). 'Pleistocene Rhine–Thames landscapes: geological background for hominin

occupation of the southern North Sea region.' *Journal of Quaternary Science*, *27*(1), 17-39.

- Hoffman, C. M. (2022); Local versus extra-local representation of Holocene vegetation change in North-East Germany, *Utrecht University*.

- IXBlue (2013), 'Delph Seismic Advanced Notes.'

- Jenny, J. G. (2013). 'High Resolution Seismic Reflection Practical Basis.'

- Kluesner, J., Brothers, D., Hart, P., Miller, N., & Hatcher, G. (2019). 'Practical approaches to maximizing the resolution of sparker seismic reflection data.' *Marine Geophysical Research*, *40*(3), 279-301.

- Knox, R. W. O. B., Bosch, J. H. A., Rasmussen, E. S., Heilmann-Clausen, C., Hiss, M., De Lugt, I. R., … Vandenberghe, N. (2010). *Cenozoic*. In J. C. Doornenbal & A. G. Stevenson (Eds.), *Petroleum geological Atlas of the southern Permian Basin area* (pp. 211–223). Houten, the Netherlands: EAGE Publications B.V.

- Kozaczka, E., Grelowska, G., Kozaczka, S., & Szymczak, W. (2013). Detection of objects buried in the sea bottom with the use of parametric echosounder. *Archives of Acoustics*, *38*(1).

- Laban, C. (1995). The Pleistocene glaciations in the Dutch sector of the North Sea. A synthesis of sedimentary and seismic data. *University of Amsterdam.*

- Laban, C. & Van der Meer, J. J. M. (2022). 'Geological development of the Southern North Sea during the Quarternary.' *Grondboor & Hamer, Staringia 17*, 76(3/4), 200-207.

- Limpenny, S.E., Barrio Froján, C., Cotterill, C., Foster-Smith, R.L., Pearce, B., Tizzard, L., Limpenny, D.L., Long, D., Walmsley, S., Kirby, S., Baker, K., Meadows, W.J., Rees, J., Hill, J., Wilson, C., Leivers, M., Churchley, S., Russell, J., Birchenough, A.C., Green, S.L., and Law, R.J. 2011. The East Coast Regional Environmental Characterisation. *Cefas Open report* 08/04. 287.

- Mathys, M. (2010). Het onderwaterreliëf van het Belgisch deel van de Noordzee. *De Grote Rede*, 26, 16-26.

- Mellett, C. L., Hodgson, D. M., Plater, A. J., Mauz, B., Selby, I., & Lang, A. (2013). 'Denudation of the continental shelf between Britain and France at the glacial–interglacial timescale.' *Geomorphology*, *203*, 79-96.

- Missiaen, T., Fitch, S., Harding, R., Muru, M., Fraser, A., De Clercq, M., Garcia Moreno, D., Versteeg, W., Busschers, F. S., Van Heteren, S., Hijma, M. P., Reichart., G. J., & Gaffney, V. (2021). 'Targeting the Mesolithic: interdisciplinary approaches to archaeological prospection in the Brown Bank area, southern North Sea.' *Quaternary International*, 584, 141-151.

- Mitchum Jr, R. M. (1977). ‘Seismic stratigraphy and global changes of sea level: Part 11. Glossary of terms used in seismic stratigraphy: Section 2.’ *Application of seismic reflection configuration to stratigraphic interpretation.*

- Mitchum Jr, R. M., & Vail, P. R. (1977). ‘Seismic stratigraphy and global changes of sea level: Part 7. Seismic stratigraphic interpretation procedure: Section 2.’ *Application of seismic reflection configuration to stratigraphic interpretation.*

- Mitchum Jr, R. M., Vail, P. R., & Sangree, J. B. (1977). ‘Seismic stratigraphy and global changes of sea level: Part 6. Stratigraphic interpretation of seismic reflection patterns in depositional sequences: Section 2.’ *Application of seismic reflection configuration to stratigraphic interpretation.*

- Mol, D. & Bakker, R. (2022). ‘Quarternary terrestrial megafaunal remains and their localities in the southern bight of the North Sea between the British Isles and The Netherlands: An overview.’ *Grondboor & Hamer*, *Staringia 17*, 76(3/4), 88-127.

- Oele, E. (1971). The Quaternary geology of the southern area of the Dutch part of the North Sea. *Geologie en Mijnbouw*, *50*(3), 461-474.

- Peeters, J., Busschers, F. S., & Stouthamer, E. (2015). ‘Fluvial evolution of the Rhine during the last interglacial-glacial cycle in the southern North Sea basin: a review and look forward.’ *Quaternary International*, 357, 176-188.

- Peeters, J., Busschers, F. S., Stouthamer, E., Bosch, J. H. A., Van den Berg, M. W., Wallinga, J., Versendaal, A. J., Bunnik, F. P. M. & Middelkoop, H. (2016). ‘Sedimentary architecture and chronostratigraphy of a late Quaternary incised-valley fill: a case study of the late Middle and Late Pleistocene Rhine system in the Netherlands.’ *Quaternary Science Reviews*, 131, 211-236.

- Rijksdienst voor Ondernemend Nederland (2019). ‘Geophysical Results Report Hollandse Kust (West) Wind Farm Zone Survey 2018 Dutch Continental Shelf, North Sea.’

- Rijsdijk, K. F., Passchier, S., Weerts, H. J. T., Laban, C., Van Leeuwen, R. J. W., & Ebbing, J. H. J. (2005). ‘Revised Upper Cenozoic stratigraphy of the Dutch sector of the North Sea Basin: towards an integrated lithostratigraphic, seismostratigraphic and allostratigraphic approach.’ *Netherlands Journal of Geosciences*, 84(2), 129-146.

- RVO (2024). ‘Hollandse Kust (west) – Soil’ Database. Accessed on March 28, 2024 via https://offshorewind.rvo.nl/page/view/f4f39d87-68f8-4925-97c4-c49f6a07a001/soll-hollandse-kust-west

- Schroeder, F. W. (2004). ‘Lecture 6 - Seismic Reflections.’ *Courtesy of ExxonMobil*.

- Slootweg, A. P. (1986). Basement imaging with side-looking seismics. *Marine geophysical researches*, *8*(2), 149-174.

- Stow, D. A. (2005). Sedimentary Rocks in the Field: A color guide. Gulf Professional Publishing.

- Stoker, M.S., Balson, P.S., Long, D. and Tappin, D.R. 2011. *An overview of the lithostratigraphical framework for the Quaternary deposits on the United Kingdom continental shelf*. British Geological Survey Research Report, RR/11/03. 48

- Stouthamer, E., Cohen, K., & Hoek, W. (2015). De vorming van het land. Geologie en geomorfologie, *Perspectief Uitgevers*, Utrecht. ISBN 978 94 91269 11 0. Website: http://www.geovorming.nl/

- Taal, M. (2023), Zeespiegel Nederlandse kust verder gestegen in 2022. Deltares. Accessed on March 7, 2024 via https://www.deltares.nl/nieuws/zeespiegel-nederlandse-kust-verder-gestegen-in-2022

- Takano, O., & Tsuji, T. (2017). 'Fluvial to bay sequence stratigraphy and seismic facies of the Cretaceous to Paleogene successions in the MITI Sanriku-oki well and the vicinities, the Sanriku-oki forearc basin, northeast Japan.' *Island Arc*, 26(4), e12184.

- Tizzard, L., Benjamin, J. and De Loecker, D. 2014. 'A Middle Palaeolithic site in the southern North Sea: Investigating the archaeology and palaeogeography of Area 240', *Journal of Quaternary Science* 29(7), 698-710.

- Tizzard, L., Bicket, A. and De Loecker, D. 2015. *Seabed Prehistory: Investigating the Palaeogeography and Early Middle Palaeolithic Archaeology in the Southern North Sea*, Wessex Archaeology Monograph 35. Internal reference 70757.

- TNO-GDN (2022a). Formatie van Naaldwijk. In: *Stratigrafische Nomenclator van Nederland, TNO – Geologische Dienst Nederland*. Accessed on July 16, 2022 via http://www.dinoloket.nl/stratigrafische-nomenclator/formatie-van-naaldwijk.

- TNO-GDN (2022b). Southern Bight Formatie. In: *Stratigrafische Nomenclator van Nederland, TNO – Geologische Dienst Nederland*. Accessed on July 16, 2022 via http://www.dinoloket.nl/stratigrafische-nomenclator/southern-bight-formatie.

- TNO-GDN (2022c). Bligh Bank Laagpakket. In: *Stratigrafische Nomenclator van Nederland, TNO – Geologische Dienst Nederland*. Accessed on July 16, 2022 via http://www.dinoloket.nl/stratigrafische-nomenclator/bligh-bank-laagpakket.

- TNO-GDN (2022d). Buitenbanken Laagpakket. In: *Stratigrafische Nomenclator van Nederland, TNO – Geologische Dienst Nederland*. Accessed on July 16, 2022 via http://www.dinoloket.nl/stratigrafische-nomenclator/buitenbanken-laagpakket.

- TNO-GDN (2022e). Formatie van Kreftenheye. In: *Stratigrafische Nomenclator van Nederland, TNO – Geologische Dienst Nederland*. Accessed on July 16, 2022 via http://www.dinoloket.nl/stratigrafische-nomenclator/formatie-van-kreftenheye.

- TNO-GDN (2022f). Eem Formatie. In: *Stratigrafische Nomenclator van Nederland, TNO – Geologische Dienst Nederland*. Accessed on July 16, 2022 via http://www.dinoloket.nl/stratigrafische-nomenclator/eem-formatie.

- TNO-GDN (2022g). Bruine Bank Laagpakket. In: *Stratigrafische Nomenclator van Nederland, TNO – Geologische Dienst Nederland*. Accessed on July 16, 2022 via http://www.dinoloket.nl/stratigrafische-nomenclator/bruine-bank-laagpakket.

- TNO-GDN (2022h). Formatie van Boxtel. In: *Stratigrafische Nomenclator van Nederland, TNO – Geologische Dienst Nederland*. Accessed on July 16, 2022 via http://www.dinoloket.nl/stratigrafische-nomenclator/formatie-van-boxtel.

- TNO-GDN (2022i). Egmond Ground Formatie. In: *Stratigrafische Nomenclator van Nederland, TNO – Geologische Dienst Nederland*. Accessed on July 16, 2022 via http://www.dinoloket.nl/stratigrafische-nomenclator/egmond-ground-formatie.

- TNO-GDN (2022j). Yarmouth Roads Formatie. In: *Stratigrafische Nomenclator van Nederland, TNO – Geologische Dienst Nederland*. Accessed on July 16, 2022 via http://www.dinoloket.nl/stratigrafische-nomenclator/yarmouth-roads-formatie.

- Van der Valk, B. (2022). 'Mollusc faunas in the Southern North Sea (Tertiary, Pleistocene, Holocene) 10-years of collecting shells on the Zandmotor coastal nourishment.' *Grondboor & Hamer, Staringia 17*, 76(3/4), 152-166.

- Vos, P. C., & van Kesteren, W. P. (2000). The long-term evolution of intertidal mudflats in the northern Netherlands during the Holocene; natural and anthropogenic processes. *Continental Shelf Research*, *20*(12-13), 1687-1710.

- Waajen, I. M., Busschers, F. S., Donders, T. H., Van Heteren, S., Plets, R., Wallinga, J., Hennekam, R., Reichart, G. J., Kinnaird, T. & Wagner-Cremer, F. (2024). Late MIS5a in the southern North Sea: new chronostratigraphic insights from the Brown Bank Formation. *Journal of Quaternary Science*.

- Wunderlich, J. & Müller, S. (2003). High-resolution sub-bottom profiling using parametric acoustics. *International Ocean Systems*, *7*(4), 6-11.

- Zagwijn, W. H. (1983). Sea-level changes in the Netherlands during the Eemian. *Geologie en Mijnbouw*, *62*(3), 437-450.

- Zagwijn, W. H. (1992). 'The beginning of the ice age in Europe and its major subdivisions.' *Quaternary Science Reviews*, 11(5), 583-591.

Appendices

1. All figures in JPG format (prints in A3 or A4 upon request).
2. Petrel System Folder upon request (also assessable via the TNO network within the folder MIS5/Garritsen)
3. Colour print of this document upon request.